

12

Spectroscopic techniques: I Spectrophotometric techniques

A. HOFMANN

- 12.1 Introduction
- 12.2 Ultraviolet and visible light spectroscopy
- 12.3 Fluorescence spectroscopy
- 12.4 Luminometry
- 12.5 Circular dichroism spectroscopy
- 12.6 Light scattering
- 12.7 Atomic spectroscopy
- 12.8 Suggestions for further reading

12.1 INTRODUCTION

Spectroscopic techniques employ light to interact with matter and thus probe certain features of a sample to learn about its consistency or structure. Light is electromagnetic radiation, a phenomenon exhibiting different energies, and dependent on that energy, different molecular features can be probed. The basic principles of interaction of electromagnetic radiation with matter are treated in this chapter. There is no obvious logical dividing point to split the applications of electromagnetic radiation into parts treated separately. The justification for the split presented in this text is purely pragmatic and based on 'common practice'. The applications considered in this chapter use visible or UV light to probe consistency and conformational structure of biological molecules. Usually, these methods are the first analytical procedures used by a biochemical scientist. The applications covered in Chapter 13 present a higher level of complexity in undertaking and are employed at a later stage in biochemical or biophysical characterisation.

An understanding of the properties of electromagnetic radiation and its interaction with matter leads to an appreciation of the variety of types of spectra and, consequently, different spectroscopic techniques and their applications to the solution of biological problems.

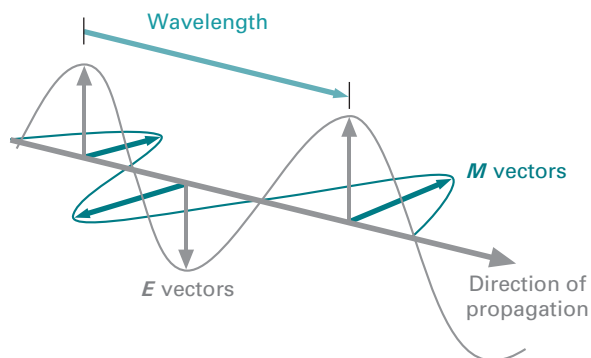


Fig. 12.1 Light is electromagnetic radiation and can be described as a wave propagating transversally in space and time. The electric (E) and magnetic (M) field vectors are directed perpendicular to each other. For UV/Vis, circular dichroism and fluorescence spectroscopy, the electric field vector is of most importance. For electron paramagnetic and nuclear magnetic resonance, the emphasis is on the magnetic field vector.

12.1.1 Properties of electromagnetic radiation

The interaction of electromagnetic radiation with matter is a **quantum phenomenon** and dependent upon both the properties of the radiation and the appropriate structural parts of the samples involved. This is not surprising, since the origin of electromagnetic radiation is due to energy changes within matter itself. The transitions which occur within matter are quantum phenomena and the spectra which arise from such transitions are principally predictable.

Electromagnetic radiation (Fig. 12.1) is composed of an electric and a perpendicular magnetic vector, each one oscillating in plane at right angles to the direction of propagation. The **wavelength** λ is the spatial distance between two consecutive peaks (one cycle) in the sinusoidal waveform and is measured in submultiples of metre, usually in nanometres (nm). The maximum length of the vector is called the **amplitude**. The **frequency** ν of the electromagnetic radiation is the number of oscillations made by the wave within the timeframe of 1 s. It therefore has the units of $1 \text{ s}^{-1} = 1 \text{ Hz}$. The frequency is related to the wavelength via the speed of light c ($c = 2.998 \times 10^8 \text{ m s}^{-1}$ in *vacuo*) by $\nu = c \lambda^{-1}$. A historical parameter in this context is the **wavenumber** $\bar{\nu}$ which describes the number of completed wave cycles per distance and is typically measured in 1 cm^{-1} .

12.1.2 Interaction with matter

Figure 12.2 shows the spectrum of electromagnetic radiation organised by increasing wavelength, and thus decreasing energy, from left to right. Also annotated are the types of radiation and the various interactions with matter and the resulting spectroscopic applications, as well as the interdependent parameters of frequency and wavenumber.

Electromagnetic phenomena are explained in terms of quantum mechanics. The **photon** is the elementary particle responsible for electromagnetic phenomena. It carries the electromagnetic radiation and has properties of a wave, as well as of

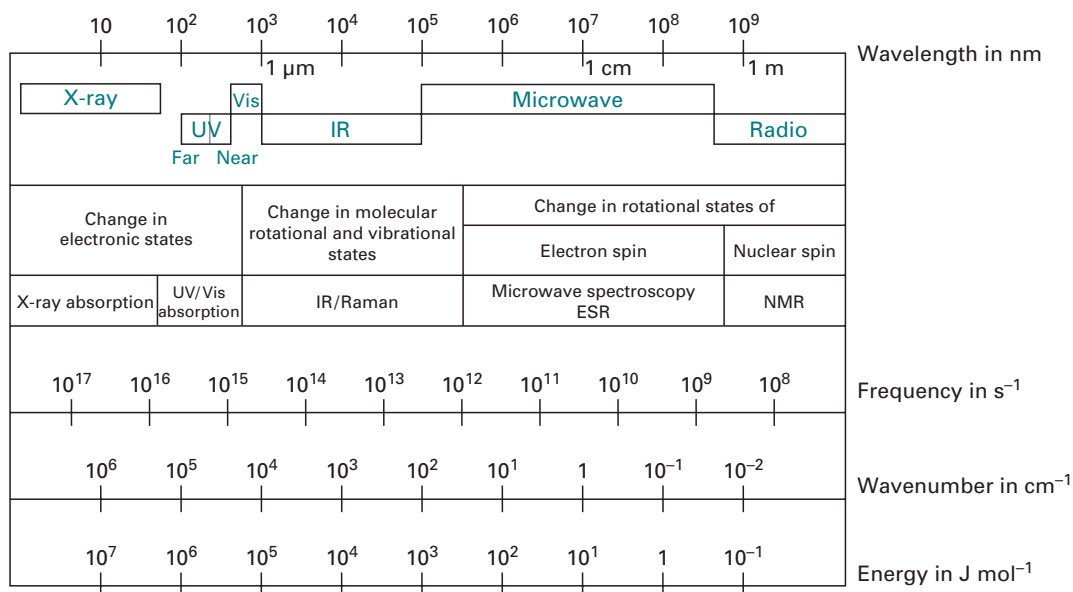


Fig. 12.2 The electromagnetic spectrum and its usage for spectroscopic methods.

a particle, albeit having a mass of zero. As a particle, it interacts with matter by transferring its energy E :

$$E = \frac{hc}{\lambda} = h\nu \quad (12.1)$$

where h is the Planck constant ($h = 6.63 \times 10^{-34}$ Js) and ν is the frequency of the radiation as introduced above.

When considering a diatomic molecule (see Fig. 12.3), **rotational** and **vibrational** levels possess discrete energies that only merge into a continuum at very high energy. Each electronic state of a molecule possesses its own set of rotational and vibrational levels. Since the kind of schematics shown in Fig. 12.3 is rather complex, the **Jablonski diagram** is used instead, where electronic and vibrational states are schematically drawn as horizontal lines, and vertical lines depict possible transitions (see Fig. 12.8 below).

In order for a **transition** to occur in the system, energy must be absorbed. The energy change ΔE needed is defined in quantum terms by the difference in absolute energies between the final and the starting state as $\Delta E = E_{\text{final}} - E_{\text{start}} = h\nu$.

Electrons in either atoms or molecules may be distributed between several energy levels but principally reside in the lowest levels (**ground state**). In order for an electron to be promoted to a higher level (**excited state**), energy must be put into the system. If this energy $E = h\nu$ is derived from electromagnetic radiation, this gives rise to an absorption spectrum, and an electron is transferred from the electronic ground state (S_0) into the first electronic excited state (S_1). The molecule will also be in an excited vibrational and rotational state. Subsequent **relaxation** of the molecule into the vibrational ground state of the first electronic excited state will occur. The electron can then revert back to the electronic ground state. For non-fluorescent molecules, this is accompanied by the emission of heat (ΔH).

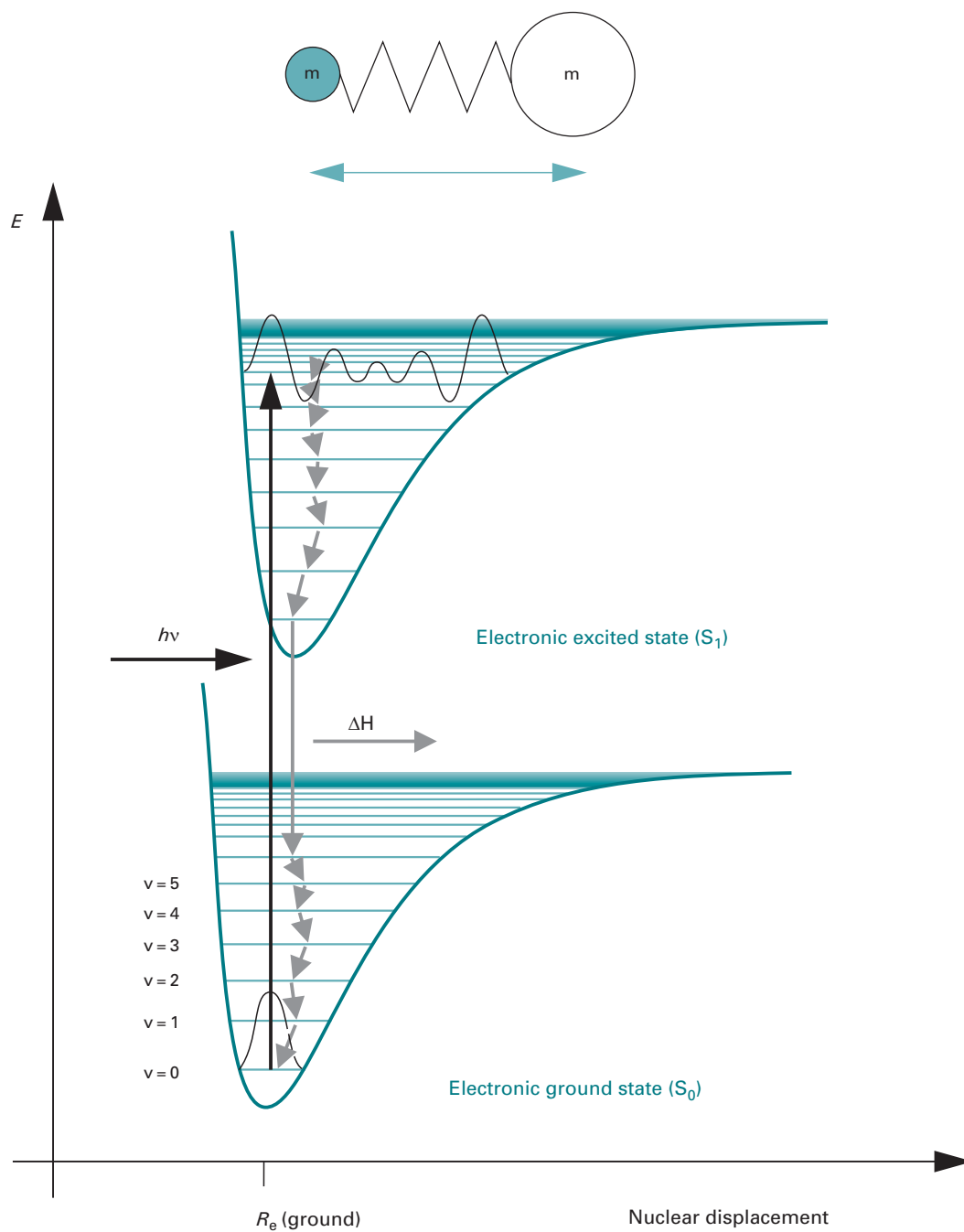


Fig. 12.3 Energy diagram for a diatomic molecule exhibiting rotation, vibration as well as an electronic structure. The distance between two masses m_1 and m_2 (nuclear displacement) is described as a Lennard–Jones potential curve with different equilibrium distances (R_e) for each electronic state. Energetically lower states always have lower equilibrium distances. The vibrational levels (horizontal lines) are superimposed on the electronic levels. Rotational levels are superimposed on the vibrational levels and not shown for reasons of clarity.

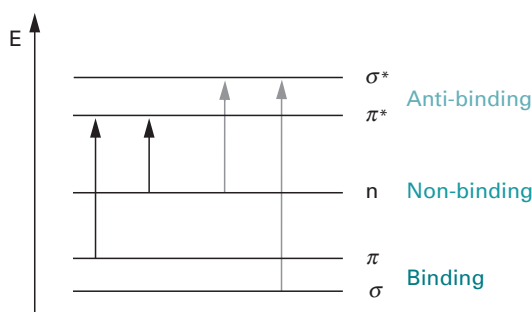


Fig. 12.4 Energy scheme for molecular orbitals (not to scale). Arrows indicate possible electronic transitions. The length of the arrows indicates the energy required to be put into the system in order to enable the transition. Black arrows depict transitions possible with energies from the UV/Vis spectrum for some biological molecules. The transitions shown by grey arrows require higher energies (e.g. X-rays).

The plot of absorption probability against wavelength is called **absorption spectrum**. In the simpler case of single atoms (as opposed to multi-atom molecules), electronic transitions lead to the occurrence of line spectra (see Section 12.7). Because of the existence of more different kinds of energy levels, molecular spectra are usually observed as band spectra (for example Fig. 12.7 below) which are molecule-specific due to the unique vibration states.

A commonly used classification of absorption transitions uses the **spin states** of electrons. Quantum mechanically, the electronic states of atoms and molecules are described by **orbitals** which define the different states of electrons by two parameters: a geometrical function defining the space and a probability function. The combination of both functions describes the localisation of an electron.

Electrons in binding orbitals are usually paired with antiparallel spin orientation (Fig. 12.8). The total spin S is calculated from the individual electron spins. The multiplicity M is obtained by $M = 2 \times S + 1$. For paired electrons in one orbital this yields:

$$S = \text{spin}(\text{electron 1}) + \text{spin}(\text{electron 2}) = (+1/2) + (-1/2) = 0$$

The multiplicity is thus $M = 2 \times 0 + 1 = 1$. Such a state is thus called a **singlet state** and denoted as 'S'. Usually, the ground state of a molecule is a singlet state, S_0 .

In case the spins of both electrons are oriented in a parallel fashion, the resulting state is characterised by a total spin of $S = 1$, and a multiplicity of $M = 3$. Such a state is called a **triplet state** and usually exists only as one of the excited states of a molecule, e.g. T_1 .

According to quantum mechanical transition rules, the multiplicity M and the total spin S must not change during a transition. Thus, the $S_0 \rightarrow S_1$ transition is allowed and possesses a high transition probability. In contrast, the $S_0 \rightarrow T_1$ is not allowed and has a small transition probability. Note that the transition probability is proportional to the intensity of the respective absorption bands.

Most biologically relevant molecules possess more than two atoms and, therefore, the energy diagrams become more complex than the ones shown in Fig. 12.3. Different orbitals combine to yield **molecular orbitals** that generally fall into one of five different classes (Fig. 12.4): s orbitals combine to the binding σ and the anti-binding σ^* orbitals. Some p orbitals combine to the binding π and the anti-binding π^*

orbitals. Other p orbitals combine to form non-binding n orbitals. The population of binding orbitals strengthens a chemical bond, and, vice versa, the population of anti-binding orbitals weakens a chemical bond.

12.1.3 Lasers

Laser is an acronym for light amplification by stimulated emission of radiation. A detailed explanation of the theory of lasers is beyond the scope of this textbook. A simplified description starts with the use of photons of a defined energy to excite an absorbing material. This results in elevation of an electron to a higher energy level. If, whilst the electron is in the excited state, another photon of precisely that energy arrives, then, instead of the electron being promoted to an even higher level, it can return to the original ground state. However, this transition is accompanied by the emission of two photons with the same wavelength and exactly in phase (**coherent photons**). Multiplication of this process will produce coherent light with extremely narrow spectral bandwidth. In order to produce an ample supply of suitable photons, the absorbing material is surrounded by a rapidly flashing light of high intensity (**pumping**).

Lasers are indispensable tools in many areas of science, including biochemistry and biophysics. Several modern spectroscopic techniques utilise laser light sources, due to their high intensity and accurately defined spectral properties. One of the probably most revolutionising applications in the life sciences, the use of lasers in DNA sequencing with fluorescence labels (see Sections 5.11.5, 5.11.6 and 12.3.3), enabled the breakthrough in whole-genome sequencing.

12.2 ULTRAVIOLET AND VISIBLE LIGHT SPECTROSCOPY

These regions of the electromagnetic spectrum and their associated techniques are probably the most widely used for analytical work and research into biological problems.

The electronic transitions in molecules can be classified according to the participating molecular orbitals (See Fig. 12.4). From the four possible transitions ($n \rightarrow \pi^*$, $\pi \rightarrow \pi^*$, $n \rightarrow \sigma^*$, $\sigma \rightarrow \sigma^*$), only two can be elicited with light from the UV/Vis spectrum for some biological molecules: $n \rightarrow \pi^*$ and $\pi \rightarrow \pi^*$. The $n \rightarrow \sigma^*$ and $\sigma \rightarrow \sigma^*$ transitions are energetically not within the range of UV/Vis spectroscopy and require higher energies.

Molecular (sub-)structures responsible for interaction with electromagnetic radiation are called **chromophores**. In proteins, there are three types of chromophores relevant for UV/Vis spectroscopy:

- peptide bonds (amide bond);
- certain amino acid side chains (mainly tryptophan and tyrosine); and
- certain prosthetic groups and coenzymes (e.g. porphyrine groups such as in haem).

The presence of several **conjugated double bonds** in organic molecules results in an extended π -system of electrons which lowers the energy of the π^* orbital through **electron delocalisation**. In many cases, such systems possess $\pi \rightarrow \pi^*$ transitions in the UV/Vis range of the electromagnetic spectrum. Such molecules are very useful tools in colorimetric applications (see Table 12.1).

Table 12.1 **Common colorimetric and UV absorption assays**

Substance	Reagent	Wavelength (nm)
Amino acids	(a) Ninhydrin	570 (proline : 420)
	(b) Cupric salts	620
Cysteine residues, thiolates	Ellman reagent (di-sodium-bis-(3-carboxy-4-nitrophenyl)-disulphide)	412
Protein	(a) Folin (phosphomolybdate, phosphotungstate, cupric salt)	660
	(b) Biuret (reacts with peptide bonds)	540
	(c) BCA reagent (bicinchoninic acid)	562
	(d) Coomassie Brilliant Blue	595
	(e) Direct	Tyr, Trp: 278, peptide bond : 190
Coenzymes	Direct	FAD: 438, NADH: 340, NAD ⁺ : 260
Carotenoids	Direct	420, 450, 480
Porphyrins	Direct	400 (Soret band)
Carbohydrate	(a) Phenol, H ₂ SO ₄	Glucose: 490, xylose: 480
	(b) Anthrone (anthrone, H ₂ SO ₄)	620 or 625
Reducing sugars	Dinitrosalicylate, alkaline tartrate buffer	540
Pentoses	(a) Bial (orcinol, ethanol, FeCl ₃ , HCl)	665
	(b) Cysteine, H ₂ SO ₄	380–415
Hexoses	(a) Carbazole, ethanol, H ₂ SO ₄	540 or 440
	(b) Cysteine, H ₂ SO ₄	380–415
	(c) Arsenomolybdate	500–570
Glucose	Glucose oxidase, peroxidase, <i>o</i> -dianisidine, phosphate buffer	420
Ketohehexose	(a) Resorcinol, thiourea, ethanoic acid, HCl	520
	(b) Carbazole, ethanol, cysteine, H ₂ SO ₄	560
	(c) Diphenylamine, ethanol, ethanoic acid, HCl	635
Hexosamines	Ehrlich (dimethylaminobenzaldehyde, ethanol, HCl)	530

Table 12.1 (cont.)

Substance	Reagent	Wavelength (nm)
DNA	(a) Diphenylamine	595
	(b) Direct	260
RNA	Bial (orcinol, ethanol, FeCl ₃ , HCl)	665
Sterols and steroids	Liebermann–Burchardt reagent (acetic anhydride, H ₂ SO ₄ , chloroform)	425, 625
Cholesterol	Cholesterol oxidase, peroxidase, 4-amino-antipyrine, phenol	500
ATPase assay	Coupled enzyme assay with ATPase, pyruvate kinase, lactate dehydrogenase: ATP → ADP (consumes ATP) phosphoenolpyruvate → pyruvate (consumes ADP) pyruvate → lactate (consumes NADH)	NADH: 340

12.2.1 Chromophores in proteins

The electronic transitions of the **peptide bond** occur in the far UV. The intense peak at 190 nm, and the weaker one at 210–220 nm is due to the $\pi \rightarrow \pi^*$ and $n \rightarrow \pi^*$ transitions. A number of amino acids (Asp, Glu, Asn, Gln, Arg and His) have weak electronic transitions at around 210 nm. Usually, these cannot be observed in proteins because they are masked by the more intense peptide bond absorption. The most useful range for proteins is above 230 nm, where there are absorptions from **aromatic side chains**. While a very weak absorption maximum of phenylalanine occurs at 257 nm, tyrosine and tryptophan dominate the typical protein spectrum with their absorption maxima at 274 nm and 280 nm, respectively (Fig. 12.5). *In praxi*, the presence of these two aromatic side chains gives rise to a band at ~ 278 nm. Cystine (Cys₂) possesses a weak absorption maximum of similar strength as phenylalanine at 250 nm. This band can play a role in rare cases in protein optical activity or protein fluorescence.

Proteins that contain **prosthetic groups** (e.g. haem, flavin, carotenoid) and some metal–protein complexes, may have strong absorption bands in the UV/Vis range. These bands are usually sensitive to local environment and can be used for physical studies of enzyme action. Carotenoids, for instance, are a large class of red, yellow and orange plant pigments composed of long carbon chains with many conjugated double bonds. They contain three maxima in the visible region of the electromagnetic spectrum (~ 420 nm, 450 nm, 480 nm).

Porphyrins are the prosthetic groups of haemoglobin, myoglobin, catalase and cytochromes. Electron delocalisation extends throughout the cyclic tetrapyrrole ring of porphyrins and gives rise to an intense transition at ~ 400 nm called the **Soret band**. The spectrum of haemoglobin is very sensitive to changes in the iron-bound ligand. These changes can be used for structure–function studies of haem proteins.

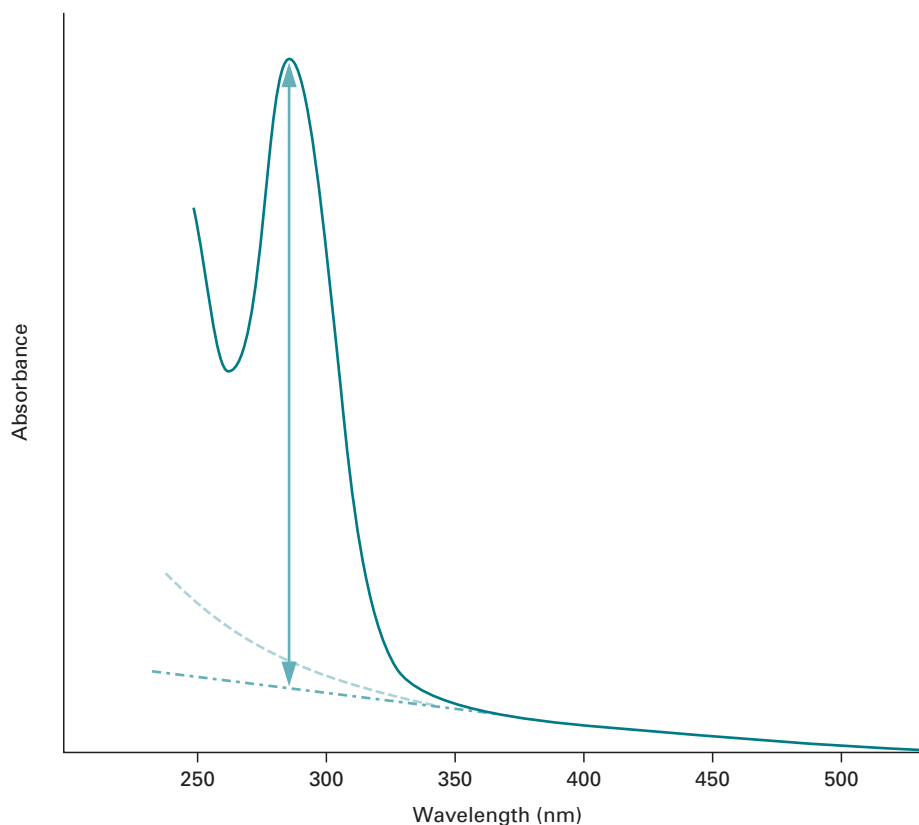


Fig. 12.5 The presence of larger aggregates in biological samples gives rise to Rayleigh scatter visible by a considerable slope in the region from 500 to 350 nm. The dashed line shows the correction to be applied to spectra with Rayleigh scatter which increases with λ^{-4} . Practically, linear extrapolation of the region from 500 to 350 nm is performed to correct for the scatter. The corrected absorbance is indicated by the double arrow.

Molecules such as FAD (flavin adenine dinucleotide), NADH and NAD^+ are important **coenzymes** of proteins involved in electron transfer reactions (RedOx reactions). They can be conveniently assayed by using their UV/Vis absorption: 438 nm (FAD), 340 nm (NADH) and 260 nm (NAD^+).

Chromophores in genetic material

The absorption of UV light by nucleic acids arises from $n \rightarrow \pi^*$ and $\pi \rightarrow \pi^*$ transitions of the purine (adenine, guanine) and pyrimidine (cytosine, thymine, uracil) bases that occur between 260 nm and 275 nm. The absorption spectra of the bases in polymers are sensitive to pH and greatly influenced by electronic interactions between bases.

12.2.2 Principles

Quantification of light absorption

The chance for a photon to be absorbed by matter is given by an **extinction coefficient** which itself is dependent on the wavelength λ of the photon. If light with the

intensity I_0 passes through a sample with appropriate transparency and the path length (thickness) d , the intensity I drops along the pathway in an exponential manner. The characteristic absorption parameter for the sample is the extinction coefficient α , yielding the correlation $I = I_0 e^{-\alpha d}$. The ratio $T = I/I_0$ is called **transmission**.

Biochemical samples usually comprise aqueous solutions, where the substance of interest is present at a molar concentration c . Algebraic transformation of the exponential correlation into an expression based on the decadic logarithm yields the **law of Beer–Lambert**:

$$\lg \frac{I_0}{I} = \lg \frac{1}{T} = \varepsilon \times c \times d = A \quad (12.2)$$

where $[d] = 1 \text{ cm}$, $[c] = 1 \text{ mol dm}^{-3}$, and $[\varepsilon] = 1 \text{ dm}^3 \text{ mol}^{-1} \text{ cm}^{-1}$. ε is the **molar absorption coefficient** (also **molar extinction coefficient**) ($\alpha = 2.303 \times c \times \varepsilon$). A is the **absorbance** of the sample, which is displayed on the spectrophotometer.

The Beer–Lambert law is valid for low concentrations only. Higher concentrations might lead to association of molecules and therefore cause deviations from the ideal behaviour. Absorbance and extinction coefficients are additive parameters, which complicates determination of concentrations in samples with more than one absorbing species. Note that in dispersive samples or suspensions scattering effects increase the absorbance, since the scattered light is not reaching the detector for read-out. The absorbance recorded by the spectrophotometer is thus overestimated and needs to be corrected (Fig. 12.5).

Deviations from the Beer–Lambert law

According to the Beer–Lambert law, absorbance is linearly proportional to the concentration of chromophores. This might not be the case any more in samples with high absorbance. Every spectrophotometer has a certain amount of stray light, which is light received at the detector but not anticipated in the spectral band isolated by the monochromator. In order to obtain reasonable signal-to-noise ratios, the intensity of light at the chosen wavelength (I_λ) should be 10 times higher than the intensity of the stray light (I_{stray}). If the stray light gains in intensity, the effects measured at the detector have nothing or little to do with chromophore concentration. Secondly, molecular events might lead to deviations from the Beer–Lambert law. For instance, chromophores might dimerise at high concentrations and, as a result, might possess different spectroscopic parameters.

Absorption or light scattering – optical density

In some applications, for example measurement of turbidity of cell cultures (determination of biomass concentration), it is not the absorption but the **scattering** of light (see Section 12.6) that is actually measured with a spectrophotometer. Extremely turbid samples like bacterial cultures do not absorb the incoming light. Instead, the light is scattered and thus, the spectrometer will record an **apparent absorbance** (sometimes also called **attenuance**). In this case, the observed parameter is called **optical density** (OD). Instruments specifically designed to measure turbid samples are **nephelometers** or Klett meters; however, most biochemical laboratories use the general UV/Vis spectrometer for determination of optical densities of cell cultures.

Factors affecting UV/Vis absorption

Biochemical samples are usually buffered aqueous solutions, which has two major advantages. Firstly, proteins and peptides are comfortable in water as a solvent, which is also the 'native' solvent. Secondly, in the wavelength interval of UV/Vis (700–200 nm) the water spectrum does not show any absorption bands and thus acts as a silent component of the sample.

The absorption spectrum of a chromophore is only partly determined by its chemical structure. The environment also affects the observed spectrum, which mainly can be described by three parameters:

- protonation/deprotonation (pH, RedOx);
- solvent polarity (dielectric constant of the solvent); and
- orientation effects.

Vice versa, the immediate environment of chromophores can be probed by assessing their absorption, which makes chromophores ideal reporter molecules for environmental factors. Four effects, two each for wavelength and absorption changes, have to be considered:

- a wavelength shift to higher values is called **red shift** or **bathochromic effect**;
- similarly, a shift to lower wavelengths is called **blue shift** or **hypsochromic effect**;
- an increase in absorption is called **hyperchromicity** ('more colour'),
- while a decrease in absorption is called **hypochromicity** ('less colour').

Protonation/deprotonation arises either from changes in pH or **oxidation/reduction** reactions, which makes chromophores pH- and RedOx-sensitive reporters. As a rule of thumb, λ_{max} and ϵ increase, i.e. the sample displays a batho- and hyperchromic shift, if a titratable group becomes charged.

Furthermore, **solvent polarity** affects the difference between the ground and excited states. Generally, when shifting to a less polar environment one observes a batho- and hyperchromic effect. Conversely, a solvent with higher polarity elicits a hypso- and hypochromic effect.

Lastly, orientation effects, such as an increase in order of nucleic acids from single-stranded to double-stranded DNA, lead to different absorption behaviour. A sample of free nucleotides exhibits a higher absorption than a sample with identical amounts of nucleotides but assembled into a single-stranded polynucleotide. Accordingly, double-stranded polynucleotides exhibit an even smaller absorption than two single-stranded polynucleotides. This phenomenon is called the hypochromicity of polynucleotides. The increased exposure (and thus stronger absorption) of the individual nucleotides in the less ordered states provides a simplified explanation for this behaviour.

12.2.3 Instrumentation

UV/Vis spectrophotometers are usually dual-beam spectrometers where the first channel contains the sample and the second channel holds the control (buffer) for correction.

Alternatively, one can record the control spectrum first and use this as internal reference for the sample spectrum. The latter approach has become very popular as many spectrometers in the laboratories are computer-controlled, and baseline correction can be carried out using the software by simply subtracting the control from the sample spectrum.

The light source is a tungsten filament bulb for the visible part of the spectrum, and a deuterium bulb for the UV region. Since the emitted light consists of many different wavelengths, a **monochromator**, consisting of either a prism or a rotating metal grid of high precision called **grating**, is placed between the light source and the sample. Wavelength selection can also be achieved by using coloured filters as monochromators that absorb all but a certain limited range of wavelengths. This limited range is called the **bandwidth** of the filter. Filter-based wavelength selection is used in **colorimetry**, a method with moderate accuracy, but best suited for specific colorimetric assays where only certain wavelengths are of interest. If wavelengths are selected by prisms or gratings, the technique is called **spectrophotometry** (Fig. 12.6).

Example 1 ESTIMATION OF MOLAR EXTINCTION COEFFICIENTS

In order to determine the concentration of a solution of the peptide MAMVSEFLKQ AWFIEENEEQE YVQTVKSSKG GPGSAVSPYP TFNPSS in water, the molar absorption coefficient needs to be estimated.

The molar extinction coefficient ϵ is a characteristic parameter of a molecule and varies with the wavelength of incident light. Because of useful applications of the law of Beer-Lambert, the value of ϵ needs to be known for a lot of molecules being used in biochemical experiments.

Very frequently in biochemical research, the molar extinction coefficient of proteins is estimated using incremental ϵ_i values for each absorbing protein residue (chromophore). Summation over all residues yields a reasonable estimation for the extinction coefficient. The simplest increment system is based on values of Gill and von Hippel.¹ The determination of protein concentration using this formula only requires an absorption value at $\lambda = 280$ nm. Increments ϵ_i are used to calculate a molar extinction coefficient at 280 nm for the entire protein or peptide by summation over all relevant residues in the protein:

Residue	Gill and von Hippel ϵ_i (280 nm) in $\text{dm}^3 \text{mol}^{-1} \text{cm}^{-1}$
Cys ₂	120
Trp	5690
Tyr	1280

For the peptide above, one obtains $\epsilon = (1 \times 5690 + 2 \times 1280) \text{ dm}^3 \text{mol}^{-1} \text{cm}^{-1} = 8250 \text{ dm}^3 \text{mol}^{-1} \text{cm}^{-1}$

¹ Gill, S. C. and von Hippel, P. H. (1989). Calculation of protein extinction coefficients from amino acid sequence data. *Analytical Biochemistry*, 182, 319–326. Erratum: *Analytical Biochemistry* (1990), 189, 283.

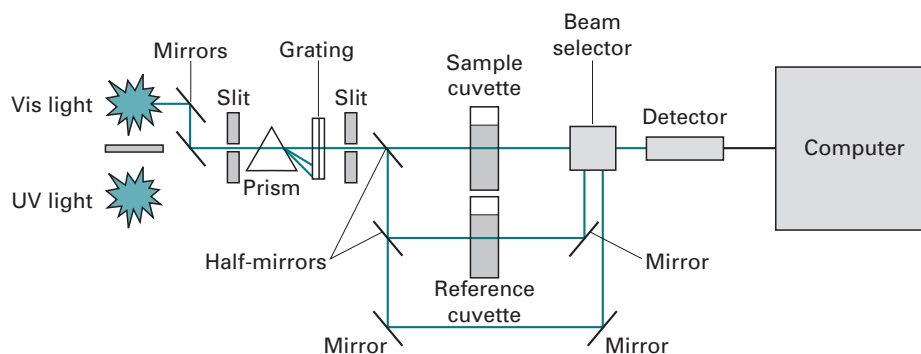


Fig. 12.6 Optical arrangements in a dual-beam spectrophotometer. Either a prism or a grating constitutes the monochromator of the instrument. Optical paths are shown as green lines.

A prism splits the incoming light into its components by refraction. Refraction occurs because radiation of different wavelengths travels along different paths in medium of higher density. In order to maintain the principle of velocity conservation, light of shorter wavelength (higher speed) must travel a longer distance (i.e. blue sky effect). At a grating, the splitting of wavelengths is achieved by diffraction. Diffraction is a reflection phenomenon that occurs at a grid surface, in this case a series of engraved fine lines. The distance between the lines has to be of the same order of magnitude as the wavelength of the diffracted radiation. By varying the distance between the lines, different wavelengths are selected. This is achieved by rotating the grating perpendicular to the optical axis. The resolution achieved by gratings is much higher than the one available by prisms. Nowadays instruments almost exclusively contain gratings as monochromators as they can be reproducibly made in high quality by photoreproduction.

The bandwidth of a colorimeter is determined by the filter used as monochromator. A filter that appears red to the human eye is transmitting red light and absorbs almost any other (visual) wavelength. This filter would be used to examine blue solutions, as these would absorb red light. The filter used for a specific colorimetric assay is thus made of a colour complementary to that of the solution being tested. Theoretically, a single wavelength is selected by the monochromator in spectrophotometers, and the emergent light is a parallel beam. Here, the bandwidth is defined as twice the half-intensity bandwidth. The bandwidth is a function of the optical slit width. The narrower the slit width the more reproducible are measured absorbance values. In contrast, the sensitivity becomes less as the slit narrows, because less radiation passes through to the detector.

In a dual-beam instrument, the incoming light beam is split into two parts by a half-mirror. One beam passes through the sample, the other through a control (blank, reference). This approach obviates any problems of variation in light intensity, as both reference and sample would be affected equally. The measured absorbance is the difference between the two transmitted beams of light recorded. Depending on the instrument, a second detector measures the intensity of the incoming beam, although some instruments use an arrangement where one detector measures the incoming and the transmitted intensity alternately. The latter design is better from an analytical point of view as it eliminates potential variations between the two

detectors. At about 350 nm most instruments require a change of the light source from visible to UV light. This is achieved by mechanically moving mirrors that direct the appropriate beam along the optical axis and divert the other. When scanning the interval of 500–210 nm, this frequently gives rise to an offset of the spectrum at the switchover point.

Since borosilicate glass and normal plastics absorb UV light, such cuvettes can only be used for applications in the visible range of the spectrum (up to 350 nm). For UV measurements, quartz cuvettes need to be used. However, disposable plastic cuvettes have been developed that allow for measurements over the entire range of the UV/Vis spectrum.

12.2.4 Applications

The usual procedure for (colorimetric) assays is to prepare a set of standards and produce a plot of concentration versus absorbance called **calibration curve**. This should be linear as long as the Beer–Lambert law applies. Absorbances of unknowns are then measured and their concentration interpolated from the linear region of the plot. It is important that one never extrapolates beyond the region for which an instrument has been calibrated as this potentially introduces enormous errors.

To obtain good spectra, the maximum absorbance should be approximately 0.5 which corresponds to concentrations of about 50 μM (assuming $\epsilon = 10\,000\text{ dm}^3\text{ mol}^{-1}\text{ cm}^{-1}$).

Qualitative and quantitative analysis

Qualitative analysis may be performed in the UV/Vis regions to identify certain classes of compounds both in the pure state and in biological mixtures (e.g. protein-bound). The application of UV/Vis spectroscopy to further analytical purposes is rather limited, but possible for systems where appropriate features and parameters are known.

Most commonly, this type of spectroscopy is used for quantification of biological samples either directly or via colorimetric assays. In many cases, proteins can be quantified directly using their intrinsic chromophores, tyrosine and tryptophan. Protein spectra are acquired by scanning from 500 to 210 nm. The characteristic features in a protein spectrum are a band at 278/280 nm and another at 190 nm (Fig. 12.6). The region from 500 to 300 nm provides valuable information about the presence of any prosthetic groups or coenzymes. Protein quantification by single wavelength measurements at 280 and 260 nm only should be avoided, as the presence of larger aggregates (contaminations or protein aggregates) gives rise to considerable **Rayleigh scatter** that needs to be corrected for (Fig. 12.6).

Difference spectra

The main advantage of difference spectroscopy is its capacity to detect small absorbance changes in systems with high background absorbance. A difference spectrum is obtained by subtracting one absorption spectrum from another. Difference spectra can be obtained in two ways: either by subtraction of one absolute absorption spectrum from another, or by placing one sample in the reference cuvette and another in the test cuvette. The latter method requires usage of a dual-beam instrument, the former method has become very popular due to most instruments being controlled

Example 2 DETERMINATION OF CONCENTRATIONS

- Question** (1) The concentration of an aqueous solution of a protein is to be determined assuming:
- (i) knowledge of the molar extinction coefficient ϵ
 - (ii) molar extinction coefficient ϵ is not known.
- (2) What is the concentration of an aqueous solution of a DNA sample?

Answer (1) (i) The protein concentration of a pure sample can be determined by using the Beer–Lambert law. The absorbance at 280 nm is determined from a protein spectrum, and the molar extinction coefficient at this wavelength needs to be experimentally determined or estimated:

$$\rho^* = \frac{A \times M}{\epsilon \times d}$$

where ρ^* is the mass concentration in mg cm^{-3} and M the molecular mass of the assayed species in g mol^{-1} .

- (ii) Alternatively, an empirical formula known as the Warburg–Christian formula can be used without knowledge of the value of the molar extinction coefficient:

$$\rho^* = (1.52 \times A_{280} - 0.75 \times A_{260}) \text{ mg cm}^{-3}$$

Other commonly used applications to determine the concentration of protein in a sample make use of colorimetric assays that are based on chemicals (folin, biuret, bicinchoninic acid or Coomassie Brilliant Blue) binding to protein groups. Concentration determination in these cases requires a calibration curve measured with a protein standard, usually bovine serum albumin.

- (2) As we have seen above, the genetic bases have absorption bands in the UV/Vis region. Thus, the concentration of a DNA sample can be determined spectroscopically. Assuming that a pair of nucleotides has a molecular mass of $M = 660 \text{ g mol}^{-1}$, the absorbance A of a solution with double-stranded DNA at 260 nm can be converted to mass concentration ρ^* by:

$$\rho^* = 50 \mu\text{g cm}^{-3} \times A_{260}$$

The ratio A_{260}/A_{280} is an indicator for the purity of the DNA solution and should be in the range 1.8–2.0.

by computers which allows easy processing and handling of data. From a purist's point of view, the direct measurement of the difference spectrum in a dual-beam instrument is the preferred method, since it reduces the introduction of inconsistencies between samples and thus the error of the measurement. Figure 12.7 shows the two absolute spectra of ubiquinone and ubiquinol, the oxidised and reduced species of the same molecular skeleton, as well as the difference spectrum.

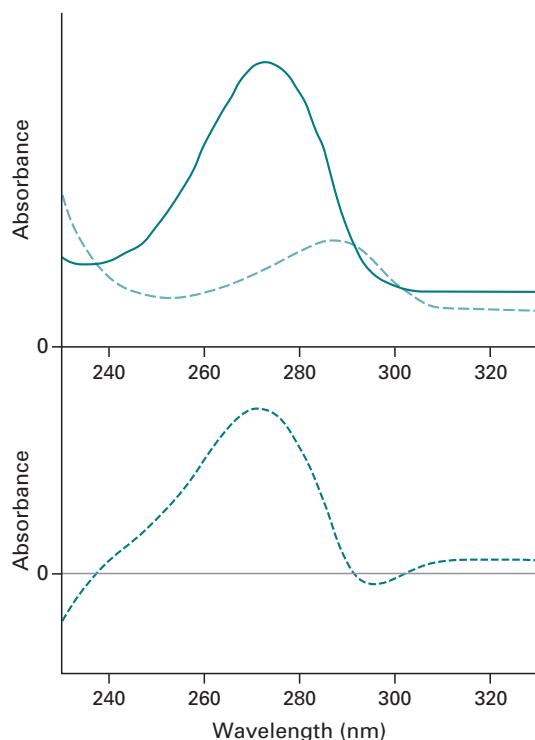


Fig. 12.7 Top: Absolute spectra of ubiquinone (solid curve) and ubiquinol (dotted curve). Bottom: Difference spectrum.

Difference spectra have three distinct features as compared to absolute spectra:

- difference spectra may contain negative absorbance values;
- absorption maxima and minima may be displaced and the extinction coefficients are different from those in peaks of absolute spectra;
- there are points of zero absorbance, usually accompanied by a change of sign of the absorbance values. These points are observed at wavelengths where both species of related molecules exhibit identical absorbances (isosbestic points), and which may be used for checking for the presence of interfering substances.

Common applications for difference UV spectroscopy include the determination of the number of aromatic amino acids exposed to solvent, detection of conformational changes occurring in proteins, detection of aromatic amino acids in active sites of enzymes, and monitoring of reactions involving ‘catalytic’ chromophores (prosthetic groups, coenzymes).

Derivative spectroscopy

Another way to resolve small changes in absorption spectra that otherwise would remain invisible is the usage of derivative spectroscopy. Here, the absolute absorption spectrum of a sample is differentiated and the differential $\delta^x A / \delta \lambda^x$ plotted against the wavelength. Since the algebraic relationship between A and λ is unknown, differentiation is carried out by numerical methods using computer software. The usefulness of this approach depends on the individual problem. Examples of successful applications

include the binding of a monoclonal antibody to its antigen with second-order derivatives and the quantification of tryptophan and tyrosine residues in proteins using fourth-order derivatives.

Solvent perturbation

As we have mentioned above, aromatic amino acids are the main chromophores of proteins in the UV region of the electromagnetic spectrum. Furthermore, the UV absorption of chromophores depends largely on the polarity in its immediate environment. A change in the polarity of the solvent changes the UV spectrum of a protein by bathochromic or hypsochromic effects without changing its conformation. This phenomenon is called **solvent perturbation** and can be used to probe the surface of a protein molecule. In order to be accessible to the solvent, the chromophore has to be accessible on the protein surface. Practically, solvents like dimethyl-sulfoxide, dioxane, glycerol, mannitol, sucrose and polyethylene glycol are used for solvent perturbation experiments, because they are miscible with water. The method of solvent perturbation is most commonly used for determination of the number of aromatic residues that are exposed to solvent.

Spectrophotometric and colorimetric assays

For biochemical assays testing for time- or concentration-dependent responses of systems, an appropriate read-out is required that is coupled to the progress of the reaction (**reaction coordinate**). Therefore, the biophysical parameter being monitored (read-out) needs to be coupled to the biochemical parameter under investigation. Frequently, the monitored parameter is the absorbance of a system at a given wavelength which is monitored throughout the course of the experiment. Preferably, one should try to monitor the changing species directly (e.g. protein absorption, starting product or generated product of a reaction), but in many cases this is not possible and a secondary reaction has to be used to generate an appropriate signal for monitoring. A common application of the latter approach is the determination of protein concentration by Lowry or Bradford assays, where a secondary reaction is used to colour the protein. The more intense the colour, the more protein is present. These assays are called **colorimetric assays** and a number of commonly used ones are listed in Table 12.1.

12.3 FLUORESCENCE SPECTROSCOPY

12.3.1 Principles

Fluorescence is an emission phenomenon where an energy transition from a higher to a lower state is accompanied by radiation. Only molecules in their excited forms are able to emit fluorescence; thus, they have to be brought into a state of higher energy prior to the emission phenomenon.

We have already seen in Section 12.1.2 that molecules possess discrete states of energy. Potential energy levels of molecules have been depicted by different Lennard-Jones potential curves with overlaid vibrational (and rotational) states (Fig. 12.3). Such diagrams can be abstracted further to yield Jablonski diagrams (Fig. 12.8).

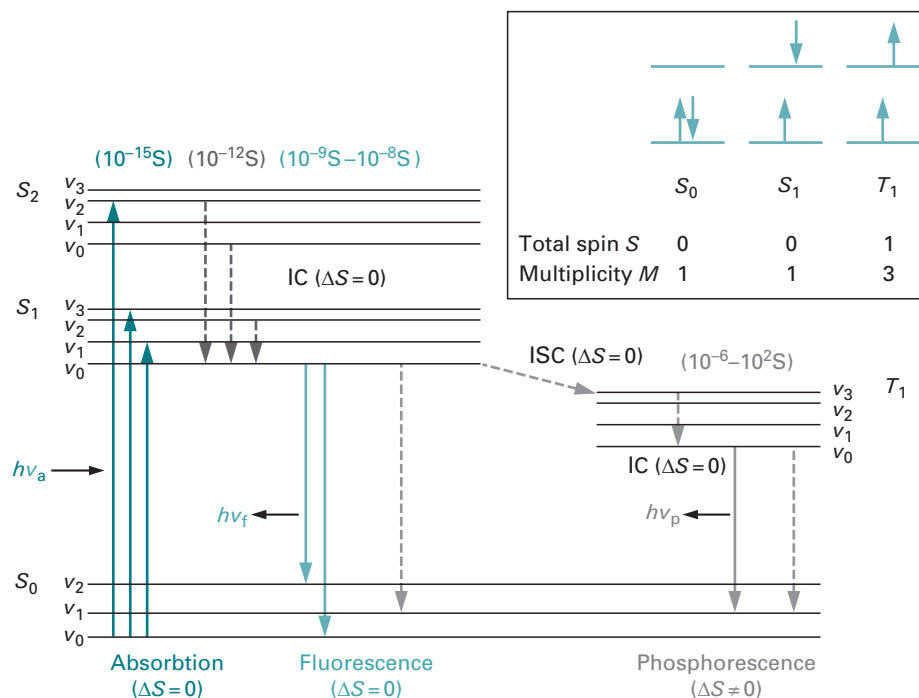


Fig. 12.8 Jablonski diagram. Shown are the electronic ground state (S_0), two excited singlet states (S_1, S_2) and a triplet state (T_1). Vibrational levels (v) are only illustrated exemplarily. Solid vertical lines indicate radiative transitions, dotted lines show non-radiative transitions. The inset shows the relationship between electron configurations, total spin number S and multiplicity M .

In these diagrams, energy transitions are indicated by vertical lines. Not all transitions are possible; allowed transitions are defined by the selection rules of quantum mechanics. A molecule in its electronic and vibrational ground state (S_0v_0) can absorb photons matching the energy difference of its various discrete states. The required photon energy has to be higher than that required to reach the vibrational ground state of the first electronic excited state (S_1v_0). The excess energy is absorbed as vibrational energy ($v > 0$), and quickly dissipated as heat by collision with solvent molecules. The molecule thus returns to the vibrational ground state (S_1v_0). These relaxation processes are non-radiating transitions from one energetic state to another with lower energy, and are called **internal conversion** (IC). From the lowest level of the first electronic excited state, the molecule returns to the ground state (S_0) either by emitting light (fluorescence) or by a non-radiative transition. Upon radiative transition, the molecule can end up in any of the vibrational states of the electronic ground state (as per quantum mechanical rules).

If the vibrational levels of the ground state overlap with those of the electronic excited state, the molecule will not emit fluorescence, but rather revert to the ground state by non-radiative internal conversion. This is the most common way for excitation energy to be dissipated and is why fluorescent molecules are rather rare. Most molecules are flexible and thus have very high vibrational levels in the ground state. Indeed, most fluorescent molecules possess fairly rigid aromatic rings or ring systems. The fluorescent group in a molecule is called a **fluorophore**.

Since radiative energy is lost in fluorescence as compared to the absorption, the fluorescent light is always at a longer wavelength than the exciting light (**Stokes shift**). The emitted radiation appears as band spectrum, because there are many closely related wavelength values dependent on the vibrational and rotational energy levels attained. The fluorescence spectrum of a molecule is independent of the wavelength of the exciting radiation and has a mirror image relationship with the absorption spectrum. The probability of the transition from the electronic excited to the ground state is proportional to the intensity of the emitted light.

An associated phenomenon in this context is **phosphorescence** which arises from a transition from a triplet state (T_1) to the electronic (singlet) ground state (S_0). The molecule gets into the triplet state from an electronic excited singlet state by a process called **intersystem crossing** (ISC). The transition from singlet to triplet is quantum-mechanically not allowed and thus only happens with low probability in certain molecules where the electronic structure is favourable. Such molecules usually contain heavy atoms. The rate constants for phosphorescence are much longer and phosphorescence thus happens with a long delay and persists even when the exciting energy is no longer applied.

The fluorescence properties of a molecule are determined by properties of the molecule itself (internal factors), as well as the environment of the protein (external factors). The fluorescence intensity emitted by a molecule is dependent on the **lifetime** of the excited state. The transition from the excited to the ground state can be treated like a decay process of first order, i.e. the number of molecules in the excited state decreases exponentially with time. In analogy to kinetics, the exponential coefficient k_r is called rate constant and is the reciprocal of the lifetime: $\tau_r = k_r^{-1}$. The lifetime is the time it takes to reduce the number of fluorescence emitting molecules to N_0/e , and is proportional to λ^3 .

The effective lifetime τ of excited molecules, however, differs from the fluorescence lifetime τ_r since other, non-radiative processes also affect the number of molecules in the excited state. τ is dependent on all processes that cause relaxation: fluorescence emission, internal conversion, quenching, fluorescence resonance energy transfer, reactions of the excited state and intersystem crossing.

The ratio of photons emitted and photons absorbed by a fluorophore is called **quantum yield** Φ (equation 12.3). It equals the ratio of the rate constant for fluorescence emission k_r and the sum of the rate constants for all six processes mentioned above.

$$\Phi = \frac{N(\text{em})}{N(\text{abs})} = \frac{k_r}{k} = \frac{k_r}{k_r + k_{IC} + k_{ISC} + k_{\text{reaction}} + k_Q c(Q) + k_{\text{FRET}}} = \frac{\tau}{\tau_r} \quad (12.3)$$

The quantum yield is a dimensionless quantity, and, most importantly, the only absolute measure of fluorescence of a molecule. Measuring the quantum yield is a difficult process and requires comparison with a fluorophore of known quantum yield. In biochemical applications, this measurement is rarely done. Most commonly, the fluorescence emissions of two or more related samples are compared and their relative differences analysed.

12.3.2 Instrumentation

Fluorescence spectroscopy works most accurately at very low concentrations of emitting fluorophores. UV/Vis spectroscopy, in contrast, is least accurate at such

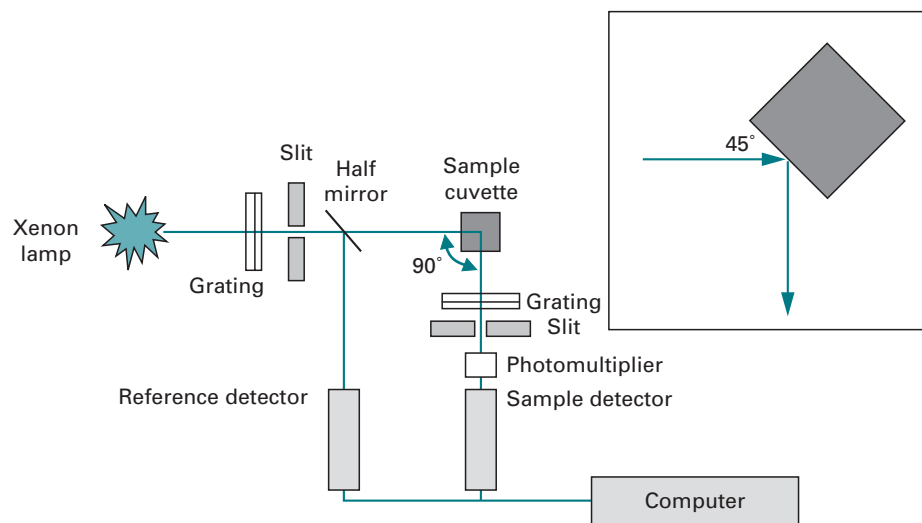


Fig. 12.9 Schematics of a spectrofluorimeter with 'T' geometry (90°). Optical paths are shown as green lines. Inset: Geometry of front-face illumination.

low concentrations. One major factor adding to the high sensitivity of fluorescence applications is the spectral selectivity. Due to the Stokes shift, the wavelength of the emitted light is different from that of the exciting light. Another feature makes use of the fact that fluorescence is emitted in all directions. By placing the detector perpendicular to the excitation pathway, the background of the incident beam is reduced.

The schematics of a typical spectrofluorimeter are shown in Fig. 12.9. Two monochromators are used, one for tuning the wavelength of the exciting beam and a second one for analysis of the fluorescence emission. Due to the emitted light always having a lower energy than the exciting light, the wavelength of the excitation monochromator is set at a lower wavelength than the emission monochromator. The better fluorescence spectrometers in laboratories have a photon-counting detector yielding very high sensitivity. Temperature control is required for accurate work as the emission intensity of a fluorophore is dependent on the temperature of the solution.

Two geometries are possible for the measurement, with the 90° arrangement most commonly used. Pre- and post-filter effects can arise owing to absorption of light prior to reaching the fluorophore and the reduction of emitted radiation. These phenomena are also called **inner filter effects** and are more evident in solutions with high concentrations. As a rough guide, the absorption of a solution to be used for fluorescence experiments should be less than 0.05. The use of microcuvettes containing less material can also be useful. Alternatively, the front-face illumination geometry (Fig. 12.9 inset) can be used which obviates the inner filter effect. Also, while the 90° geometry requires cuvettes with two neighbouring faces being clear (usually, fluorescence cuvettes have four clear faces), the front-face illumination technique requires only one clear face, as excitation and emission occur at the same face. However, front-face illumination is less sensitive than the 90° illumination.

12.3.3 Applications

There are many and highly varied applications for fluorescence despite the fact that relatively few compounds exhibit the phenomenon. The effects of pH, solvent composition and the polarisation of fluorescence may all contribute to structural elucidation. Measurement of fluorescence lifetimes can be used to assess rotation correlation coefficients and thus particle sizes. Non-fluorescent compounds are often labelled with fluorescent probes to enable monitoring of molecular events. This is termed **extrinsic fluorescence** as distinct from intrinsic fluorescence where the native compound exhibits the property. Some fluorescent dyes are sensitive to the presence of metal ions and can thus be used to track changes of these ions in *in vitro* samples, as well as whole cells.

Since fluorescence spectrometers have two monochromators, one for tuning the excitation wavelength and one for analysing the emission wavelength of the fluorophore, one can measure two types of spectra: excitation and emission spectra. For fluorescence **excitation spectrum** measurement, one sets the emission monochromator at a fixed wavelength (λ_{em}) and scans a range of excitation wavelengths which are then recorded as ordinate (*x*-coordinate) of the excitation spectrum; the fluorescence emission at λ_{em} is plotted as abscissa. Measurement of **emission spectra** is achieved by setting a fixed excitation wavelength (λ_{exc}) and scanning a wavelength range with the emission monochromator. To yield a spectrum, the emission wavelength λ_{em} is recorded as ordinate and the emission intensity at λ_{em} is plotted as abscissa.

Intrinsic protein fluorescence

Proteins possess three intrinsic fluorophores: tryptophan, tyrosine and phenylalanine, although the latter has a very low quantum yield and its contribution to protein fluorescence emission is thus negligible. Of the remaining two residues, tyrosine has the lower quantum yield and its fluorescence emission is almost entirely quenched when it becomes ionised, or is located near an amino or carboxyl group, or a tryptophan residue. Intrinsic protein fluorescence is thus usually determined by tryptophan fluorescence which can be selectively excited at 295–305 nm. Excitation at 280 nm excites tyrosine and tryptophan fluorescence and the resulting spectra might therefore contain contributions from both types of residues.

The main application for intrinsic protein fluorescence aims at conformational monitoring. We have already mentioned that the fluorescence properties of a fluorophore depend significantly on environmental factors, including solvent, pH, possible quenchers, neighbouring groups, etc.

A number of empirical rules can be applied to interpret protein fluorescence spectra:

- As a fluorophore moves into an environment with less polarity, its emission spectrum exhibits a hypsochromic shift (λ_{max} moves to shorter wavelengths) and the intensity at λ_{max} increases.
- Fluorophores in a polar environment show a decrease in quantum yield with increasing temperature. In a non-polar environment, there is little change.
- Tryptophan fluorescence is quenched by neighbouring protonated acidic groups.

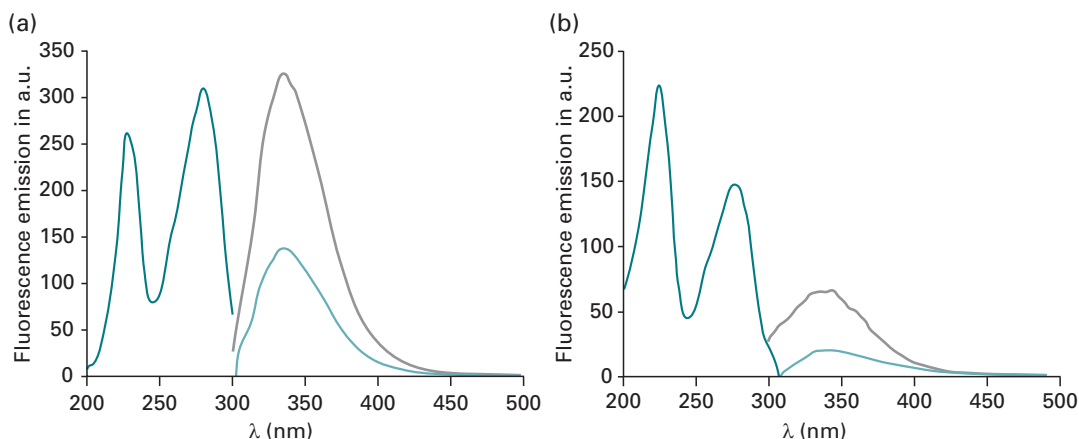


Fig. 12.10 Comparison of fluorescence excitation and emission spectra can yield insights into internal quenching. Excitation spectra with emission wavelength 340 nm are shown in dark green. Emission spectra with excitation wavelength 295 nm are shown in light green; emission spectra with excitation wavelength 280 nm are grey. (a) PDase homologue (*Escherichia coli*). (b) CPDase (*Arabidopsis thaliana*); in this protein, the fluorophores are located in close proximity to each other which leads to the effect of intrinsic quenching, as obvious from the lower intensity of the emission spectrum as compared to the excitation spectrum.

When interpreting effects observed in fluorescence experiments, one has to consider carefully all possible molecular events. For example, a compound added to a protein solution can cause quenching of tryptophan fluorescence. This could come about by binding of the compound at a site close to the tryptophan (i.e. the residue is surface-exposed to a certain degree), or due to a conformational change induced by the compound.

The comparison of protein fluorescence excitation and emission spectra can yield insights into the location of fluorophores. The close spatial arrangement of fluorophores within a protein can lead to quenching of fluorescence emission; this might be seen by the lower intensity of the emission spectrum when compared to the excitation spectrum (Fig. 12.10).

Extrinsic fluorescence

Frequently, molecules of interest for biochemical studies are non-fluorescent. In many of these cases, an external fluorophore can be introduced into the system by chemical coupling or non-covalent binding. Some examples of commonly used external fluorophores are shown in Fig. 12.11. Three criteria must be met by fluorophores in this context. Firstly, it must not affect the mechanistic properties of the system under investigation. Secondly, its fluorescence emission needs to be sensitive to environmental conditions in order to enable monitoring of the molecular events. And lastly, the fluorophore must be tightly bound at a unique location.

A common non-conjugating extrinsic chromophore for proteins is 1-anilino-8-naphthalene sulphonate (ANS) which emits only weak fluorescence in polar environment, i.e. in aqueous solution. However, in non-polar environment, e.g. when bound to hydrophobic patches on proteins, its fluorescence emission is significantly increased and the spectrum shows a hypsochromic shift; λ_{max} shifts from 475 nm to 450 nm. ANS

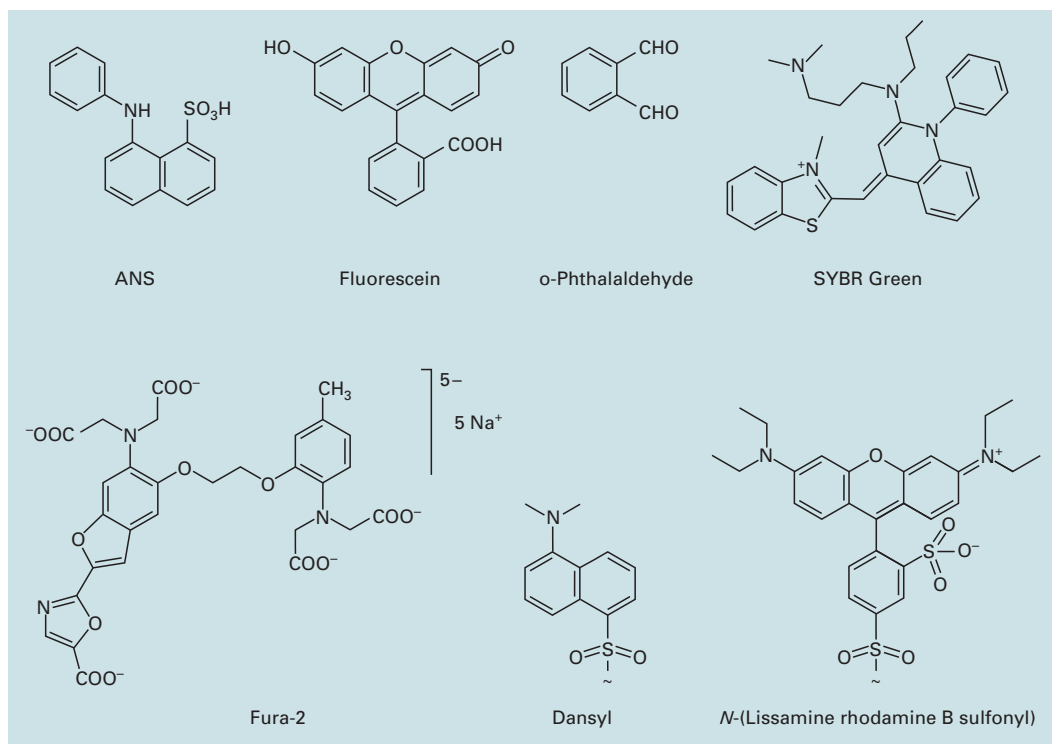


Fig. 12.11 Structures of some extrinsic fluorophores. Fura-2 is a fluorescent chelator for divalent and higher valent metal ions (Ca^{2+} , Ba^{2+} , Sr^{2+} , Pb^{2+} , La^{3+} , Mn^{2+} , Ni^{2+} , Cd^{2+}).

is thus a valuable tool for assessment of the degree of non-polarity. It can also be used in competition assays to monitor binding of ligands and prosthetic groups.

Reagents such as fluorescamine, *o*-phthalaldehyde or 6-aminoquinolyl-*N*-hydroxysuccinimidyl carbamate have been very popular conjugating agents used to derivatise amino acids for analysis (see Section 8.4.2). *o*-Phthalaldehyde, for example, is a non-fluorescent compound that reacts with primary amines and β -mercaptoethanol to yield a highly sensitive fluorophore.

Metal-chelating compounds with fluorescent properties are useful tools for a variety of assays, including monitoring of metal homeostasis in cells. Widely used probes for calcium are the chelators Fura-2, Indo-1 and Quin-1. Since the chemistry of such compounds is based on metal chelation, cross-reactivity of the probes with other metal ions is possible.

The intrinsic fluorescence of nucleic acids is very weak and the required excitation wavelengths are too far in the UV region to be useful for practical applications. Numerous extrinsic fluorescent probes spontaneously bind to DNA and display enhanced emission. While in earlier days ethidium bromide was one of the most widely used dyes for this application, it has nowadays been replaced by SYBR Green, as the latter probe poses fewer hazards for health and environment and has no teratogenic properties like ethidium bromide. These probes bind DNA by intercalation of the planar aromatic ring systems

between the base pairs of double-helical DNA. Their fluorescence emission in water is very weak and increases about 30-fold upon binding to DNA.

Quenching

In Section 12.3.1, we have seen that the quantum yield of a fluorophore is dependent on several internal and external factors. One of the external factors with practical implications is the presence of a **quencher**. A quencher molecule decreases the quantum yield of a fluorophore by non-radiating processes. The absorption (excitation) process of the fluorophore is not altered by the presence of a quencher. However, the energy of the excited state is transferred onto the quenching molecules. Two kinds of quenching processes can be distinguished:

- dynamic quenching which occurs by collision between the fluorophore in its excited state and the quencher; and
- static quenching whereby the quencher forms a complex with the fluorophore. The complex has a different electronic structure compared to the fluorophore alone and returns from the excited state to the ground state by non-radiating processes.

It follows intuitively that the efficacy of both processes is dependent on the concentration of quencher molecules. The mathematical treatment for each process is different, because of two different chemical mechanisms. Interestingly, in both cases the degree of quenching, expressed as $I_0 I^{-1}$, is directly proportional to the quencher concentration. For collisional (dynamic) quenching, the resulting equation has been named the **Stern–Volmer equation** (equation 12.4).

$$\frac{I_0}{I} - 1 = k_Q c_Q \tau_0 \quad (12.4)$$

$$\frac{I_0}{I} - 1 = K_a c_Q \quad (12.5)$$

The Stern–Volmer equation relates the degree of quenching (expressed as $I_0 I^{-1}$) to the molar concentration of the quencher c_Q , the lifetime of the fluorophore τ_0 , and the rate constant of the quenching process k_Q . In case of static quenching (equation 12.5), $I_0 I^{-1}$ is related to the equilibrium constant K_a that describes the formation of the complex between the excited fluorophore and the quencher, and the concentration of the quencher. Importantly, a plot of $I_0 I^{-1}$ versus c_Q yields for both quenching processes a linear graph with a y-intercept of 1.

Thus, fluorescence data obtained by intensity measurements alone cannot distinguish between static or collisional quenching. The measurement of fluorescence lifetimes or the temperature/viscosity dependence of quenching can be used to determine the kind of quenching process. It should be added, that both processes can also occur simultaneously in the same system.

The fact that static quenching is due to complex formation between the fluorophore and the quencher makes this phenomenon an attractive assay for binding of a ligand to a protein. In the simplest case, the fluorescence emission being monitored is the

intrinsic fluorescence of the protein. While this is a very convenient titration assay when validated for an individual protein–ligand system, one has to be careful when testing unknown pairs, because the same decrease in intensity can occur by collisional quenching.

Highly effective quenchers for fluorescence emission are oxygen, as well as the iodide ion. Usage of these quenchers allows surface mapping of biological macromolecules. For instance, iodide can be used to determine whether tryptophan residues are exposed to solvent.

Fluorescence resonance energy transfer (FRET)

Fluorescence resonance energy transfer (FRET) was first described by Förster in 1948. The process can be explained in terms of quantum mechanics by a non-radiative energy transfer from a donor to an acceptor chromophore. The requirements for this process are a reasonable overlap of emission and excitation spectra of donor and acceptor chromophores, close spatial vicinity of both chromophores (10–100 Å), and an almost parallel arrangement of their transition dipoles. Of great practical importance is the correlation

$$\text{FRET} \propto \frac{1}{R_0^6} \quad (12.6)$$

showing that the FRET effect is inversely proportional to the distance between donor and acceptor chromophores, R_0 .

The FRET effect is particularly suitable for biological applications, since distances of 10–100 Å are in the order of the dimensions of biological macromolecules. Furthermore, the relation between FRET and the distance allows for measurement of molecular distances and makes this application a kind of ‘spectroscopic ruler’. If a process exhibits changes in molecular distances, FRET can also be used to monitor the molecular mechanisms.

The high specificity of the FRET signal allows for monitoring of molecular interactions and conformational changes with high spatial (1–10 nm) and temporal resolution (<1 ns). Especially the possibility of localising and monitoring cellular structures and proteins in physiological environments makes this method very attractive. The effects can be observed even at low concentrations (as low as single molecules), in different environments (different solvents, including living cells), and observations may be done in real time.

In most cases, different chromophores are used as donor and acceptor, presenting two possibilities to record FRET: either as donor-stimulated fluorescence emission of the acceptor or as fluorescence quenching of the donor by the acceptor. However, the same chromophore may be used as donor and acceptor simultaneously; in this case, the depolarisation of fluorescence is the observed parameter. Since non-FRET stimulated fluorescence emission by the acceptor can result in undesirable background fluorescence, a common approach is usage of non-fluorescent acceptor chromophores.

FRET-based assays may be used to elucidate the effects of new substrates for different enzymes or putative agonists in a quick and quantitative manner. Furthermore, FRET detection might be used in high-throughput screenings (see Sections 17.3.2 and 18.2.3), which makes it very attractive for drug development.

Example 3 FRET APPLICATIONS IN DNA SEQUENCING AND INVESTIGATION OF MOLECULAR MECHANISMS

BigDyes™ are a widely used application of FRET fluorophores (Fig. 12.12). Since 1997, these fluorophores are generally used as chain termination markers in automated DNA sequencing. As such, BigDyes™ are in major parts responsible for the great success of genome projects.

In many instances, FRET allows monitoring of conformational changes, protein folding, as well as protein–protein, protein–membrane and protein–DNA interactions. For instance, the three subunits of T4 DNA polymerase holoenzyme arrange around DNA in torus-like geometry. Using the tryptophan residue in one of the subunits as FRET donor and a coumarine label conjugated to a cysteine residue in the adjacent subunit (FRET acceptor), the distance change between both subunits could be monitored and seven steps involved in opening and closing of the polymerase could be identified. Other examples of this approach include studies of the architecture of *Escherichia coli* RNA polymerase, the calcium-dependent change of troponin and structural studies of neuropeptide Y dimers.

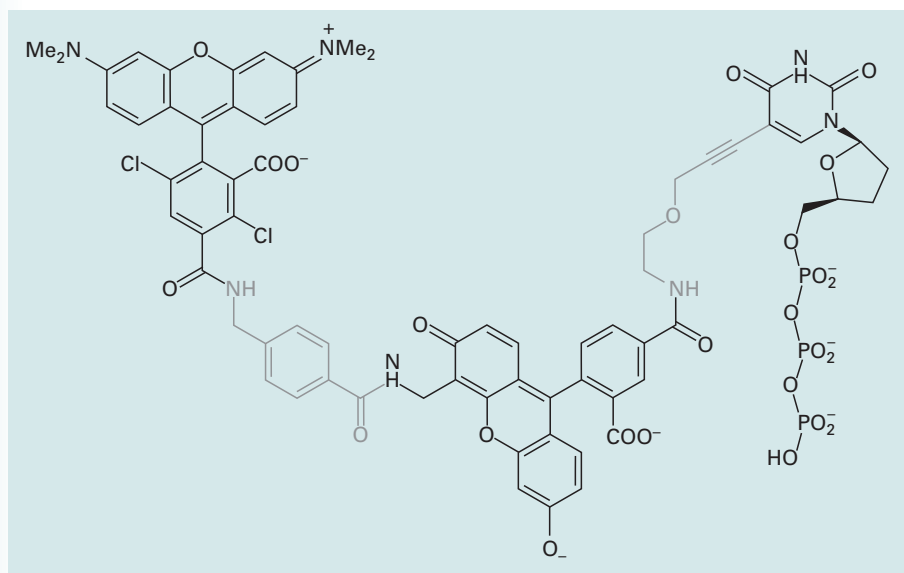


Fig. 12.12 Structure of one of the four BigDye™ terminators, ddT-E0-6CFB-dTMR. The moieties from left to right are: 5-carboxy-dichloro-rhodamine (FRET acceptor), 4-aminomethyl benzoate linker, 6-carboxy-4'-aminomethylfluorescein (FRET donor), propargyl ethoxyamino linker, dUTP.

Bioluminescence Resonance Energy Transfer (BRET)

Bioluminescence resonance energy transfer (BRET) uses the FRET effect with native fluorescent or luminescent proteins as chromophores. The phenomenon is observed naturally for example with the sea pansy *Renilla reniformis*. It contains the enzyme

luciferase, which oxidises luciferin (coelenterazin) by simultaneously emitting light at $\lambda_{\text{exc}} = 480$ nm. This light directly excites green fluorescent protein (GFP), which, in turn, emits fluorescence at $\lambda_{\text{em}} = 509$ nm.

Fluorescence labelling of proteins by other proteins presents a useful approach to study various processes *in vivo*. Labelling can be done at the genetic level by generating fusion proteins. Monitoring of protein expression by GFP is an established technique and further development of 'living colours' will lead to promising new tools.

While nucleic acids have been the main players in the genomic era, the postgenomic/proteomic era focusses on gene products, the proteins. New proteins are being discovered and characterised, others are already used within biotechnological processes. In particular for classification and evaluation of enzymes and receptors, reaction systems can be designed such that the reaction of interest is detectable quantitatively using FRET donor and acceptor pairs.

For instance, detection methods for protease activity can be developed based on BRET applications. A protease substrate is fused to a GFP variant on the N-terminal side and dsRED on the C-terminal side. The latter protein is a red fluorescing FRET acceptor and the GFP variant acts as a FRET donor. Once the substrate is cleaved by a protease, the FRET effect is abolished. This is used to directly monitor protease activity. With a combination of FRET analysis and two-photon excitation spectroscopy it is also possible to carry out a kinetic analysis.

A similar idea is used to label human insulin receptor (see Section 17.4.4) in order to quantitatively assess its activity. Insulin receptor is a glycoprotein with two α and two β subunits, which are linked by dithioether bridges. The binding of insulin induces a conformational change and causes a close spatial arrangement of both β subunits. This, in turn, activates tyrosine kinase activity of the receptor.

In pathological conditions such as diabetes, the tyrosine kinase activity is different than in healthy conditions. Evidently, it is of great interest to find compounds that stimulate the same activity as insulin. By fusing the β subunit of human insulin receptor to *Renilla reniformis* luciferase and yellow fluorescent protein (YFP) a FRET donor-acceptor pair is obtained, which reports the ligand-induced conformational change and precedes the signal transduction step. This reporter system is able to detect the effects of insulin and insulin-mimicking ligands in order to assess dose-dependent behaviour.

Fluorescence recovery after photo bleaching (FRAP)

If a fluorophore is exposed to high intensity radiation it may be irreversibly damaged and lose its ability to emit fluorescence. Intentional bleaching of a fraction of fluorescently labelled molecules in a membrane can be used to monitor the motion of labeled molecules in certain (two-dimensional) compartments. Moreover, the time-dependent monitoring allows determination of the diffusion coefficient. A well-established application is the usage of phospholipids labelled with NBD (e.g. NBD-phosphatidylethanolamine, Fig. 12.13b) which are incorporated into a biological or artificial membrane. The specimen is subjected to a pulse of high-intensity light (photo bleaching), which causes a sharp drop of fluorescence in the observation area (Fig. 12.13). Re-emergence of fluorescence emission in this area is monitored as unbleached molecules diffused into the observation area. From the time-dependent increase of fluorescence emission, the rate of diffusion of the

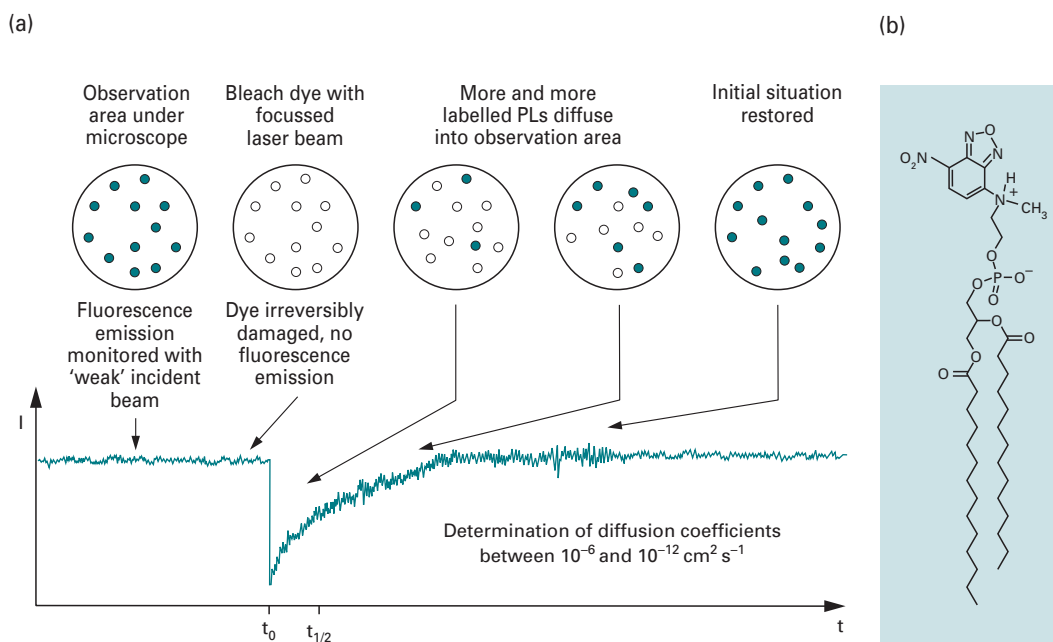


Fig. 12.13 (a) Schematic of a FRAP experiment. Time-based monitoring of fluorescence emission intensity enables determination of diffusion coefficients in membranes. (b) A commonly used fluorescence label in membrane FRAP experiments: chemical structure of phosphatidylethanolamine conjugated to the fluorophore NBD.

phospholipid molecules can be calculated. Similarly, membrane proteins such as receptors or even proteins in a cell can be conjugated to fluorescence labels and their diffusion coefficients can be determined.

Fluorescence polarisation

A light source usually consists of a collection of randomly oriented emitters, and the emitted light is a collection of waves with all possible orientations of the E vectors (non-polarised light). Linearly polarised light is obtained by passing light through a polariser that transmits light with only a single plane of **polarisation**; i.e. it passes only those components of the E vector that are parallel to the axis of the polariser (Fig. 12.14). The intensity of transmitted light depends on the orientation of the polariser. Maximum transmission is achieved when the plane of polarisation is parallel to the axis of the polariser; the transmission is zero when the orientation is perpendicular. The polarisation P is defined as

$$P = \frac{I_{\uparrow} - I_{\leftrightarrow}}{I_{\uparrow} + I_{\leftrightarrow}} \quad (12.7)$$

I_{\uparrow} and I_{\leftrightarrow} are the intensities observed parallel and perpendicular to an arbitrary axis. The polarisation can vary between -1 and $+1$; it is zero when the light is unpolarised. Light with $0 < |P| < 0.5$ is called partially polarised.

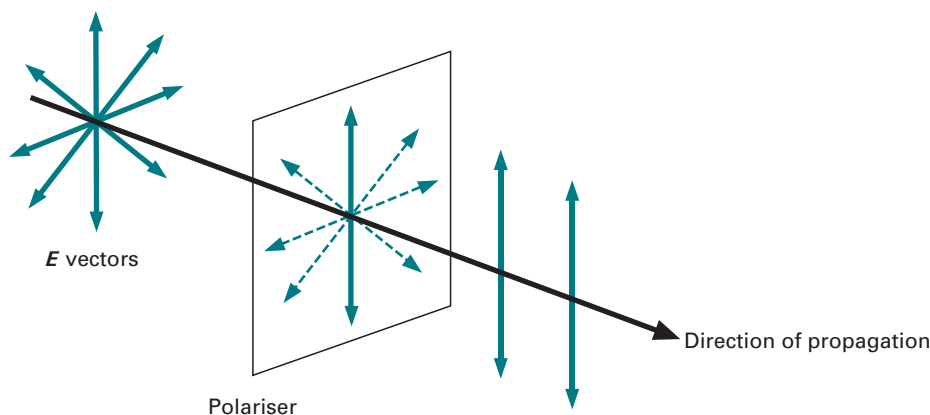


Fig. 12.14 Generation of linearly polarised light.

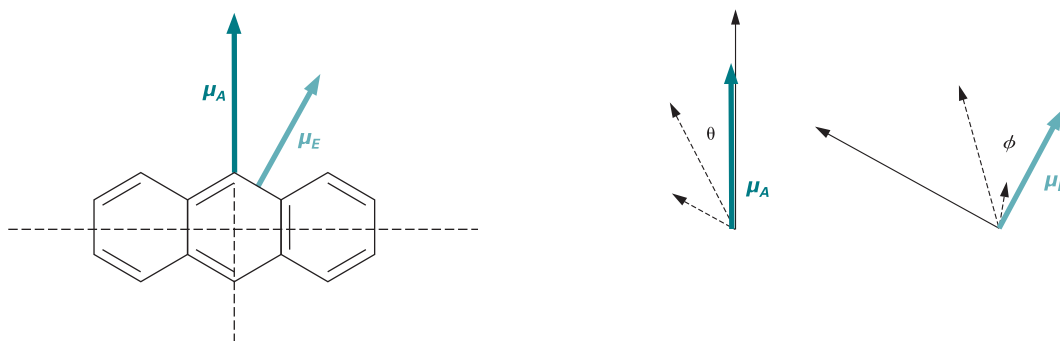


Fig. 12.15 Absorption dipole moment μ_A (describing the probability of photon absorption) and transition dipole moment μ_E (describing the probability for photon emission) for any chromophore are usually not parallel. Absorption of linearly polarised light varies with $\cos^2\theta$ and is at its maximum parallel to μ_A . Emission of linearly polarised light varies with $\sin^2\phi$ and is highest at a perpendicular orientation to μ_E .

Experimentally, this can be achieved in a fluorescence spectrometer by placing a polariser in the excitation path in order to excite the sample with polarised light. A second polariser is placed between the sample and the detector with its axis either parallel or perpendicular to the axis of the excitation polariser. The emitted light is either partially polarised or entirely unpolarised. This loss of polarisation is called **fluorescence depolarisation**.

Absorption of polarised light by a chromophore is highest when the plane of polarisation is parallel to the **absorption dipole moment** μ_A (Fig. 12.15). More generally, the probability of absorption of exciting polarised light by a chromophore is proportional to $\cos^2\theta$, with θ being the angle between the direction of polarisation and the absorption dipole moment. Fluorescence emission, in contrast, does not depend on the absorption dipole moment, but on the **transition dipole moment** μ_E . Usually, μ_A and μ_E are tilted against each other by about 10° to 40° . The probability of emission of polarised light at

an angle ϕ with respect to the transition dipole moment is proportional to $\sin^2 \phi$, and thus at its maximum in a perpendicular orientation.

As a result if the chromophores are randomly oriented in solution, the polarisation P is less than 0.5. It is thus evident that any process that leads to a deviation from random orientation will give rise to a change of polarisation. This is certainly the case when a chromophore becomes more static. Furthermore, one needs to consider Brownian motion. If the chromophore is a small molecule in solution, it will be rotating very rapidly. Any change in this motion due to temperature changes, changes in viscosity of the solvent, or binding to a larger molecule, will therefore result in a change of polarisation.

Fluorescence cross-correlation spectroscopy

With **fluorescence cross-correlation spectroscopy** the temporal fluorescence fluctuations between two differently labelled molecules can be measured as they diffuse through a small sample volume. Cross-correlation analysis of the fluorescence signals from separate detection channels extracts information of the dynamics of the dual-labelled molecules. Fluorescence cross-correlation spectroscopy has thus become an essential tool for the characterisation of diffusion coefficients, binding constants, kinetic rates of binding and determining molecular interactions in solutions and cells (see also Section 17.3.2).

Fluorescence microscopy, high-throughput assays

Fluorescence emission as a means of monitoring is a valuable tool for many biological and biochemical applications. We have already seen the usage of fluorescence monitoring in DNA sequencing; the technique is inseparably tied in with the success of projects such as genome deciphering.

Fluorescence techniques are also indispensable methods for cell biological applications with fluorescence microscopy (see Sections 4.6 and 17.3.2). Proteins (or biological macromolecules) of interest can be tagged with a fluorescent label such as e.g. the green fluorescent protein (GFP) from the jelly fish *Aequorea victoria* or the red fluorescent protein from *Discosoma striata*, if spatial and temporal tracking of the tagged protein is desired. Alternatively, the use of GFP spectral variants such as cyan fluorescent protein (CFP) as a fluorescence donor and yellow fluorescent protein (YFP) as an acceptor allows investigation of mechanistic questions by using the FRET phenomenon. Specimens with cells expressing the labelled proteins are illuminated with light of the excitation wavelength, and then observed through a filter that excludes the exciting light and only transmits the fluorescence emission. The recorded fluorescence emission can be overlaid with a visual image computationally, and the composite image then allows for localisation of the labelled species. If different fluorescence labels with distinct emission wavelengths are used simultaneously, even co-localisation studies can be performed.

Time-resolved fluorescence spectroscopy

The emission of a single photon from a fluorophore follows a probability distribution. With time-correlated single photon counting, the number of emitted photons can be recorded in a time-dependent manner following a pulsed excitation of the sample.

By sampling the photon emission for a large number of excitations, the probability distribution can be constructed. The time-dependent decay of an individual fluorophore species follows an exponential distribution, and the time constant is thus termed the lifetime of this fluorophore. Curve fitting of fluorescence decays enables the identification of the number of species of fluorophores (within certain limits), and the calculation of the lifetimes for these species. In this context, different species can be different fluorophores or distinct conformations of the same fluorophore.

12.4 LUMINOmetry

In the preceding section, we mentioned the method of bioluminescence resonance energy transfer (BRET) and its main workhorse, luciferase. Generally, fluorescence phenomena depend on the input of energy in the form of electromagnetic radiation. However, emission of electromagnetic radiation from a system can also be achieved by prior excitation in the course of a chemical or enzymatic reaction. Such processes are summarised as **luminescence**. Luminometry is not strictly speaking a spectrophotometric technique, but is included here due to its importance in the life sciences.

12.4.1 Principles

Luminometry is the technique used to measure luminescence, which is the emission of electromagnetic radiation in the energy range of visible light as a result of a reaction. **Chemiluminescence** arises from the relaxation of excited electrons transitioning back to the ground state. The prior excitation occurs through a chemical reaction that yields a fluorescent product. For instance, the reaction of luminol with oxygen produces 3-aminophthalate which possesses a fluorescence spectrum that is then observed as a chemiluminescence. In other words, the chemiluminescence spectrum is the same as the fluorescence spectrum of the product of the chemical reaction.

Bioluminescence describes the same phenomenon, only the reaction leading to a fluorescent product is an enzymatic reaction. The most commonly used enzyme in this context is certainly luciferase (see Section 15.3.2). The light is emitted by an intermediate complex of luciferase with the substrate ('photoprotein'). The colour of the light emitted depends on the source of the enzyme and varies between 560 nm (greenish yellow) and 620 nm (red) wavelengths. Bioluminescence is a highly sensitive method, due to the high quantum yield of the underlying reaction. Some luciferase systems work with almost 100% efficiency. For comparison, the incandescent light bulb loses about 90% of the input energy to heat.

Because luminescence does not depend on any optical excitation, problems with autofluorescence in assays are eliminated.

12.4.2 Instrumentation

Since no electromagnetic radiation is required as a source of energy for excitation, no light source and monochromator are required. Luminometry can be performed with a

rather simple set-up, where a reaction is started in a cuvette or mixing chamber, and the resulting light is detected by a photometer. In most cases, a photomultiplier tube is needed to amplify the output signal prior to recording. Also, it is fairly important to maintain a strict temperature control, as all chemical, and especially enzymatic, reactions are sensitive to temperature.

12.4.3 Applications

Chemiluminescence

Luminol and its derivatives can undergo chemiluminescent reactions with high efficiency. For instance, enzymatically generated H_2O_2 may be detected by the emission of light at 430 nm wavelength in the presence of luminol and microperoxidase (see Section 15.3.2).

Competitive binding assays (see Section 15.2) may be used to determine low concentrations of hormones, drugs and metabolites in biological fluids. These assays depend on the ability of proteins such as antibodies and cell receptors to bind specific ligands with high affinity. Competition between labelled and unlabelled ligand for appropriate sites on the protein occurs. If the concentration of the protein, i.e. the number of available binding sites, is known, and a limited but known concentration of labelled ligand is introduced, the concentration of unlabelled ligand can be determined under saturation conditions when all sites are occupied. Exclusive use of labelled ligand allows the determination of the concentration of the protein and thus the number of available binding sites.

During the process of phagocytosis by leukocytes, molecular oxygen is produced in its singlet state (see Section 12.1.2) which exhibits chemiluminescence. The effects of pharmacological and toxicological agents on leukocytes and other phagocytic cells can be studied by monitoring this luminescence.

Bioluminescence

Firefly luciferase is mainly used to measure ATP concentrations. The bioluminescence assay is rapidly carried out with accuracies comparable to spectrophotometric and fluorimetric assays. However, with a detection limit of 10^{-15} M, and a linear range of 10^{-12} to 10^{-6} M ATP, the luciferase assay is vastly superior in terms of sensitivity. Generally, all enzymes and metabolites involved in ATP interconversion reactions may be assayed in this method, including ADP, AMP, cyclic AMP and the enzymes pyruvate kinase, adenylate kinase, phosphodiesterase, creatine kinase, hexokinase and ATP sulphurase (see Section 15.3.2). Other substrates include creatine phosphate, glucose, GTP, phosphoenolpyruvate and 1,3-diphosphoglycerate.

The main application of bacterial luciferase is the determination of electron transfer co-factors, such as nicotine adenine dinucleotides (and phosphates) and flavin mononucleotides in their reduced states, for example NADH, NADPH and FMNH₂. Similar to the firefly luciferase assays, this method can be applied to a whole range of coupled RedOx enzyme reaction systems. The enzymatic assays are again much more sensitive

Example 4 ENZYMATIC CALCIUM MONITORING

Question Calcium signalling is a common mechanism, since the ion, once it enters the cytoplasm, exerts allosteric regulatory effects on many enzymes and proteins. How can intracellular calcium be monitored?

Answer The EF-hand protein aequorin from *Aequorea* species (jellyfish) has been used for determination of intracellular calcium concentrations. Despite the availability of calcium-specific electrodes, this bioluminescence assay presents advantages due to its high sensitivity to and specificity for calcium. Since the protein is non-toxic, has a low leakage rate from cells and is not intracellularly compartmentalised, it is ideally suited for usage in living cells. Its disadvantages are the scarcity, large molecular size, consumption during the reaction and the non-linearity of the light emission relative to calcium concentration. The reaction is further sensitive to the chemical environment and the limited speed in which it can respond to rapid changes in calcium concentration, for example influx and efflux in certain cell types. The protein possesses a reflective yellow colour and is non-fluorescent in its apo- (non-calcium-bound) state. In the calcium-bound form, the prosthetic group coelenterazine, a molecule belonging to the luciferin family, is oxidised to coelenteramide and CO_2 . Upon relaxation to the ground state, blue light of 469 nm wavelength is emitted.

than the corresponding spectrophotometric and fluorimetric assays, and a concentration range of 10^{-9} to 10^{-12} M can be achieved. The NADPH assay is by a factor of 20 less sensitive than the NADH assay.

12.5 CIRCULAR DICHROISM SPECTROSCOPY**12.5.1 Principles**

In Section 12.3.3 we have already seen that electromagnetic radiation oscillates in all possible directions and that it is possible to preferentially select waves oscillating in a single plane, as applied for fluorescence polarisation. The phenomenon first known as **mutarotation** (described by Lowry in 1898) became manifest in due course as a special property of **optically active** isomers allowing the rotation of plane-polarised light. Optically active isomers are compounds of identical chemical composition and topology, but whose mirror images cannot be superimposed; such compounds are called **chiral**.

Linearly and circularly polarised light

Light is electromagnetic radiation where the electric vector (E) and the magnetic vector (M) are perpendicular to each other. Each vector undergoes an oscillation as the light

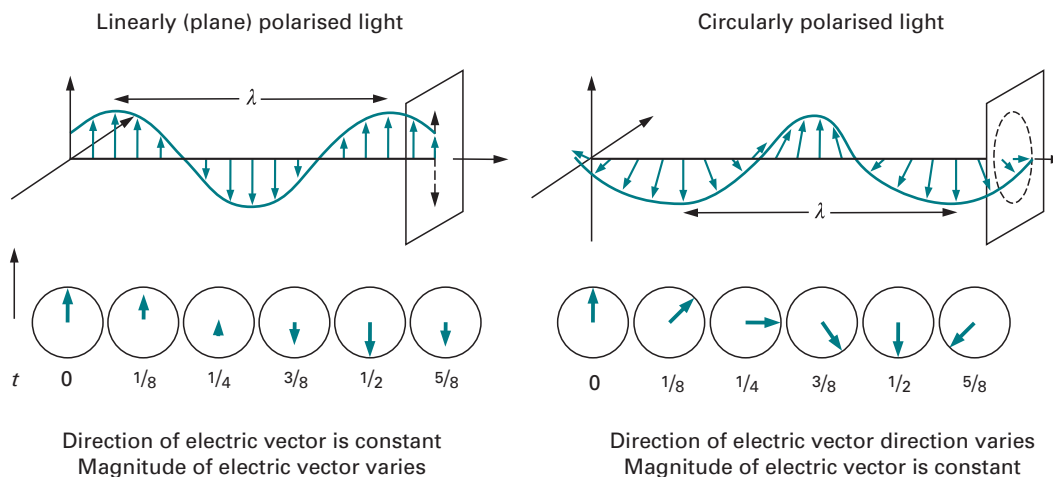


Fig. 12.16 Linearly (plane) and circularly polarised light.

travels along the direction of propagation, resulting in a sine-like waveform of each, the E and the M vectors. A light source usually consists of a collection of randomly oriented emitters. Therefore, the emitted light is a collection of waves with all possible orientations of the E vectors. This light is non-polarised. Linearly or plane-polarised light is obtained by passing light through a polariser that transmits light with only a single plane of polarisation, i.e. it passes only those components of the E vector that are parallel to the axis of the polariser (Fig. 12.14). If the E vectors of two electromagnetic waves are $1/4$ wavelength out of phase and perpendicular to each other, the vector that is the sum of the E vectors of the two components rotates around the direction of propagation so that its tip follows a helical path. Such light is called **circularly polarised** (Fig. 12.16).

While the E vector of circularly polarised light always has the same magnitude but a varying direction, the direction of the E vector of linearly polarised light is constant; it is its magnitude that varies. With the help of vector algebra, one can now reversely think of linearly polarised light as a composite of two circularly polarised beams with opposite handedness (Fig. 12.17a).

Polarimetry and optical rotation dispersion

Polarimetry essentially measures the angle through which the plane of polarisation is changed after linearly polarised light is passed through a solution containing a chiral substance. **Optical rotation dispersion** (ORD) spectroscopy is a technique that measures this ability of a chiral substance to change the plane-polarisation as a function of the wavelength. The angle α_λ between the plane of the resulting linearly polarised light against that of the incident light is dependent on the refractive index for left (n_{left}) and right (n_{right}) circularly polarised light. The refractive index can be calculated as the ratio of the speed of light *in vacuo* and the speed of light in matter. After normalisation against the amount of substance present in the sample (thickness of sample/cuvette length d , and mass concentration ρ^*), a substance-specific constant $[\alpha]_\lambda$ is obtained that can be used to characterise chiral compounds.

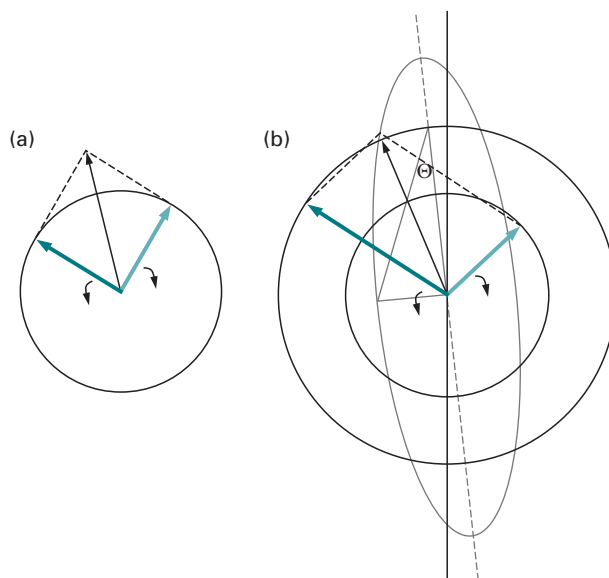


Fig. 12.17 (a) Linearly polarised light can be thought of consisting of two circularly polarised components with opposite 'handedness'. The vector sum of the left- and right-handed circularly polarised light yields linearly polarised light. (b) If the amplitudes of left- and right-handed polarised components differ, the resulting light is elliptically polarised. The composite vector will trace the ellipse shown in grey. The ellipse is characterised by a major and a minor axis. The ratio of minor and major axis yields $\tan \Theta$. Θ is the ellipticity.

Circular dichroism

In addition to changing the plane of polarisation, an optically active sample also shows unusual absorption behaviour. Left- and right-handed polarised components of the incident light are absorbed differently by the sample, which yields a difference in the absorption coefficients $\Delta\varepsilon = \varepsilon_{\text{left}} - \varepsilon_{\text{right}}$. This latter difference is called **circular dichroism** (CD). The difference in absorption coefficients $\Delta\varepsilon$ (i.e. CD) is measured in units of $\text{cm}^2 \text{g}^{-1}$, and is the observed quantity in CD experiments. Historically, results from CD experiments are reported as ellipticity Θ_λ . Normalisation of Θ_λ similar to the ORD yields the molar ellipticity:

$$\theta_\lambda = \frac{M \times \Theta_\lambda}{10 \times \rho^* \times d} = \frac{\ln 10}{10} \times \frac{180^\circ}{2\pi} \times \Delta\varepsilon \quad (12.8)$$

It is common practice to display graphs of CD spectra with the molar ellipticity in units of $1^\circ \text{cm}^2 \text{dmol}^{-1} = 10^\circ \text{cm}^2 \text{mol}^{-1}$ on the ordinate axis (Fig. 12.18).

Three important conclusions can be drawn:

- ORD and CD are the manifestation of the same underlying phenomenon;
- if an optically active molecule has a positive CD, then its enantiomer will have a negative CD of exactly the same magnitude; and
- the phenomenon of CD can only be observed at wavelengths where the optically active molecule has an absorption band.

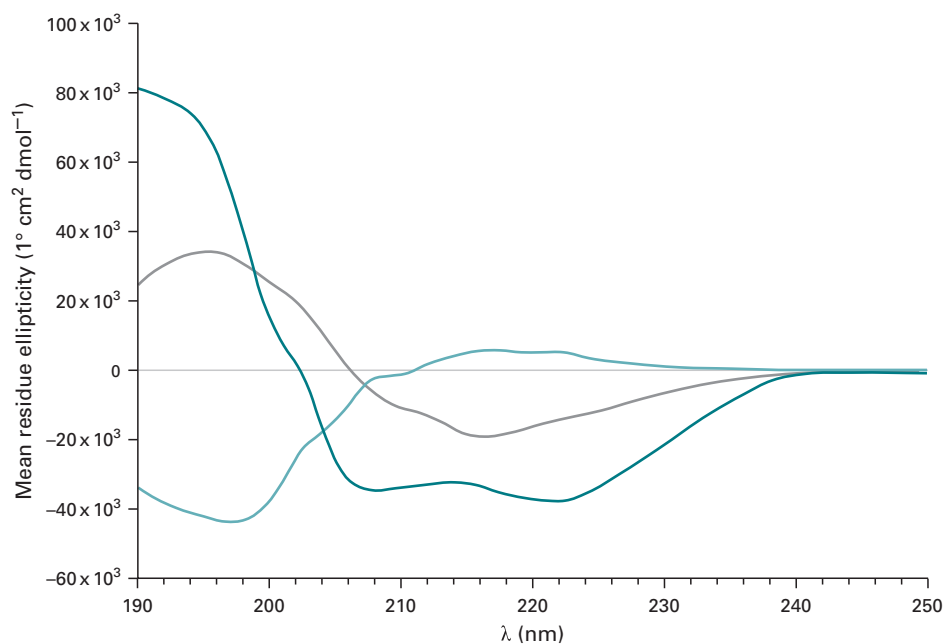


Fig. 12.18 Circular dichroism spectra for three standard secondary structures according to Fasman. An α -helical peptide is shown in dark green, a peptide adopting β -strand structure in grey, and a random coil peptide in light green.

The chromophores of protein secondary structure

In Section 12.2, we saw that the peptide bond in proteins possesses UV absorption bands in the area of 220–190 nm. The carbon atom vicinal to the peptide bond (the C_α atom) is asymmetric and a chiral centre in all amino acids except glycine. This chirality induces asymmetry into the peptide bond chromophore. Because of the serial arrangement of the peptide bonds making up the backbone of a protein, the individual chromophores couple with each other. The (secondary) structure of a polypeptide thus induces an ‘overall chirality’ which gives rise to the CD phenomenon of a protein in the wavelength interval 260–190 nm.

With protein circular dichroism, the molar ellipticity θ also appears as **mean residue ellipticity** θ_{res} , owing to the fact that the chromophores responsible for the chiral absorption phenomenon are the peptide bonds. Therefore, the number of chromophores of a polypeptide in this context is equal to the number of residues. Because of the law of Beer–Lambert (Equation 12.2), the number of chromophores is proportional to the magnitude of absorption, i.e. in order to normalise the spectrum of an individual polypeptide for reasons of comparison, the CD has to be scaled by the number of peptide bonds.

12.5.2 Instrumentation

The basic layout of a CD spectrometer follows that of a single-beam UV absorption spectrometer. Owing to the nature of the measured effects, an electro-optic modulator, as well as a more sophisticated detector are needed, though.

Generally, left and right circularly polarised light passes through the sample in an alternating fashion. This is achieved by an electro-optic modulator which is a crystal that transmits either the left- or right-handed polarised component of linearly polarised light, depending on the polarity of the electric field that is applied by alternating currents. The photomultiplier detector produces a voltage proportional to the ellipticity of the resultant beam emerging from the sample. The light source of the spectrometer is continuously flushed with nitrogen to avoid the formation of ozone and help to maintain the lamp.

CD spectrometry involves measuring a very small difference between two absorption values which are large signals. The technique is thus very susceptible to noise and measurements must be carried out carefully. Some practical considerations involve having a clean quartz cuvette, and using buffers with low concentrations of additives. While this is sometimes tricky with protein samples, reducing the salt concentrations to values as low as 5 mM helps to obtain good spectra. Also, filtered solutions should be used to avoid any turbidity of the sample that could produce scatter. Saturation of the detector must be avoided, this becoming more critical with lower wavelengths. Therefore, good spectra are obtained in a certain range of protein concentrations only where enough sample is present to produce a good signal and does not saturate the detector. Typical protein concentrations are $0.03\text{--}0.3\text{ mg cm}^{-3}$.

In order to calculate specific ellipticities (mean residue ellipticities) and be able to compare the CD spectra of different samples with each other, the concentration of the sample must be known. Provided the protein possesses sufficient amounts of UV/Vis-absorbing chromophores, it is thus advisable to subject the CD sample to a protein concentration determination by UV/Vis as described in Section 12.2.3.

12.5.3 Applications

The main application for protein CD spectroscopy is the verification of the adopted secondary structure. The application of CD to determine the tertiary structure is limited, owing to the inadequate theoretical understanding of the effects of different parts of the molecules at this level of structure.

Rather than analysing the secondary structure of a 'static sample', different conditions can be tested. For instance, some peptides adopt different secondary structures when in solution or membrane-bound. The comparison of CD spectra of such peptides in the absence and presence of small unilamellar phospholipid vesicles shows a clear difference in the type of secondary structure. Measurements with lipid vesicles are tricky, because due to their physical extensions they give rise to scatter. Other options in this context include CD experiments at lipid monolayers which can be realised at synchrotron beam lines, or by usage of optically clear vesicles (reverse micelles).

CD spectroscopy can also be used to monitor changes of secondary structure within a sample over time. Frequently, CD instruments are equipped with temperature control units and the sample can be heated in a controlled fashion. As the protein undergoes its transition from the folded to the unfolded state, the CD at a certain wavelength (usually 222 nm) is monitored and plotted against the temperature, thus yielding a thermal denaturation curve which can be used for stability analysis.

Example 5 DETERMINATION OF THE SECONDARY STRUCTURE CONTENT OF A PROTEIN SAMPLE

Question You have purified a recombinant protein and wonder whether it adopts a folded structure. How might you address this problem?

Answer CD spectra of poly-L-amino acids as well as proteins with known three-dimensional structure have been obtained and are used as standards for deducing the secondary structure composition of unknown proteins. The simplest approach is a visual comparison of the shape of the CD spectrum with the three 'Fasman standard spectra' (Fig. 12.18), allowing conclusions as to α helix, β strand and random coil structure. CD deconvolution is a curve-fitting process where the experimental CD spectrum is fitted with a given set of basis spectra using a weighting scheme. The estimated weighting coefficients determined in the fitting process reveal the percentage of each form of secondary structure in proteins. Different algorithms for deconvolution have been generated, ranging from a simple linear combination of three or five basis sets, to fitting procedures using 10–30 basis spectra and different mathematical algorithms (CONTIN fit, neural networks, etc.).

Further applications include the use of circular dichroism for an observable for kinetic measurements using the stopped flow technique (see Section 15.3).

12.6 LIGHT SCATTERING

The scattering of light can yield a number of valuable insights into the properties of macromolecules, including the molecular mass, dimensions and diffusion coefficients, as well as association/dissociation properties and internal dynamics. The incident light hitting a macromolecule is scattered into all directions with the intensity of the scatter being only about 10^{-5} of the original intensity. The scattered light is measured at angles higher than 0° and less than 180° . Most of the scattered light possesses the same wavelength as the incident light; this phenomenon is called **elastic light scattering**. When the scattered light has a wavelength higher or lower than the incident light, the phenomenon is called **inelastic light scattering**. The special properties of lasers (see Section 12.1.3) with high monochromaticity, narrow focus and strong intensity, make them ideally suited for light scattering applications.

12.6.1 Elastic (static) light scattering

Elastic light scattering is also known as **Rayleigh scattering** and involves measuring the intensity of light scattered by a solution at an angle relative to the incident laser beam. The scattering intensity of macromolecules is proportional to the squared

molecular mass, and thus ideal for determination of M , since the contribution of small solvent molecules can be neglected. In an ideal solution, the macromolecules are entirely independent from each other, and the light scattering can be described as:

$$\frac{I_\theta}{I_0} \sim R_\theta = P_\theta \times K \times c \times M \quad (12.9)$$

where I_θ is the intensity of the scattered light at angle θ , I_0 is the intensity of the incident light, K is a constant proportional to the squared refractive index increment, c is the concentration and R_θ the Rayleigh ratio. P_θ describes the angular dependence of the scattered light.

For non-ideal solutions, interactions between molecules need to be considered. The scattering intensity of real solutions has been calculated by Debye and takes into account concentration fluctuations. This results in an additional correction term comprising the **second virial coefficient** B which is a measure for the strength of interactions between molecules:

$$\frac{Kc}{R_\theta} = \frac{1}{P_\theta} \left(\frac{1}{M} + 2Bc \right) \quad (12.10)$$

Determination of molecular mass with multi-angle light scattering

In solution, there are only three methods for absolute determination of molecular mass: membrane osmometry, sedimentation equilibrium centrifugation and light scattering. These methods are absolute, because they do not require any reference to molecular mass standards. In order to determine the molecular mass from light scattering, three parameters must be measured: the intensity of scattered light at different angles, the concentration of the macromolecule and the specific refractive index increment of the solvent. As minimum instrumentation, this requires a light source, a **multi-angle light scattering** (MALS) detector, as well as a refractive index detector. These instruments can be used in batch mode, but can also be connected to an HPLC to enable online determination of the molecular mass of eluting macromolecules. The chromatography of choice is **size-exclusion chromatography** (SEC), also called gel filtration (see Section 11.7), and the combination of these methods is known as SEC-MALS. Unlike conventional size-exclusion chromatography, the molecular mass determination from MALS is independent of the elution volume of the macromolecule. This is a valuable advantage, since the retention time of a macromolecule on the size-exclusion column can depend on its shape and conformation.

12.6.2 Quasi-elastic (dynamic) light scattering – photon correlation spectroscopy

While intensity and angular distribution of scattered light yields information about molecular mass and dimension of macromolecules, the wavelength analysis of scattered light allows conclusions as to the transport properties of macromolecules. Due to rotation and translation, macromolecules move into and out of a very small region in the solution. This Brownian motion happens at a timescale of microseconds to

milliseconds, and the translation component of this motion is a direct result of diffusion, which leads to a broader wavelength distribution of the scattered light compared to the incident light. This analysis is the subject of dynamic light scattering, and yields the distribution of diffusion coefficients of macromolecules in solution.

The diffusion coefficient is related to the particle size by an equation known as the **Stokes–Einstein relation**. The parameter derived is the hydrodynamic radius, or **Stokes radius**, which is the size of a spherical particle that would have the same diffusion coefficient in a solution with the same viscosity. Most commonly, data from dynamic light scattering are presented as a distribution of hydrodynamic radius rather than wavelength of scattered light.

Notably, the hydrodynamic radius describes an idealised particle and can differ significantly from the true physical size of a macromolecule. This is certainly true for most proteins which are not strictly spherical and their hydrodynamic radius thus depends on their shape and conformation.

In contrast to size exclusion chromatography, dynamic light scattering measures the hydrodynamic radius directly and accurately, as the former method relies on comparison with standard molecules and several assumptions.

Applications of dynamic light scattering include determination of diffusion coefficients and assessment of protein aggregation, and can aid many areas *in praxi*. For instance, the development of ‘stealth’ drugs that can hide from the immune system or certain receptors relies on the PEGylation of molecules. Since conjugation with PEG (polyethylene glycol) increases the hydrodynamic size of the drug molecules dramatically, dynamic light scattering can be used for product control and as a measure of efficiency of the drug.

12.6.3 Inelastic light scattering – Raman spectroscopy

When the incident light beam hits a molecule in its ground state, there is a low probability that the molecule is excited and occupies the next higher vibrational state (Figs. 12.3, 12.8). The energy needed for the excitation is a defined increment which will be missing from the energy of the scattered light. The wavelength of the scattered light is thus increased by an amount associated with the difference between two vibrational states of the molecule (**Stokes shift**). Similarly, if the molecule is hit by the incident light in its excited state and transitions to the next lower vibrational state, the scattered light has higher energy than the incident light which results in a shift to lower wavelengths (**anti-Stokes shift**). These lines constitute the Raman spectrum. If the wavelength of the incident light is chosen such that it coincides with an absorption band of an electronic transition in the molecule, there is a significant increase in the intensity of bands in the Raman spectrum. This technique is called resonance Raman spectroscopy (see Section 13.2).

12.7 ATOMIC SPECTROSCOPY

So far, all methods have dealt with probing molecular properties. In Section 12.1.2, we discussed the general theory of electronic transitions and said that molecules give rise

to band spectra, but atoms yield clearly defined line spectra. In **atomic emission spectroscopy** (AES), these lines can be observed as light of a particular wavelength (colour). Conversely, black lines can be observed against a bright background in **atomic absorption spectroscopy** (AAS). The wavelengths emitted from excited atoms may be identified using a spectroscope with the human eye as the 'detector' or a spectrophotometer.

12.7.1 Principles

In a spectrum of an element, the absorption or emission wavelengths are associated with transitions that require a minimum of energy change. In order for energy changes to be minimal, transitions tend to occur between orbitals close together in energy terms. For example, excitation of a sodium atom and its subsequent relaxation gives rise to emission of orange light ('D-line') due to the transition of an electron from the 3s to the 3p orbital and return (Fig. 12.19).

Electron transitions in an atom are limited by the availability of empty orbitals. Filling orbitals with electrons is subject to two major rules:

- one orbital can be occupied with a maximum of two electrons; and
- the spins of electrons in one orbital need to be paired in an antiparallel fashion (**Pauli principle**).

Together, these limitations mean that emission and absorption lines are characteristic for an individual element.

12.7.2 Instrumentation

In general, atomic spectroscopy is not carried out in solution. In order for atoms to emit or absorb monochromatic radiation, they need to be volatilised by exposing them to high thermal energy. Usually, nebulisers are used to spray the sample solution into a flame or an oven. Alternatively, the gaseous form can be generated by using **inductively coupled plasma** (ICP). The variations in temperature and composition of a flame make standard conditions difficult to achieve. Most modern instruments thus use an ICP.

Atomic emission spectroscopy (AES) and atomic absorption spectroscopy (AAS) are generally used to identify specific elements present in the sample and to determine their concentrations. The energy absorbed or emitted is proportional to the number of atoms in the optical path. Strictly speaking, in the case of emission, it is the number of excited atoms that is proportional to the emitted energy. Concentration determination with AES or AAS is carried out by comparison with calibration standards.

Sodium gives high backgrounds and is usually measured first. Then, a similar amount of sodium is added to all other standards. Excess hydrochloric acid is commonly added, because chloride compounds are often the most volatile salts. Calcium and magnesium emission can be enhanced by the addition of alkali metals and suppressed by addition of phosphate, silicate and aluminate, as these form non-dissociable salts. The suppression effect can be relieved by the addition of lanthanum and strontium salts. Lithium is frequently used as an internal standard. For storage of

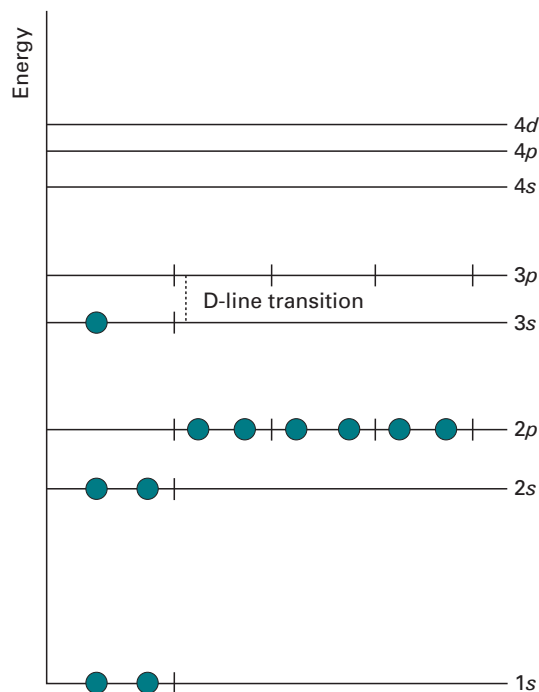


Fig. 12.19 Energy levels of atomic orbitals in the sodium atom. Each atomic orbital can be occupied by electrons following the rules of quantum chemistry until the total number of electrons for that element is reached (in case of sodium: 11 electrons). The energy gap between the 3s and the 3p orbitals in the sodium atom is such that it can be overcome by absorption of orange light.

samples and standards, polyethylene bottles are used, since glass can absorb and release metal ions, and thus impact the accuracy of this sensitive technique.

Cyclic analysis may be performed that involves the estimation of each interfering substance in a mixture. Subsequently, the standards for each component in the mixture are doped with each interfering substance. This process is repeated two or three times with refined estimates of interfering substance, until self-consistent values are obtained for each component.

Flame instability requires experimental protocols where determination of an unknown sample is bracketed by measurements of the appropriate standard, in order to achieve the highest possible accuracy.

Biological samples are usually converted to ash prior to determination of metals. Wet ashing in solution is often used, employing an oxidative digestion similar to the Kjeldahl method (see Section 8.3.2).

12.7.3 Applications

Atomic emission and atomic absorption spectrophotometry

Sodium and potassium are assayed at concentrations of a few p.p.m. using simple filter photometers. The modern emission spectrophotometers allow determination of about

20 elements in biological samples, the most common being calcium, magnesium and manganese. Absorption spectrophotometers are usually more sensitive than emission instruments and can detect less than 1 p.p.m. of each of the common elements with the exception of alkali metals. The relative precision is about 1% in a working range of 20–200 times the detection limit of an element.

AES and AAS have been widely used in analytical chemistry, such as environmental and clinical laboratories. Nowadays, the technique has been superseded largely by the use of ion-selective electrodes (see Section 16.2.2).

Atomic fluorescence spectrophotometry

Despite being limited to only a few metals, the main importance of **atomic fluorescence spectrophotometry** (AFS) lies in the extreme sensitivity. For example, zinc and cadmium can be detected at levels as low as 1–2 parts per 10^{10} .

AFS uses the same basic setup as AES and AAS. The atoms are required to be vaporised by one of three methods (flame, electric, ICP). The atoms are excited using electromagnetic radiation by directing a light beam into the vaporised sample. This beam must be intense, but not spectrally pure, since only the resonant wavelengths will be absorbed, leading to fluorescence (see Section 12.3.1).

12.8 SUGGESTIONS FOR FURTHER READING

General biophysics

Hoppe, W., Lohmann, W., Markl, H. and Ziegler, H. (1982). *Biophysik*, 2nd edn. Berlin: Springer-Verlag. (A rich and authoritative compendium of the physical basics of the life sciences.)

WEBSITES

<http://lectureonline.cl.msu.edu/%7Emmp/applist/Spectrum/s.htm>
<http://www.colorado.edu/physics/2000/lasers/index.html>

Ultraviolet and visible light spectroscopy

Simonian, M. H. and Smith, J. A. (2006). Spectrophotometric and colorimetric determination of protein concentration. *Current Protocols in Molecular Biology*, Chapter 10, Unit 10.1A. New York: Wiley Interscience

WEBSITES

<http://teaching.shu.ac.uk/hwb/chemistry/tutorials/molspec/uvvisab1.htm>
<http://www.cem.msu.edu/~reusch/VirtualText/Spectrpy/UV-Vis/spectrum.htm#uv1>
<http://www.srs.dl.ac.uk/VUV/>
<http://phys.educ.ksu.edu/vqm/html/absorption.html>

Fluorescence spectroscopy

Brown, M. P. and Royer, C. (1997). Fluorescence spectroscopy as a tool to investigate protein interactions. *Current Opinion in Biotechnology*, 8, 45–49.
 Groemping, Y. and Hellmann, N. (2005). Spectroscopic methods for the determination of protein interactions. *Current Protocols in Protein Science*, Chapter 20, Unit 20.8. New York: Wiley Interscience.
 Hwang, L. C. and Wohland, T. (2007). Recent advances in fluorescence cross-correlation spectroscopy. *Cell Biochemistry and Biophysics*, 49, 1–13.

- Lakowicz, J. R. (1999). *Principles of Fluorescence Spectroscopy* 2nd edn. New York: Kluwer/Plenum. (An authoritative textbook on fluorescence spectroscopy.)
- Langowski, J. (2008). Protein–protein interactions determined by fluorescence correlation spectroscopy. *Methods in Cell Biology*, **85**, 471–484.
- Prinz, A., Reither, G., Diskar, M. and Schultz, C. (2008). Fluorescence and bioluminescence procedures for functional proteomics. *Proteomics*, **8**, 1179–1196.
- Roy, R., Hohng, S. and Ha, T. (2008). A practical guide to single-molecule FRET. *Nature Methods*, **5**, 507–516.
- VanEngelenburg, S. B. and Palmer, A. E. (2008). Fluorescent biosensors of protein function. *Current Opinion in Chemical Biology*, **12**, 60–65.

WEBSITES

- <http://www.invitrogen.com/site/us/en/home/support/Tutorials.html>
- <http://www.microscopyu.com/tutorials/java/fluorescence/excitationbalancer/index.html>

Luminometry

- Bacart, J., Corbel, C., Jockers, R., Bach, S. and Couturier, C. (2008). The BRET technology and its application to screening assays. *Biotechnology Journal*, **3**, 311–324.
- Deshpande, S. S. (2001). Principles and applications of luminescence spectroscopy. *Critical Reviews in Food Science Nutrition*, **41**, 155–224.
- Jia, Y., Quinn, C. M., Kwak, S. and Talanian, R. V. (2008). Current in vitro kinase assay technologies: the quest for a universal format. *Current Drug Discovery Technology*, **5**, 59–69.
- Meaney, M. S. and McGuffin, V. L. (2008). Luminescence-based methods for sensing and detection of explosives. *Analytical and Bioanalytical Chemistry*, **391**, 2557–2576.

WEBSITES

- http://www.turnerbiosystems.com/doc/appnotes/998_2620.html

Circular dichroism spectroscopy

- Fasman, G. D. (1996). *Circular Dichroism and the Conformational Analysis of Biomolecules*. New York: Plenum Press. (An authoritative textbook on circular dichroism in biochemistry.)
- Gottarelli, G., Lena, S., Masiero, S., Pieraccini, S. and Spada, G. P. (2008). The use of circular dichroism spectroscopy for studying the chiral molecular self-assembly: an overview. *Chirality*, **20**, 471–485.
- Kelly, S. M. and Price, N. C. (2006). Circular dichroism to study protein interactions. *Current Protocols in Protein Science*, Chapter 20, Unit 20.10. New York: Wiley Interscience.
- Martin, S. R. and Schilstra, M. J. (2008). Circular dichroism and its application to the study of biomolecules. *Methods in Cell Biology*, **84**, 263–293.

WEBSITES

- <http://www.cryst.bbk.ac.uk/cdweb/html/>
- http://www.ap-lab.com/circular_dichroism.htm

Light scattering

- Lindner, P. and Zemb, T. (2002). *Neutron, X-rays and Light. Scattering Methods Applied to Soft Condensed Matter*, rev. edn. Amsterdam: North-Holland. (In-depth coverage of theory and applications of light scattering at expert level.)
- Villari, V. and Micali, N. (2008). Light scattering as spectroscopic tool for the study of disperse systems useful in pharmaceutical sciences. *Journal of Pharmaceutical Science*, **97**, 1703–1730.

WEBSITES

- http://www.ap-lab.com/light_scattering.htm
- <http://www.people.vcu.edu/~ecarpenter2/Tutorial.html>

Atomic spectroscopy

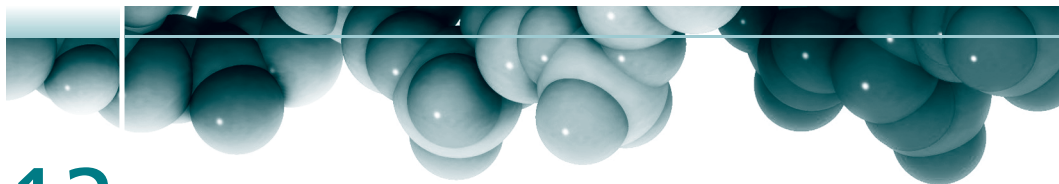
L'vov, B. V. (2005). Fifty years of atomic absorption spectrometry. *Journal of Analytical Chemistry*, **60**, 382–392.

Zybin, A., Koch, J., Wizemann, H. D., Franzke, J. and Niemax, K. (2005). Diode laser atomic absorption spectrometry. *Spectrochimica Acta*, **B60**, 1–11.

WEBSITES

<http://www.colorado.edu/physics/2000/quantumzone/index.html>

<http://zebu.uoregon.edu/nsf/emit.html>



13

Spectroscopic techniques: II Structure and interactions

A. HOFMANN

- 13.1 Introduction
- 13.2 Infrared and Raman spectroscopy
- 13.3 Surface plasmon resonance
- 13.4 Electron paramagnetic resonance
- 13.5 Nuclear magnetic resonance
- 13.6 X-ray diffraction
- 13.7 Small-angle scattering
- 13.8 Suggestions for further reading

13.1 INTRODUCTION

The overarching theme of techniques such as mass spectrometry (Chapter 9), electron microscopy and imaging (Chapter 4), analytical centrifugation (Chapter 3) and molecular exclusion chromatography (Chapter 11) is the aim to obtain clues about the structure of biomolecules and larger assemblies thereof. The spectroscopic techniques discussed in Chapters 12 and 13 are further complementary methods, and by assembling the jigsaw of pieces of information, one can gain a comprehensive picture of the structure of the biological object under study. In addition, the spectroscopic principles established in Chapter 12 are often employed as read-out in a huge variety of biochemical assays, and several more sophisticated technologies employ these basic principles in a 'hidden' way.

In the previous chapter, we established that the electromagnetic spectrum is a continuum of frequencies from the long wavelength region of the radio frequencies to the high-energy γ -rays of nuclear origin. While the methods and techniques discussed in Chapter 12 concentrated on the use of visible and UV light, there are other spectroscopic techniques that employ electromagnetic radiation of higher as well as lower energy. Another shared property of the techniques in this chapter is the higher level of complexity in undertaking. These applications are usually employed at a later stage of biochemical characterisation and aimed more at investigation of the three-dimensional structure, and in the case of proteins and peptides, address the tertiary and quaternary structure.

13.2 INFRARED AND RAMAN SPECTROSCOPY

13.2.1 Principles

Within the electromagnetic spectrum (Fig. 12.1), the energy range below the UV/Vis is the infrared region, encompassing the wavelength range of about 700 nm to 25 μm , and thus reaching from the red end of the visible to the microwave region. The absorption of infrared light by a molecule results in transition to higher levels of **vibration** (Fig. 12.3).

For the purpose of this discussion, the bonds between atoms can be considered as flexible springs, illustrating the constant vibrational motion within a molecule (Fig. 13.1). Bond vibrations can thus be either **stretching** or **bending** (deformation) actions. Theory predicts that a molecule with n atoms will have a total of $3n - 6$ fundamental vibrations ($3n - 5$, if the molecule is linear): $2n - 5$ bending, and $n - 1$ stretching modes (Fig. 13.2).

Infrared and Raman spectroscopy give similar information about a molecule, but the criteria for the phenomena to occur are different for each type. For asymmetric molecules, incident infrared light will give rise to an absorption band in the infrared spectrum, as well as a peak in the Raman spectrum. However, as shown in Fig. 13.2, symmetric molecules, such as for example CO_2 , that possess a centre of symmetry show a selective behaviour: bands that appear in the infrared spectrum do not appear in the Raman spectrum, and vice versa.

An **infrared spectrum** arises from the fact that a molecule absorbs incident light of a certain wavelength which will then be 'missing' from the transmitted light. The recorded spectrum will show an absorption band.

A **Raman spectrum** arises from the analysis of scattered light, and we have already introduced the basics of inelastic light scattering in Section 12.6.3. The largest part of an incident light beam passes through the sample (transmission). A small part is scattered isotropically, i.e. uniformly in all directions (**Rayleigh scatter**), and possesses the same wavelength as the incident beam. The Raman spectrum arises from the fact

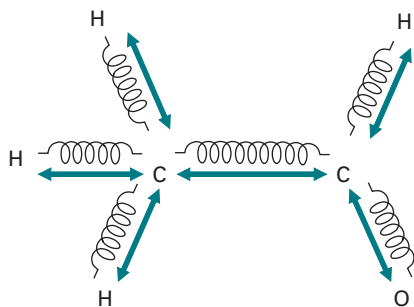


Fig. 13.1 Possible stretching vibrations in acetaldehyde.

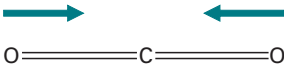
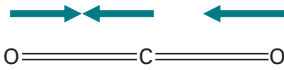
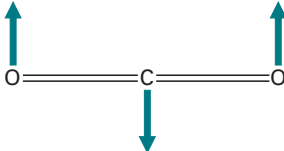
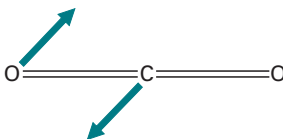
Mode		Wavenumber	IR	Raman
Stretching, symmetric		1340 cm ⁻¹	–	+
Stretching, asymmetric		2349 cm ⁻¹	+	–
Deformation		667 cm ⁻¹	+	–
Deformation		667 cm ⁻¹	+	–

Fig. 13.2 Normal vibrational modes for CO₂. For symmetric molecules that possess a centre of symmetry, bands that appear in the IR do not appear in the Raman spectrum.

that a very small proportion of light scattered by the sample will have a different frequency than the incident light. As different vibrational states are excited, energy portions will be missing, thus giving rise to peaks at lower frequencies than the incident light (**Stokes lines**). Notably, higher frequencies are also observed (**anti-Stokes lines**); these arise from excited molecules returning to ground state. The emitted energy is dumped onto the incident light which results in scattered light of higher energy than the incident light.

The criterion for a band to appear in the infrared spectrum is that the transition to the excited state is accompanied by a change in **dipole moment**, i.e. a change in charge displacement. Conversely, the criterion for a peak to appear in the Raman spectrum is a change in **polarisability** of the molecule during the transition.

Infrared spectroscopy

The fundamental frequencies observed are characteristic of the **functional groups** concerned, hence the term **fingerprint**. Figure 13.3 shows the major bands of an FT-IR spectrum of the drug phenacetin. As the number of functional groups increases in more complex molecules, the absorption bands become more difficult to assign. However, groups of certain bands regularly appear near the same wavelength and may be assigned to specific functional groups. Such group frequencies are thus extremely helpful in structural diagnosis. A more detailed analysis of the structure of a molecule is possible, because the wavenumber associated with a particular functional group varies slightly, owing to the influence of the molecular environment.

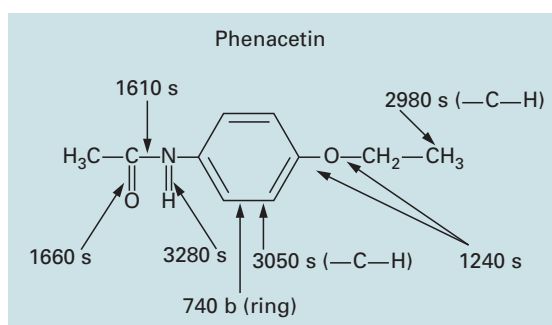
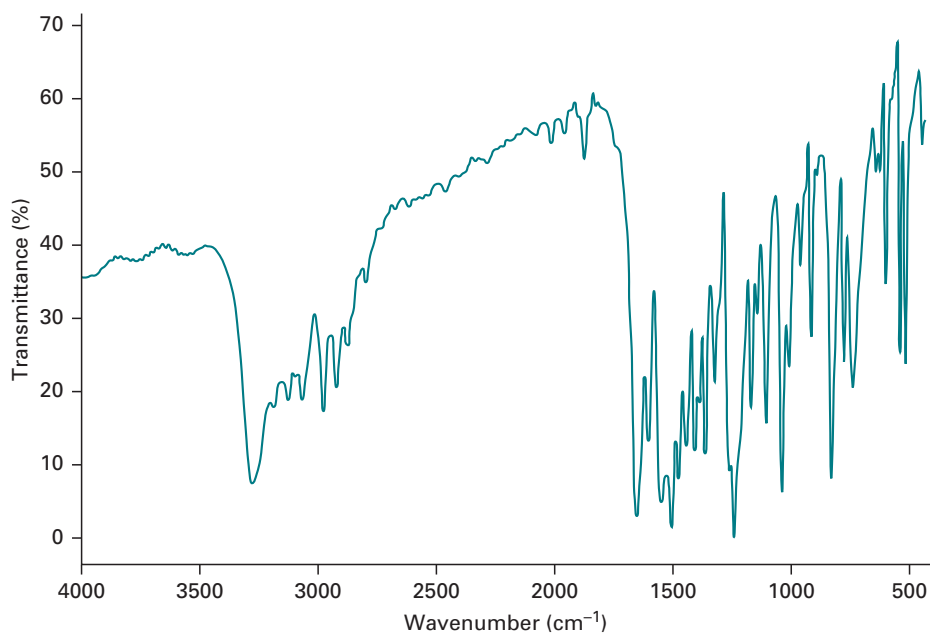


Fig. 13.3 FT-IR spectrum of phenacetin, the historically first synthetic fever reducer to go on the market. Bands at the appropriate wavenumbers (cm^{-1}) are shown, indicating the bonds with which they are associated, and the type (s, stretching; b, bending).

For example, it is possible to distinguish between C-H vibrations in methylene ($-\text{CH}_2-$) and methyl groups ($-\text{CH}_3$).

Raman spectroscopy

The assignment of peaks in Raman spectra usually requires consideration of peak position, intensity and form, as well as **depolarisation**. This allows identification of the type of **symmetry of individual vibrations**, but not the determination of structural elements of a molecule. The depolarisation is calculated as the ratio of two intensities with perpendicular and parallel polarisation with respect to the incident beam. The use of lasers as light source for Raman spectroscopy easily facilitates the use of linearly polarised light. Practically, the Raman spectrum is measured twice. In the second measurement, the polarisation plane of the incident beam is rotated by 90° .

13.2.2 Instrumentation

The most common source for infrared light is white-glowing zircon oxide or the so-called globar made of silicon carbide with a glowing temperature of 1500 K. The beam of infrared light passes a monochromator and splits into two separate beams: one runs through the sample, the other through a reference made of the substance the sample is prepared in. After passing through a splitter alternating between both beams, they are reflected into the detector. The reference is used to compensate for fluctuations in the source, as well as to cancel possible effects of the solvent. Samples of solids are either prepared in thick suspensions (mulls) such as nujol, and held as layers between NaCl planes or pressed into KBr disks. Non-covalent materials must be used for sample containment and in the optics, as these materials are transparent to infrared. All materials need to be free of water, because of the strong absorption of the O–H vibration.

Analysis using a Michelson interferometer enables **Fourier transform infrared spectroscopy** (FT-IR). The entire light emitted from the source is passed through the sample at once, and then split into two beams that are reflected back onto the point of split (interferometer plate). Using a movable mirror, path length differences are generated between both beams yielding an interferogram that is recorded by the detector. The interferogram is related with a conventional infrared spectrum by a mathematical operation called Fourier transform (see also Fig. 13.9).

For Raman spectroscopy, aqueous solutions are frequently used, since water possesses a rather featureless weak Raman spectrum. The Raman effect can principally be observed with bright, monochromatic light of any wavelength; however, light between the visible region of the spectrum is normally used due to few unwanted absorption effects. The ideal light source for Raman spectrometers is therefore a laser. Because the Raman effect is observed in light scattered off the sample, typical spectrometers use a 90° configuration.

13.2.3 Applications

The use of infrared and Raman spectroscopy is mainly in chemical and biochemical research of small compounds such as drugs, metabolic intermediates and substrates. Examples are the identification of synthesised compounds, or identification of sample constituents (e.g. in food) when coupled to a separating method such as gas chromatography (GC-IR).

FT-IR is increasingly used for analysis of peptides and proteins. The peptide bond gives rise to nine characteristic bands, named amide A, B, I, II, III, . . . , VII. The amide I (1600–1700 cm⁻¹) and amide II (1500–1600 cm⁻¹) bands are the major contributors to the protein infrared spectrum. Both bands are directly related to the backbone conformation and have thus been used for assessment of the secondary structure of peptides and proteins. The interpretation of spectra of molecules with a large number of atoms usually involves deconvolution of individual bands and second derivative spectra.

Time-resolved FT-IR (trFT-IR) enables the observation of protein reactions at the sub-millisecond timescale. This technique has been established by investigation of

the light-driven proton pump bacteriorhodopsin. For instance, the catalytic steps in the proton pumping mechanism have been validated with trFT-IR, and involve transfer of a proton from the Schiff base ($R_1R_2C=N-R_3$) to a catalytic aspartate residue, followed by re-protonation of a second catalytic aspartate residue.

13.3 SURFACE PLASMON RESONANCE

13.3.1 Principles

Surface plasmon resonance (SPR) is a surface-sensitive method for monitoring smallest changes of the **refractive index** or the thickness of thin films. It is mainly used for monitoring the interaction of two components (e.g. ligand and receptor, Section 17.3.2) one of which is immobilised on a **sensor chip** surface (Fig. 13.4a), such as a hydrogel layer on a glass slide, via either biotin-avidin interactions or covalent coupling using amine or thiol reagents similar to those used for cross-linking to affinity chromatography resins (see Section 11.8). Typical surface concentrations of the bound protein component are in the range of $1\text{--}5\text{ ng mm}^{-2}$. The sensor chip forms one wall of a microflow cell so that an aqueous solution of the ligand can be pumped at a continuous, pulse-free rate across the surface. This ensures that the concentration of ligand at the surface is maintained at a constant value. Environmental parameters such as temperature, pH and ionic strength are carefully controlled, as is the duration of exposure of the immobilised component to the ligand. Replacing the ligand solution by a buffer solution enables investigation of the dissociation of bound ligand.

Binding of ligand to the immobilised component causes an increase in mass at the surface of the chip. Vice versa, dissociation of ligand causes a reduction of mass. These mass changes, in turn, affect the refractive index of the medium at the surface of the chip, the value of which determines the propagation velocity of electromagnetic radiation in that medium.

Plasmon is a term for a collection of conduction electrons in a metal or semiconductor. Excitation of a plasmon wave requires an optical prism with a metal film of about 50 nm thickness. **Total internal reflection** (TIR) occurs when a light beam travelling through a medium of higher refractive index (e.g. glass prism with gold-coated surface) meets at an interface with a medium of lower refractive index (e.g. aqueous sample) at an angle larger than the critical angle. TIR of an incident light beam at the prism-metal interface elicits a propagating plasmon wave by leaking an electrical field intensity, called an **evanescent field wave**, into the medium of lower refractive index where it decays at an exponential rate and effectively only travels one wavelength.

Since the interface between the prism and the medium is coated with a thin layer of gold, incident photons excite a vibrational state of the electrons of the conducting band of the metal. In thin metal films this propagates as a longitudinal vibration. The electrons vibrate with a resonance frequency (hence the term 'resonance') that is dependent on metal and prism properties, as well as the wavelength and the angle of

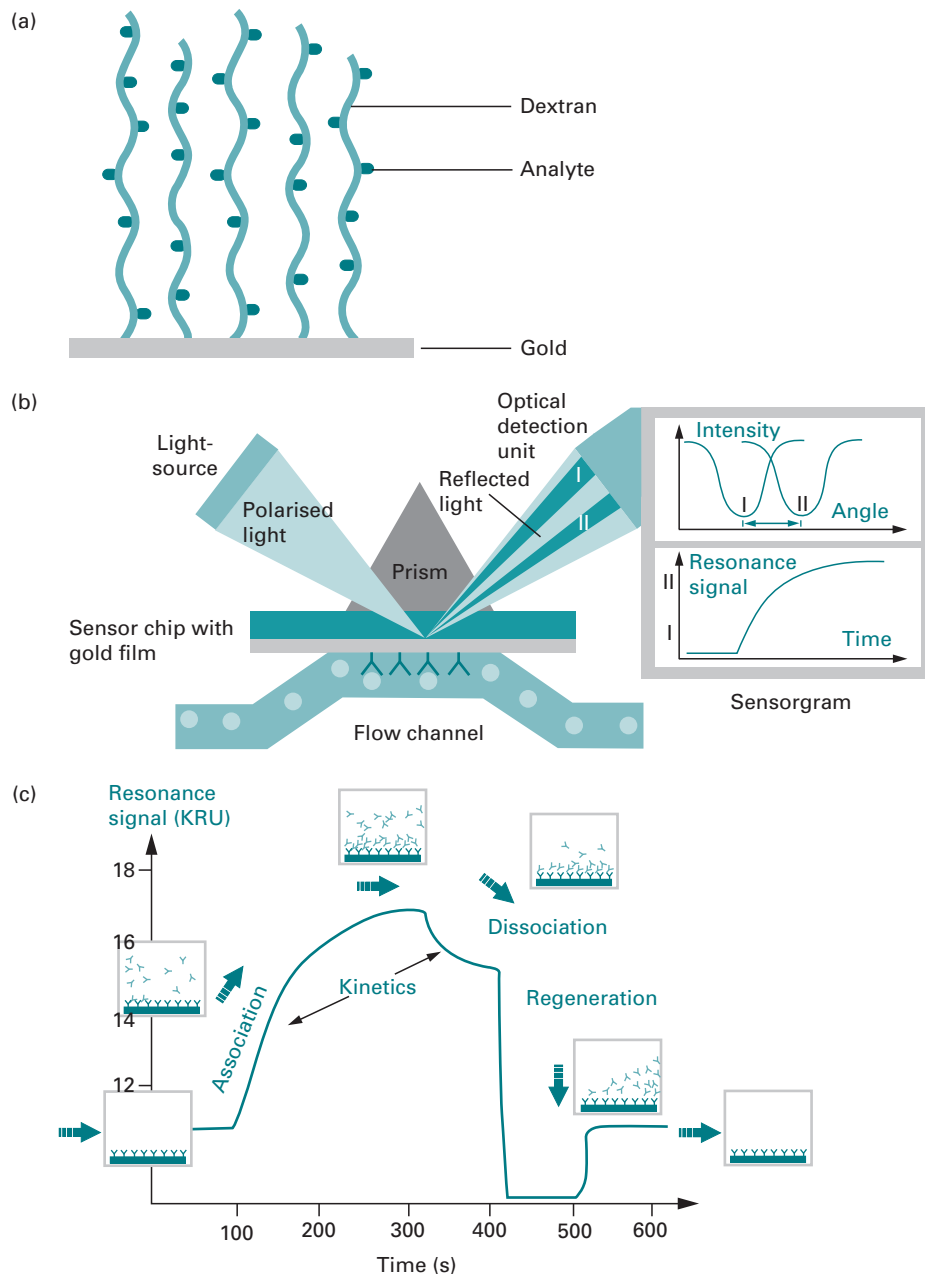


Fig. 13.4 The principles of surface plasmon resonance technology. (a) The sensor 'chip' surface. (b) The flow channel. Insert: change in intensity of reflected light as a function of angle of incidence of the light beam, and change in resonance signal as a function of time. (c) The sensorgram. (Reproduced by permission of GE Healthcare.)

the incident beam. Excitation of the plasmon wave leads to a decreased intensity of the **reflected light**. Thus, SPR produces a dip in the reflected light intensity at a specific angle of reflection. The propagating surface plasmon wave enhances the amplitude of the evanescent field wave, which extends into the sample region (Fig. 13.4b).

When binding to the chip occurs, the refractive index on the sample side of the interface increases. This alters the angle of incidence required to produce the SPR effect and hence also alters the angle of reflected light. The change in angle brings about a change in detector position, which can be plotted against time to give a sensorgram reading (Fig. 13.4c). The angle is expressed in resonance units (RU), such that 1000 RU corresponds to a change in mass at the surface of the chip of about 1 ng mm^{-2} .

Since in SPR instruments the angle and the wavelength of the incident beam are constant, a shift in the plasmon resonance leads to a change in the intensity of the reflected beam. The shift is restricted locally and happens only in areas where the optical properties have changed. The usage of an array detector as compared to a single detector cell therefore allows for measurement of an SPR image. SPR can detect changes in the refractive index of less than 10^{-4} or changes in layer heights of about 1 nm. This enables not only the detection of binding events between biomolecules but also binding at protein domains or changes in molecular monolayers with a lateral resolution of a few μm . For SPR, light of wavelengths between infrared (IR) and near-infrared (NIR) may be used. In general, the higher the wavelength of the light used the better the sensitivity but the less the lateral resolution. Vice versa, if high lateral resolution is required, red light is to be used because the propagation length of the plasmon wave is approximately proportional to the wavelength of the exciting light.

13.3.2 Applications

The SPR technique enjoys frequent use in modern life science laboratories, due to its general applicability and the fact that there are no special requirements for the molecules to be studied (**label-free**), such as fluorescent properties, spectral labels or radio labels. It can even be used with coloured or opaque solutions.

Generally, all two-component binding reactions can be investigated, which opens a variety of applications in the areas of drug design (protein–ligand interactions), as well as mechanisms of membrane-associated proteins (protein–membrane binding) and DNA-binding proteins. SPR has thus successfully been used to study the kinetics of receptor–ligand interactions, antibody–antigen and protein–protein interactions. The method is extensively used in proteomic research and drug development.

SPR imaging

The focus of SPR imaging experiments has shifted in recent years from characterisation of ultrathin films to analysis of biosensor chips, especially affinity sensor arrays. SPR imaging can detect DNA–DNA, DNA–protein and protein–protein interactions in a two-dimensional manner. The detection limit for such biosensor chips is in the order of nM to fM. Apart from the detection of binding events as such, the quality of binding (low affinity, high affinity) can also be assessed by SPR imaging. Promising future applications for SPR imaging include peptide arrays that can be prepared on modified gold surfaces. This can prove useful for assessing peptide–antibody interactions. The current time resolution of less than 1 s for an entire image also allows for high-throughput screenings and *in situ* measurements.

13.4 ELECTRON PARAMAGNETIC RESONANCE

Prior to any detailed discussion of electron paramagnetic resonance (EPR) and nuclear magnetic resonance (NMR) methods, it is worthwhile considering the more general phenomena applicable to both.

13.4.1 Magnetic phenomena

Magnetism arises from the **motion of charged particles**. This motion is controlled by internal forces in a system. For the purpose of this discussion, the major contribution to magnetism in molecules is due to the **spin** of the charged particle.

In chemical bonds of a molecule, the negatively charged electrons have a spin controlled by strict **quantum rules**. A bond is constituted by two electrons with opposite spins occupying the appropriate molecular orbital. According to the **Pauli principle**, the two electrons must have opposite spins, leading to the term **paired electrons**. Each of the spinning electronic charges generates a magnetic effect, but in electron pairs the effect is almost self-cancelling. In atoms, a value for magnetic susceptibility may be calculated and is of the order of -10^{-6} g^{-1} . This **diamagnetism** is a property of all substances, because they all contain the minuscule magnets, i.e. electrons. Diamagnetism is temperature independent.

If an electron is unpaired, there is no counterbalancing opposing spin and the magnetic susceptibility is of the order of $+10^{-3}$ to $+10^{-4} \text{ g}^{-1}$. The effect of an **unpaired electron** exceeds the 'background' diamagnetism, and gives rise to **paramagnetism**. Free electrons can arise in numerous cases. The most notable example is certainly the paramagnetism of metals such as iron, cobalt and nickel, which are the materials that permanent magnets are made of. The paramagnetism of these metals is called **ferromagnetism**. In biochemical investigations, systems with free electrons (radicals) are frequently used as probes.

Similar arguments can be made regarding **atomic nuclei**. The nucleus of an atom is constituted by protons and neutrons, and has a net charge that is normally compensated by the extra-nuclear electrons. The number of all nucleons (Z) is the sum of the number of protons (P) and the number of neutrons (N). P and Z determine whether a nucleus will exhibit paramagnetism. Carbon-12 (^{12}C), for example, consists of six protons ($P = 6$) and six neutrons ($N = 6$) and thus has $Z = 12$. P and Z are even, and therefore the ^{12}C nucleus possesses no nuclear magnetism. Another example of a nucleus with no residual magnetism is oxygen-16 (^{16}O). All other nuclei with P and Z being uneven possess residual nuclear magnetism.

The way in which a substance behaves in an externally applied magnetic field allows us to distinguish between dia- and paramagnetism. A paramagnetic material is attracted by an external magnetic field, while a diamagnetic substance is rejected. This principle is employed by the **Guoy balance**, which allows quantification of magnetic effects. A balance pan is suspended between the poles of a suitable electro-magnet supplying the external field. The substance under test is weighed in air with the current switched off. The same sample is then weighed again with the current

(i.e. external magnetic field) on. A paramagnetic substance appears to weigh more, and a diamagnetic substance appears to weigh less.

13.4.2 The resonance condition

In both EPR and NMR techniques, two possible energy states exist for either electronic or nuclear magnetism in the presence of an **external magnetic field**. In the low-energy state, the field generated by the spinning charged particle is parallel to the external field. Conversely, in the high-energy state, the field generated by the spinning charged particle is antiparallel to the external field. When enough energy is input into the system to cause a transition from the low- to the high-energy state, the condition of resonance is satisfied. Energy must be absorbed as a discrete dose (quantum) $h\nu$, where h is the Planck constant and ν is the frequency (see equation 12.1). The quantum energy required to fulfil the resonance condition and thus enable transition between the low- and high-energy states may be quantified as:

$$h\nu = g\beta B \quad (13.1)$$

where g is a constant called **spectroscopic splitting factor**, β is the magnetic moment of the electron (termed the Bohr magneton), and B is the strength of the applied external magnetic field. The frequency ν of the absorbed radiation is a function of the paramagnetic species β and the applied magnetic field B . Thus, either ν or B may be varied to the same effect.

With appropriate external magnetic fields, the frequency of applied radiation for EPR is in the microwave region, and for NMR in the region of radio frequencies. In both techniques, two possibilities exist for determining the absorption of electromagnetic energy (i.e. enabling the resonance phenomenon):

- constant frequency ν is applied and the external magnetic field B is swept; or
- constant external magnetic field B is applied and the appropriate frequency ν is selected by sweeping through the spectrum.

For technical reasons, the more commonly used option is a sweep of the external magnetic field.

13.4.3 Principles

The absorption of energy is recorded in the EPR spectrum as a function of the magnetic induction measured in Tesla (T) which is proportional to the **magnetic field strength** applied. The area under the absorption peak is proportional to the number of unpaired electron spins. Most commonly, the first derivative of the absorption peak is the signal that is actually recorded.

For a delocalised electron, as observed e.g. in free radicals, the g value is 2.0023; but for localised electrons such as in transition metal atoms, g varies, and its precise value contains information about the nature of bonding in the environment of the unpaired electron within the molecule. When resonance occurs, the absorption

peak is broadened owing to interactions of the unpaired electron with the rest of the molecule (**spin-lattice interactions**). This allows further conclusions as to the molecular structure.

High-resolution EPR may be performed by examining the **hyperfine splitting** of the absorption peak which is caused by interaction of the unpaired electron with adjacent nuclei, thus yielding information about the spatial location of atoms in the molecule. The proton hyperfine splitting for free radicals occurs in the range of $0-3 \times 10^{-3}$ T, and yields data analogous to those obtained in high-resolution NMR (see Section 13.5).

The effective resolution of an EPR spectrum can be considerably improved by combining the method with NMR, a technique called **electron nuclear double resonance** (ENDOR). Here, the sample is irradiated simultaneously with microwaves for EPR and radio frequencies (RF) for NMR. The RF signal is swept for fixed points in the EPR spectrum, yielding the EPR signal height versus nuclear RF. This approach is particularly useful when there are a large number of nuclear levels that broaden the normal electron resonance lines.

The technique of **electron double resonance** (ELDOR) finds an application in the separation of overlapping multiradical spectra and the study of relaxation phenomena, for example chemical spin exchange. In ELDOR, the sample is irradiated with two microwave frequencies simultaneously. One is used for observation of the EPR signal at a fixed point in the spectrum, the other is used to sweep other parts of the spectrum. The recorded spectrum is plotted as a function of the EPR signal as a function of the difference of the two microwave frequencies.

13.4.4 Instrumentation

Figure 13.5 shows the main components of an EPR instrument. The magnetic fields generated by the electromagnets are of the order of 50 to 500 mT, and variations of less than 10^{-6} are required for highest accuracy. The monochromatic microwave radiation is produced in a **klystron** oscillator with wavelengths around 3 cm (9 GHz).

The samples are required to be in the solid state; hence biological samples are usually frozen in liquid nitrogen. The technique is also ideal for investigation of membranes and membrane proteins. Instead of plotting the absorption A versus B , it is the first-order differential (dA/dB) that is usually plotted against B (Fig. 13.6). Such a shape is called a 'line' in EPR spectroscopy. Generally, there are relatively few unpaired electrons in a molecule, resulting in fewer than 10 lines, which are not closely spaced.

13.4.5 Applications

Metalloproteins

EPR spectroscopy is one of the main methods to study metalloproteins, particularly those containing molybdenum (xanthine oxidase), copper (cytochrome oxidase, copper blue enzymes) and iron (cytochrome, ferredoxin). Both copper and non-haem iron, which do not absorb in the UV/Vis region, possess EPR absorption peaks in one

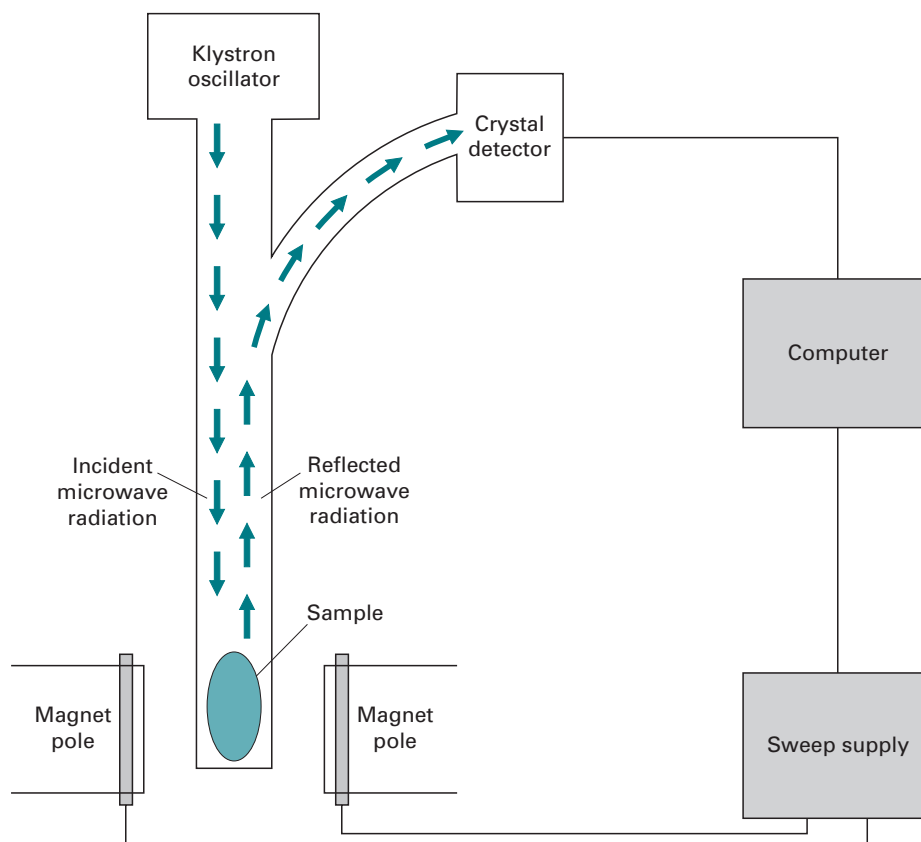


Fig. 13.5 Diagram of an EPR spectrometer.

of their oxidised states. The appearance and disappearance of their EPR signals are used to monitor the activity of these proteins in the multi-enzyme systems of intact mitochondria and chloroplasts, as well as in isolated enzymes. In many metallo-proteins, the ligands coordinating the metal ion are the amino acid residues of the protein. Coordination chemistry requires a specific stereochemical structure of the ligands, and EPR studies show that the geometry is frequently distorted in proteins when compared to model systems. Such distortions may be related to biological function.

Spin labels

Spin labels are stable and non-reactive unpaired electrons used as reporter groups or probes for EPR. The procedure of spin labelling is the attachment of these probes to biological molecules that lack unpaired electrons. The label can be attached to either a substrate or a ligand. Often, a spin label contains the nitric oxide moiety. These labels enable the study of events that occur with a frequency of 10^7 to 10^{11} s^{-1} . If the motion is restricted in some directions, only anisotropic motion (movement in one particular direction) may be studied, for example in membrane-rigid spin labels in bilayers. Here, the label is attached so that the NO group lies parallel to the long axis of the lipid.

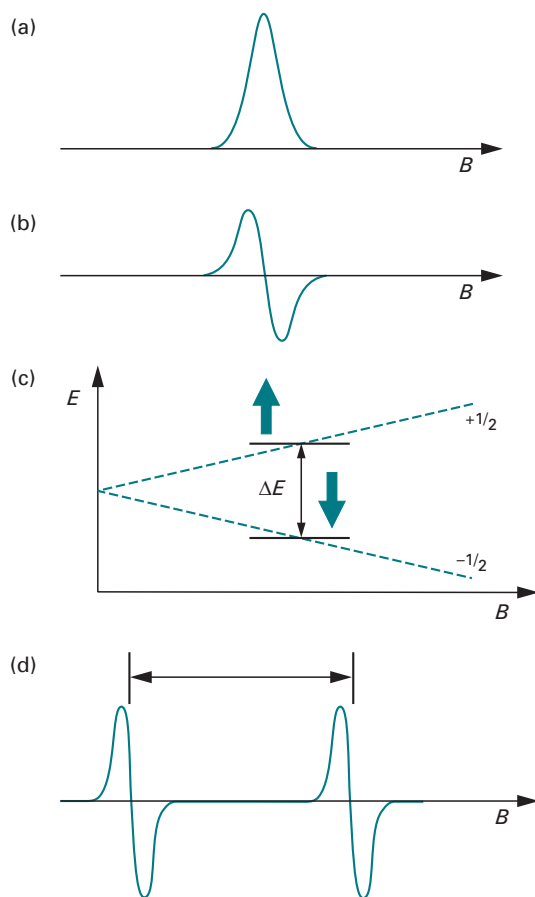


Fig. 13.6 Instead of the absorption signal (a), EPR spectrometry records its first derivative (b). (c) The energy of the two spin states of a free electron is shown as a function of the external magnetic field B . Resonance happens when the energy of the applied microwave radiation is the same as the energy difference ΔE . (d) Hyperfine splitting due to coupling of an unpaired electron with a nuclear spin of $1/2$. For the hydrogen atom, the distance between the two signals is 50.7 mT.

Intramolecular motions and lateral diffusion of lipid through the membrane, as well as the effect of proteins and other factors on these parameters may be observed. Quantification of effects often involves calculation of the **order parameter** Z . Spin-labelled lipids are either concentrated into one region of the bilayer or randomly incorporated into model membranes. The diffusion of spin labels allows them to come into contact with each other, which causes line-broadening in the spectrum. Labelling of phospholipids with 2,2,6,6-tetramethylpiperidine-1-oxyl (TEMPOL) is used for measurement of the flip rate of phospholipids between inner and outer surfaces as well as lateral diffusion.

Free radicals

Molecules in their **triplet states** (Fig. 12.8) have unpaired electrons and thus are amenable to EPR spectroscopy. Such molecules possess the property of phosphorescence

and EPR may deliver data complementary to the UV/Vis region of the spectrum. For instance, free radicals due to the triplet state of tryptophan have been observed in cataractuous lenses.

Spin trapping is a process whereby an unstable free radical is being stabilised by reaction with a compound such as 5,5-dimethylpyrroline-1-oxide (DMPO). Hyperfine splittings (Fig. 13.6) are observed that depend upon the nature of the radical.

Carcinogenesis is an area where free radicals have been implicated. While free radicals promote the generation of tumours through damage due to their high reactivity, there is, in general, a lower concentration of radicals in tumours than in normal tissue. Also, a gradient has been observed with higher concentrations of radicals in the peripheral non-necrotic surface layers than in the inner regions of the tumour. EPR has been used to study implanted tumours in mice, but also in evaluation of potential chemical carcinogens. Polycyclic hydrocarbons, such as naphthalene, anthracene and phenanthrene, consist of multiple aromatic ring systems. These extended aromatic systems allow for single free electrons to be accommodated and thus yield long-lived free radicals, extending the periods of time in which damage can be done. Many of the precursors of these radicals exist in natural sources such as coal tar, tobacco smoke and other products of combustion, hence the environmental risk. Another source of free radicals is irradiation with UV light or γ -rays. Ozone is an oxygen radical that is

Example 1 **FREE RADICALS IN THE HEALTHY ORGANISM**

An important concern for humans today is environmental pollution and its effects on our bodies. Environmental pollutants – from auto exhaust, second-hand cigarette smoke, pesticides, or even ultraviolet radiation from the Sun – create what are known as free radicals in our bodies.

A lot of metabolic studies have made use of EPR spectroscopy. Free radicals are found in many metabolic pathways and as degradation products of drugs and toxins. Electron transfer mechanisms in mitochondria and chloroplasts involve paramagnetic species, such as the Fe-S centres. Other RedOx processes involving the flavin derivatives FAD, FMN and semiquinons lend themselves readily to exploration by EPR spectroscopy. The signal of $g = 2.003$ mainly stems from mitochondria. However, different cell lines show different intensities, because this phenomenon also depends on the metabolic state. Factors increasing the metabolic activity also lead to an increase in organic radical signal. Many studies in this context have focussed on the free radical polymer melanin (the skin pigment) and the ascorbyl radical (vitamin C metabolite).

Nitric oxide (NO) operates as a physiological messenger regulating the nervous, immune and cardiovascular systems. It has been implicated in septic (toxic) shock, hypertension, stroke and neurodegenerative diseases. Although NO is involved in normal synaptic transmission, excess levels are neurotoxic. Enzymes such as superoxide dismutase attenuate the neurotoxicity by removal of radical oxygen species, hence limiting their availability for reaction with NO to produce peroxynitrite.

present as a protective shield around the Earth, filtering the dangers of cosmic UV irradiation by complex radical chemistry. The pollution of the Earth's atmosphere with radical-forming chemicals has destroyed large parts of the ozone layer, increasing the risk of skin cancer from sun exposure. EPR can be used to study biological materials, including bone or teeth, and detect radicals formed due to exposure to high energy radiation.

Another major application for EPR is the examination of irradiated foodstuffs for residual free radicals, and it is mostly used to establish whether packed food has been irradiated.

13.5 NUCLEAR MAGNETIC RESONANCE

The essential background theory of the phenomena that allow NMR to occur have been introduced in Sections 13.4.1 and 13.4.2. However, the miniature magnets involved here are not electrons, but the nuclei. The specific principles, instrumentation and applications are discussed below.

13.5.1 Principles

Most studies in organic chemistry involve the use of ^1H , but NMR spectroscopy with ^{13}C , ^{15}N and ^{31}P isotopes is frequently used in biochemical studies. The resonance condition in NMR is satisfied in an external magnetic field of several hundred mT, with absorptions occurring in the region of radio waves (frequency 40 MHz) for resonance of the ^1H nucleus. The actual field scanned is small compared with the field strengths applied, and the radio frequencies absorbed are specifically stated on such spectra.

Similar to other spectroscopic techniques discussed earlier, the energy input in the form of electromagnetic radiation promotes the transition of 'entities' from lower to higher energy states (Fig. 13.7). In case of NMR, these entities are the nuclear magnetic spins which populate energy levels according to quantum chemical rules. After a certain time-span, the spins will return from the higher to the lower energy level, a process that is known as **relaxation**.

The energy released during the transition of a nuclear spin from the higher to the lower energy state can be emitted as heat into the environment and is called **spin-lattice relaxation**. This process happens with a rate of T_1^{-1} , and T_1 is termed the **longitudinal relaxation time**, because of the change in magnetisation of the nuclei parallel to the field. The transverse magnetisation of the nuclei is also subject to change over time, due to interactions between different nuclei. The latter process is thus called **spin-spin relaxation** and is characterised by a **transverse relaxation time** T_2 .

The molecular environment of a proton governs the value of the applied external field at which the nucleus resonates. This is recorded as the **chemical shift** (δ) and is measured relative to an internal standard, which in most cases is tetramethylsilane

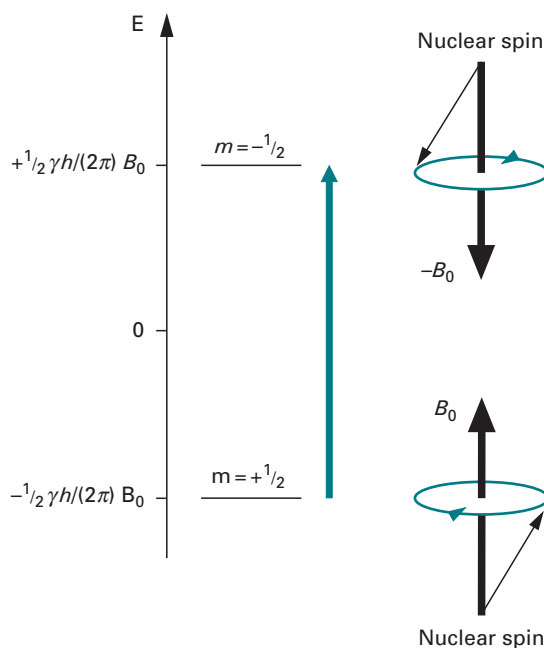


Fig. 13.7 Energy levels of a proton in the magnetic field B_0 . The nuclear spin of a nucleus is characterised by its magnetic quantum number m . For protons, m can only adopt $+\frac{1}{2}$ and $-\frac{1}{2}$. The corresponding energies are calculated by $-m\gamma h/(2\pi)H_0$, where γ is a constant characteristic for a particular nucleus, h is the Planck constant, and H_0 is the strength of the magnetic field B_0 .

(TMS; $(\text{H}_3\text{C})_4\text{Si}$) because it contains 12 identical protons. The chemical shift arises from the applied field inducing secondary fields of about 0.15–0.2 mT at the proton by interacting with the adjacent bonding electrons.

- If the induced field opposes the applied field, the latter will have to be at a slightly higher value for resonance to occur. The nucleus is said to be **shielded**, the magnitude of the shielding being proportional to the electron-withdrawing power of proximal substituents.
- Alternatively, if the induced and applied fields are aligned, the latter is required to be at a lower value for resonance. The nucleus is then said to be **deshielded**.

Usually, **deuterated solvents** such as CDCl_3 are used for sample preparation of organic compounds. For peptides and proteins D_2O is the solvent of choice. Because the stability of the magnetic field is critical for NMR spectroscopy, the magnetic flux needs to be tuned, e.g. by locking with deuterium resonance frequencies. The use of deuterated solvents thus eliminates the need for further experiments.

The chemical shift is plotted along the x -axis, and measured in p.p.m. instead of the actual magnetic field strengths. This conversion makes the recorded spectrum independent of the magnetic field used. The signal of the internal standard TMS appears at $\delta = 0$ p.p.m. The type of proton giving rise to a particular band may thus be identified by the resonance peak position, i.e. its chemical shift, and the area under each peak

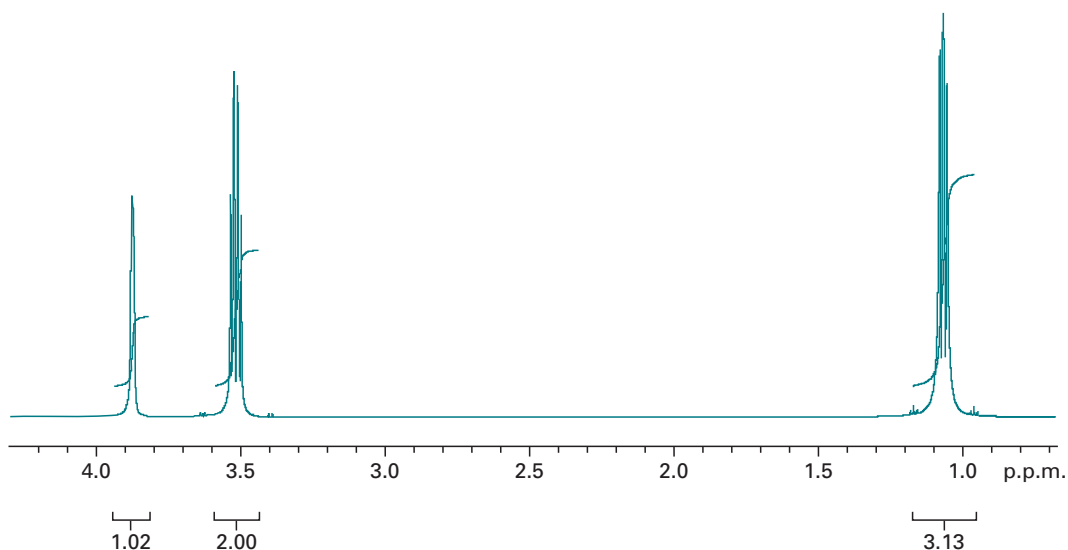


Fig. 13.8 ^1H NMR spectrum of ethyl alcohol ($\text{H}_3\text{C}-\text{CH}_2-\text{OH}$) with integrated peaks.

is proportional to the number of protons of that particular type. Figure 13.8 shows an ^1H NMR spectrum of ethyl alcohol, in which there are three methyl, two methylene and one alcohol group protons. The peak areas are integrated, and show the proportions 3 : 2 : 1. Owing to the interaction of bonding electrons with like or different spins, a phenomenon called **spin-spin coupling** (also termed **scalar** or **J-coupling**) arises that can extend to nuclei four or five bonds apart. This results in the splitting of the three bands in Fig. 13.8 into several finer bands (hyperfine splitting). The hyperfine splitting yields valuable information about the near-neighbour environment of a nucleus.

NMR spectra are of great value in elucidating chemical structures. Both qualitative and quantitative information may be obtained. The advances in computing power have made possible many more advanced NMR techniques. Weak signals can be enhanced by running many scans and accumulating the data. Baseline noise, which is random, tends to cancel out whereas the signal increases. This approach is known as computer averaging of transients or CAT scanning, and significantly improves the signal-to-noise ratio.

Despite the value and continued use of such 'conventional' ^1H NMR, much more structural information can be obtained by resorting to pulsed input of radio frequency energy, and subjecting the output to Fourier transform. This approach has given rise to a wide variety of procedures using multidimensional spectra, ^{13}C and other odd-isotope NMR spectra and the determination of multiplicities and scan images.

Pulse-acquire and Fourier transform methods

In 'conventional' NMR spectroscopy, the electromagnetic radiation (energy) is supplied from the source as a continuously changing frequency over a preselected spectral range (continuous wave method). The change is smooth and regular between fixed limits. Figure 13.9a illustrates this approach. During the scan, radiation of

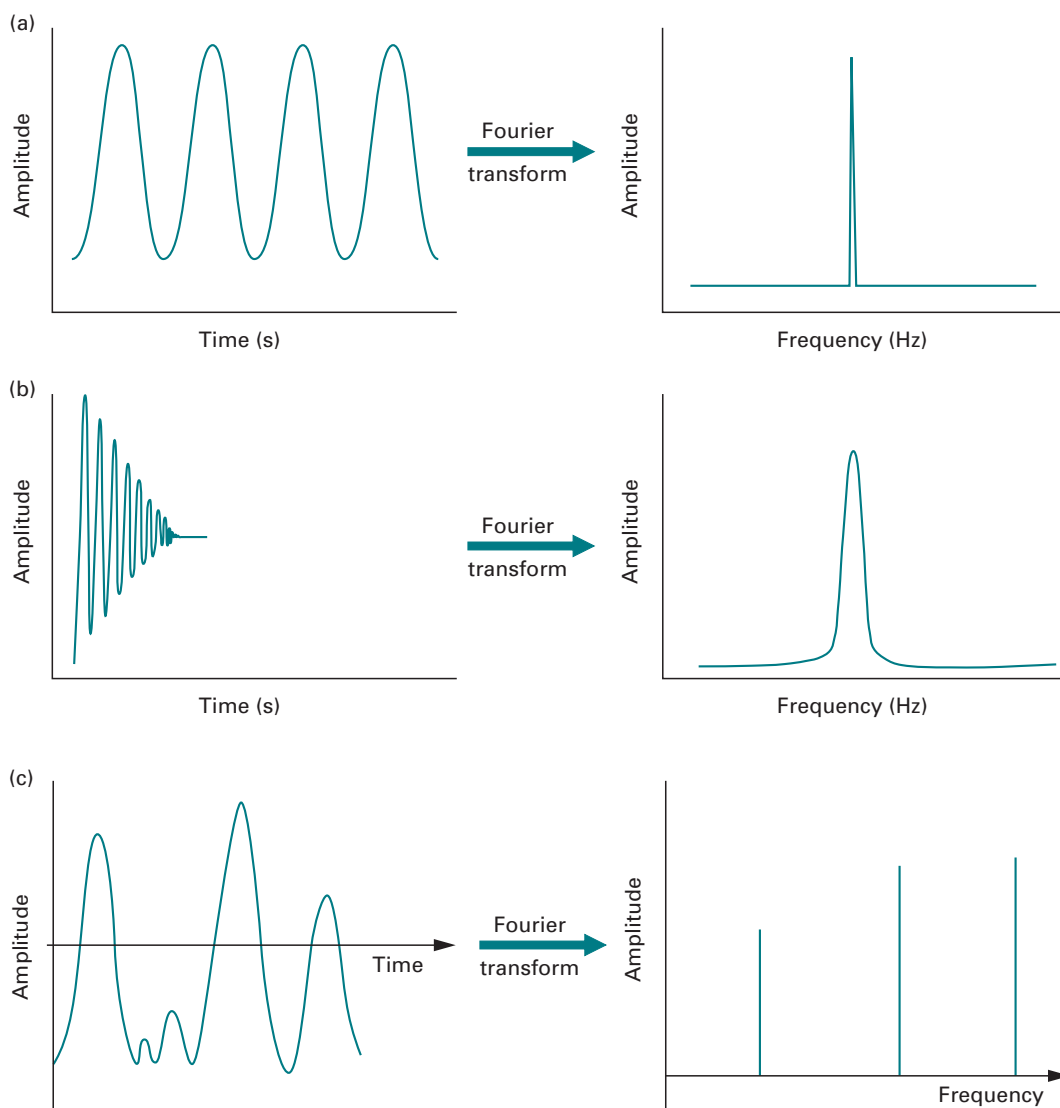


Fig. 13.9 Diagrammatic representation of the Fourier transformation of (a) a single frequency sine wave, (b) a single frequency FID, and (c) a three-sine-wave combination.

certain energy in the form of a sine wave is recorded. By using the mathematical procedure of **Fourier transform**, the 'time domain' can be resolved into a 'frequency domain'. For a single-frequency sine wave, this procedure yields a single peak of fixed amplitude. However, because the measured signal in NMR is the re-emission of energy as the nuclei return from their high-energy into their low-energy states, the recorded radiation will decay with time, as fewer and fewer nuclei will return to the ground state. The signal measured is thus called the **free induction decay** (FID). Figure 13.9b shows the effect of the FID on the corresponding Fourier transform. The frequency band broadens, but the peak position and the amplitude remain the same. The resolved frequency peak represents the chemical shift of a nucleus resonating at this energy.

Alternatively, the total energy comprising all frequencies between the fixed limits can be put in all at the same time. This is achieved by irradiating the sample with a broadband pulse of all frequencies at one go. The output will measure all resonance energies simultaneously and will result in a very complicated interference pattern. However, Fourier transform is able to resolve this pattern into the constituting frequencies (Fig. 13.9c).

In the presence of an external magnetic field, nuclear spins precess around the axis of that field with the so-called **Larmor frequency**. The vector sum of all nuclear magnetic moments yields a magnetisation parallel to the external field, i.e. a **longitudinal magnetisation**. When a high-frequency pulse is applied, the overall magnetisation is forced further off the precession by a pulse angle. This introduces a new vector component to the overall magnetisation which is perpendicular to the external field; this component is called **transverse magnetisation**. The FID measured in pulse-acquired spectra is, in fact, the decay of that transverse magnetisation component.

Nuclear Overhauser effect

It has already been mentioned above that nuclear spins generate magnetic fields which can exert effects through space, for example as observed in spin-spin coupling. This coupling is mediated through chemical bonds connecting the two coupling spins. However, magnetic nuclear spins can also exert effects in their proximal neighbourhood via dipolar interactions. The effects encountered in the dipolar interaction are transmitted through space over a limited distance on the order of 0.5 nm or less. These interactions can lead to the **nuclear Overhauser effects** (NOEs), as observed in a changing signal intensity of a resonance when the state of a near neighbour is perturbed from the equilibrium. Because of the spatial constraint, this information enables conclusions to be drawn about the three-dimensional geometry of the molecule being examined.

^{13}C NMR

Due to the low abundance of the ^{13}C isotope, the chance of finding two such species next to each other in a molecule is very small (see Chapter 9). As a consequence, ^{13}C - ^{13}C couplings (homonuclear couplings) do not arise. While ^1H - ^{13}C interactions (heteronuclear coupling) are possible, one usually records decoupled ^{13}C spectra where all bands represent carbon only. ^{13}C spectra are thus much simpler and cleaner when compared to ^1H spectra. The main disadvantage though is the fact that multiplicities in these spectra cannot be observed, i.e. it cannot be decided whether a particular ^{13}C is associated with a methyl (H_3C), a methylene (H_2C) or a methyne (HC) group. Some of this information can be regained by irradiating with an off-resonance frequency during a decoupling experiment. Another routinely used method is called **distortionless enhancement by polarisation transfer** (DEPT), where sequences of multiple pulses are used to excite nuclear spins at different angles, usually 45° , 90° or 135° . Although interactions have been decoupled, in this situation the resonances exhibit positive or negative signal intensities dependent on the number of protons bonded to the carbon. In DEPT-135, for example, a methylene group yields a negative intensity, while methyl and methyne groups yield positive signals.

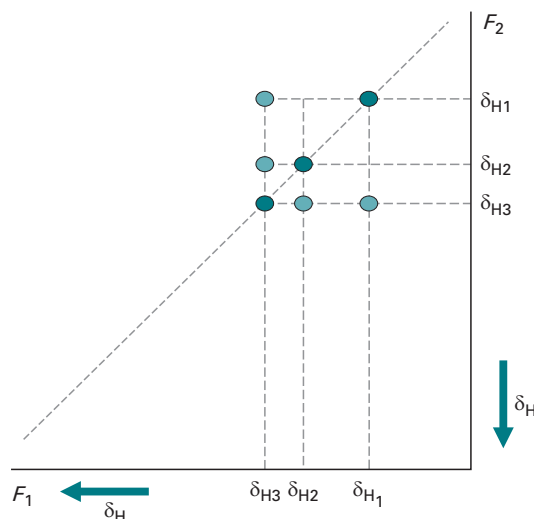


Fig. 13.10 Schematics of a correlated 2D- ^1H NMR spectrum. H3 couples with H2 and H1. H1 and H2 show no coupling.

Multidimensional NMR

As we learned above, the observable in pulse-acquired Fourier transform NMR is the decay of the transverse magnetisation, called **free induction decay** (FID). The detected signal thus is a function of the detection time t_2 . Within the pulse sequence, the time t_1 (evolution time) describes the time between the first pulse and signal detection. If t_1 is systematically varied, the detected signal becomes a function of both t_1 and t_2 , and its Fourier transform comprises two frequency components. The two components form the basis of a two-dimensional spectrum.

Correlated 2D-NMR spectra show chemical shifts on both axes. Utilising different pulse sequences leads to different methods, such as correlated spectroscopy (COSY), nuclear overhauser effect spectroscopy (NOESY), etc. Such methods yield the homonuclear ^1H couplings. The 1D-NMR spectrum now appears along the diagonal and long-range couplings between particular nuclei appear as off-diagonal signals (Fig. 13.10).

Summary of NMR parameters

The parameters obtained from NMR spectra used to derive structural determinants of a small molecule or protein are summarised in Table 13.1.

13.5.2 Instrumentation

Schematically, an analytical NMR instrument is very similar to an EPR instrument, except that instead of a klystron generating microwaves two sets of coils are used to generate and detect radio frequencies (Fig. 13.11). Samples in solution are contained in sealed tubes which are rotated rapidly in the cavity to eliminate irregularities and imperfections in sample distribution. In this way, an average and uniform signal

Table 13.1 **NMR-derived structural parameters of molecules**

Parameter	Information	Example/Comment
Chemical shift	Chemical group	^1H , ^{13}C , ^{15}N , ^{31}P
	Secondary structure	
J-couplings (through bond)	Dihedral angles	$^3J(\text{amide-H}, \text{H}\alpha)$, $^3J(\text{H}\alpha, \text{H}\beta)$, . . .
NOE (through space)	Interatomic distances	<0.5 nm
Solvent exchange	Hydrogen bonds	Hydrogen-bonded amide protons are protected from H/D exchange, while the signals of other amides disappear quickly
Relaxation/line widths	Mobility, dynamics, conformational/chemical exchange	The exchange between two conformations, but also chemical exchange, gives rise to two distinct signals for a particular spin
	Torsion angles	
Residual dipolar coupling	Torsion angles	^1H - ^{15}N , ^1H - ^{13}C , ^{13}C - ^{13}C , . . .

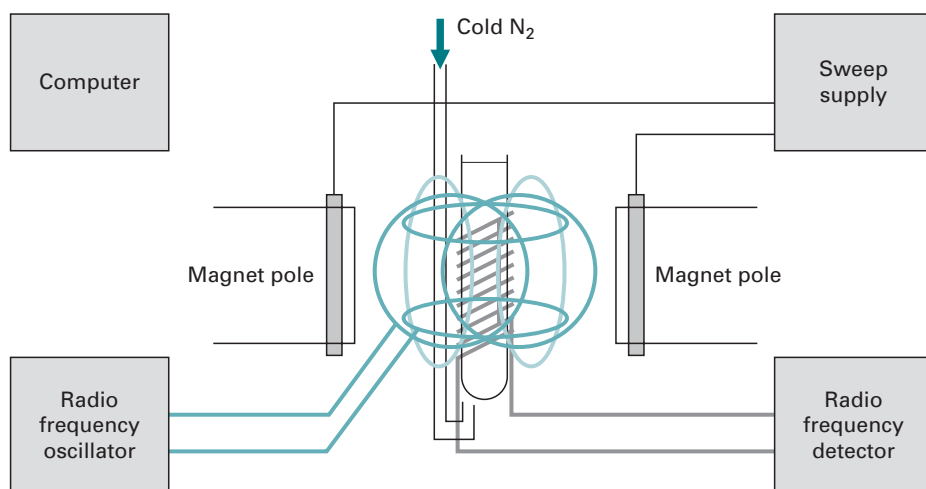


Fig. 13.11 Schematic diagram of an NMR spectrometer with cryoprobe.

is reflected to the receiver to be processed and recorded. In solid samples, the number of spin-spin interactions is greatly enhanced due to intermolecular interactions that are absent in dissolved samples due to translation and rotation movements. As a result, the resonance signals broaden significantly. However, high-resolution spectra can be obtained by spinning the solid sample at an angle of 54.7° (**magic angle spinning**). The sophisticated pulse sequences necessary for multidimensional NMR require

a certain geometric layout of the radio frequency coils and sophisticated electronics. Advanced computer facilities are needed for operation of NMR instruments, as well as analysis of the acquired spectra.

13.5.3 Applications

Molecular structure determination

Traditionally, NMR spectroscopy is the main method of structure determination for organic compounds. The chemical shift provides a clue about the environment of a particular proton or carbon, and thus allows conclusions as to the nature of functional groups. Spin-spin interactions allow conclusions as to how protons are linked with the carbon skeleton. For structure determination, the fine structure usually is the most useful information because it provides a unique criterion while chemical shifts of some groups can vary over an extended range. Additionally, the signal intensity provides information as to how many protons contribute to a particular signal.

Solution structure of proteins and peptides

The structures of proteins up to a mass of about 50 kDa can be determined with biomolecular NMR spectroscopy. The development of magnets with very high field strengths (currently 900 MHz) continues to push the size limit. The preparation of proteins or selected domains for NMR requires recombinant expression and isotopic labelling to enrich the samples with ^{13}C and ^{15}N ; ^2H labelling might be required as well. Sample amounts in the order of 10 mg used to be required for NMR experiments; however, the introduction of cryoprobe technology has reduced the sample amount significantly. Heteronuclear multidimensional NMR spectra need to be recorded for the assignment of all chemical shifts (^1H , ^{13}C , ^{15}N). For interproton NOEs, ^{13}C - and ^{15}N -edited 3D NOESY spectra are required. The data acquisition can take several weeks, after which spectra are processed (Fourier transformation) and improved with respect to digital resolution and signal-to-noise. Assignment of chemical shifts and interatomic distances is carried out with the help of software programs. All experimentally derived parameters are then used as restraints in a molecular dynamics or simulated annealing structure calculation. The result of a protein NMR structure is an ensemble of structures, all of which are consistent with the experimentally determined restraints, but converge to the same fold.

Magnetic resonance imaging

The basic principles of NMR can be applied to imaging of live samples. Because the proton is one of the more sensitive nuclides and is present in all biological systems abundantly, ^1H resonance is used almost exclusively in the clinical environment. The most important compound in biological samples in this context is water. It is distributed differently in different tissues, but constitutes about 55% of body mass in the average human. In soft tissues, the water distribution varies between 60% and 90%. In NMR, the resonance frequency of a particular nuclide is proportional to the

Example 2 ASSESSING PROTEIN CONFORMATIONAL EXCHANGE BY NMR

Question Identification of protein–protein interaction sites is crucial for understanding the basis of molecular recognition. How can such sites be identified?

Answer Apart from providing the absolute three-dimensional structure of molecules, NMR methods can also yield insights into protein interactions by mapping. In a technique called saturation transfer difference NMR, protein resonances can be selectively saturated. One then calculates the ^1H NMR difference spectrum of the ligand from the saturation experiment subtracted from the ligand spectrum without saturation of the protein. Intensities of protons in close contact with the ligand appear enhanced in the difference spectrum, allowing the identification of chemical groups of the ligand interacting with the protein. Using titration experiments, this technique also allows determination of binding constants.

Beyond mapping the flexibility of residues in known protein binding sites, NMR techniques can also be used to identify novel binding sites in proteins. Protein motions on the timescale of microseconds to milliseconds are accessible to NMR spectroscopy, and the diffusion constants for rotation around the three principal axes x , y and z (called rotational diffusion tensor) can be determined. The principal axes are fixed in the protein, and the principal components as well as the orientation can be derived from analysis of the ratio of the spin–spin and spin–lattice relaxation times T_2/T_1 . Analysing these values for the protons of the rigid amide (CO–NH) groups allows a characterisation of the conformational exchange of proteins.

Residues constituting the ligand-binding interface often experience a different environment in the bound state as compared to the free state. The amide signals of these residues are thus broadened due to exchange between these two environments when the free and bound states are in equilibrium.

This approach has been successfully applied to identify the amino acids at the binding site of a 16 kDa protein that binds to and regulates the 251 kDa hydroxylase of the methane monooxygenase protein system. The free and bound forms of the regulatory protein exchange on the timescale of milliseconds.

Other examples include the identification of specific sites involved in the weak self-association of the N-terminal domain of the rat T-cell adhesion protein CD2 (CD2d1) using the concentration dependence of the T_2 values.

strength of the applied external magnetic field. If an external magnetic field gradient is applied then a range of resonant frequencies are observed, reflecting the spatial distribution of the spinning nuclei. **Magnetic resonance imaging (MRI)** can be applied to large volumes in whole living organisms and has a central role in routine clinical imaging of large-volume soft tissues.

The number of spins in a particular defined spatial region gives rise to the spin density as an observable parameter. This measure can be combined with analysis of



Fig. 13.12 Magnetic resonance imaging: 2-mm thick coronal T_2 weighted fast spin echo image at the level of the foramina monroi connecting the anterior horns of the lateral ventricles with the third ventricle. The sequence consisting of 40 images was acquired at a field strength of 3 tesla and generates $0.47 \times 0.64 \times 2$ mm voxels. (Image courtesy of Professor H. Urbach, University of Bonn.)

the principal relaxation times (T_1 and T_2). The imaging of flux, as either bulk flow or localised diffusion, adds considerably to the options available. In terms of whole-body scanners, the entire picture is reconstructed from images generated in contiguous slices. MRI can be applied to the whole body or specific organ investigations on head, thorax, abdomen, liver, pancreas, kidney and musculoskeletal regions (Fig. 13.12). The use of contrast agents with paramagnetic properties has enabled investigation of organ function, as well as blood flow, tissue perfusion, transport across the blood-brain barrier and vascular anatomy. Resolution and image contrast are major considerations for the technique and subject to continuing development. The resolution depends on the strength of the magnetic field and the availability of labels that yield high signal strengths. MRI instruments used for clinical imaging typically operate with field strengths of up to 3 T, but experimental instruments can operate at more than 20 T, allowing the imaging of whole live organisms with almost enough spatial and temporal resolution to follow regenerative processes continuously at the single-cell level. Equipment cost and data acquisition time remain important issues. On the other hand, according to current knowledge, MRI has no adverse effects on human health, and thus provides a valuable diagnostic tool, especially due to the absence of the hazards of ionising radiation.

13.6 X-RAY DIFFRACTION

13.6.1 Principles

The interaction of electromagnetic radiation with matter causes the electrons in the exposed sample to oscillate. The accelerated electrons, in turn, will emit radiation of the same frequency as the incident radiation, called the secondary waves. The superposition of waves gives rise to the phenomenon of **interference**. Depending on the displacement (phase difference) between two waves, their amplitudes either reinforce or cancel each other out. The maximum reinforcement is called **constructive interference**, the cancelling is called **destructive interference**. The interference gives rise to dark and bright rings, lines or spots, depending on the geometry of the object causing the diffraction. Diffraction effects increase as the physical dimension of the diffracting object (aperture) approaches the wavelength of the radiation. When the aperture has a periodic structure, for example in a diffraction grating, repetitive layers or crystal lattices, the features generally become sharper. **Bragg's law** (Fig. 13.13) describes the condition that waves of a certain wavelength will constructively interfere upon partial reflection between surfaces that produce a path difference only when that path difference is equal to an integral number of wavelengths. From the constructive interferences, i.e. diffraction spots or rings, one can determine dimensions in solid materials.

Since the distances between atoms or ions are on the order of 10^{-10} m (1 Å), diffraction methods used to determine structures at the atomic level require radiation in the X-ray region of the electromagnetic spectrum, or beams of electrons or neutrons with a similar wavelength. While electrons and neutrons are particles, they also possess wave properties with the wavelength depending on their energy (**de Broglie hypothesis**). Accordingly, diffraction can also be observed using electron and neutron beams. However, each method also has distinct features, including the penetration depth which increases in the series electrons – X-rays – neutrons.

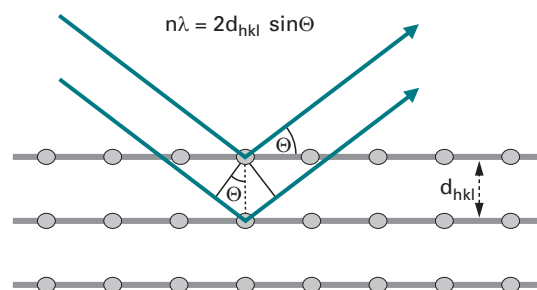


Fig. 13.13 Bragg's law. Interference effects are observable only when radiation interacts with physical dimensions that are approximately the same size as the wavelength of the radiation. Only diffracted beams that satisfy the Bragg condition are observable (constructive interference). Diffraction can thus be treated as selective reflection. n is an integer ('order'), λ is the wavelength of the radiation, d is the spacing between the lattice planes and Θ is the angle between the incident/reflected beam and the lattice plane.

13.6.2 X-ray diffraction

X-rays for chemical analysis are commonly obtained by **rotating anode generators** (in-house) or **synchrotron** facilities (Fig. 13.14). In rotating anode generators, a rotating metal target is bombarded with high-energy (10–100 keV) electrons that knock out core electrons. An electron in an outer shell fills the hole in the inner shell and emits the energy difference between the two states as an X-ray photon. Common targets are copper, molybdenum and chromium, which have strong distinct X-ray emission at 1.54 Å, 0.71 Å and 2.29 Å, respectively, that is superimposed on a continuous spectrum known as **Bremsstrahlung**. In synchrotrons, electrons are accelerated in a ring, thus producing a continuous spectrum of X-rays. Monochromators are required to select a single wavelength.

As X-rays are diffracted by electrons, the analysis of X-ray diffraction data sets produces an **electron density** map of the crystal. Since hydrogen atoms have very little electron density, they are not usually determined experimentally by this technique.

Unfortunately, the detection of light beams is restricted to recording the intensity of the beam only. Other properties, such as polarisation, can only be determined with rather complex measurements. The phase of the light waves is even systematically lost in the measurement. This phenomenon has thus been termed the **phase problem**

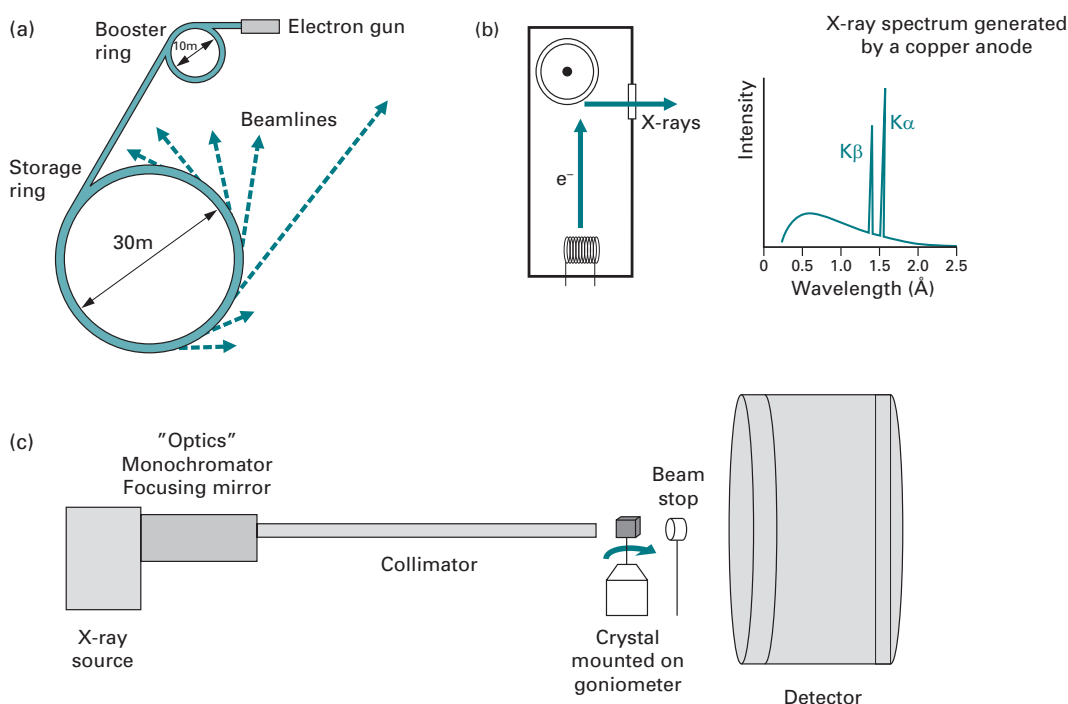


Fig. 13.14 Instrumentation for X-ray diffraction. The most common X-ray sources are (a) particle storage rings which produce synchrotron radiation, and (b) rotating anode tubes. The schematics of an X-ray diffractometer are shown in (c).

owing to the essential information contained in the phase in diffraction and microscopy experiments. The X-ray diffraction data can be used to calculate the amplitudes of the three-dimensional Fourier transform of the electron density. Only together with the phases can the electron density be calculated, in a process called Fourier synthesis.

Different methods to overcome the phase problem in X-ray crystallography have been developed, including:

- molecular replacement, where phases from a structurally similar molecule are used;
- experimental methods that require incorporation of heavy element salts (multiple isomorphous replacement);
- experimental methods where methionine has been replaced by seleno-methionine in proteins (multi-wavelength anomalous diffraction);
- experimental methods using the anomalous diffraction of the intrinsic sulphur in proteins (single wavelength anomalous diffraction);
- direct methods, where a statistical approach is used to determine phases. This approach is limited to very high resolution data sets and is the main method for small molecule crystals as these provide high-quality diffraction with relatively few numbers of reflections.

13.6.3 Applications

Single-crystal diffraction

A crystal is a solid in which atoms or molecules are packed in a particular arrangement within the **unit cell** which is repeated indefinitely along three principal directions in space. Crystals can be formed by a wide variety of materials, such as salts, metals, minerals and semiconductors, as well as various inorganic, organic and biological molecules.

A crystal grown in the laboratory is mounted on a goniometer and exposed to X-rays produced by rotating anode generators (in-house) or a synchrotron facility. A diffraction pattern of regularly spaced spots known as reflections is recorded on a detector, most frequently image plates or CCD cameras for proteins, and moveable proportional counters for small molecules.

An incident X-ray beam is diffracted by a crystal such that beams at specific angles are produced, depending on the X-ray wavelength, the crystal orientation and the structure of the crystal (i.e. unit cell).

To record a data set, the crystal is gradually rotated and a diffraction pattern is acquired for each distinct orientation. These two-dimensional images are then analysed by identifying the appropriate reflection for each **lattice plane** and measuring its intensity, measuring the cell parameters of the unit cell and determining the appropriate space group. If information about the phases is available, this data can then be used to calculate a three-dimensional model of the electron density within the unit cell using the mathematical method of Fourier synthesis. The positions of the atomic nuclei are then deduced from the electron density by computational refinement and manual intervention using molecular graphics.

Fibre diffraction

Certain biological macromolecules, such as DNA and cytoskeletal components, cannot be crystallised, but form fibres. In fibres, the axes of the long polymeric structures are parallel to each other. While this can be an intrinsic property, for example in muscle fibres, in some cases the parallel alignment needs to be induced. As fibres show **helical symmetry**, by analysing the diffraction from oriented fibres one can deduce the helical symmetry of the molecule, and in favourable cases the molecular structure. Generally, a model of the fibre is constructed and the expected diffraction pattern is compared with the observed diffraction.

Historically, fibre diffraction was of central significance in enabling the determination of the three-dimensional structure of DNA by Crick, Franklin, Watson and Wilkins.

Two classes of fibre diffraction patterns can be distinguished. In **crystalline fibres** (e.g. A form of DNA), the long fibrous molecules pack to form thin micro-crystals randomly arranged around a shared common axis. The resulting diffraction pattern is equivalent to taking a long crystal and spinning it about its axis during the X-ray exposure. All Bragg reflections are recorded at once. In **non-crystalline fibres** (e.g. B form of DNA), the molecules are arranged parallel to each other but in a random orientation around the common axis. The reflections in the diffraction pattern are now a result of the periodic repeat of the fibrous molecule. The diffraction intensity can be calculated via Fourier–Bessel transformation replacing the Fourier transformation used in single-crystal diffraction.

Powder diffraction

Powder diffraction is a rapid method to analyse multicomponent mixtures without the need for extensive sample preparation. Instead of using single crystals, the solid material is analysed in the form of a powder where, ideally, all possible crystalline orientations are equally represented.

From powder diffraction patterns, the interplanar spacings d of the lattice planes (Fig. 13.13) are determined and then compared to a known standard or to a database (Powder Diffraction File by the International Centre for Diffraction Data or the Cambridge Structural Database) for identification of the individual components.

13.7 SMALL-ANGLE SCATTERING

The characteristics of molecules at larger size scales are fundamentally different than at atomic scales. While atomic scale structures are characterised by high degrees of order (e.g. crystals), on the nano scale, the building blocks of matter are rarely well organised and are composed of rather complex building blocks (i.e. shapes). Consequently, sharp diffraction peaks are observed in X-ray diffraction from single crystals, but diffuse patterns are obtained from X-ray scattering from biological molecules or nano-structures.

In Section 12.6, we learned that incident light scattered by a particle in the form of **Rayleigh scattering** has the same frequency as the incident light. It is thus called elastic light scattering. The light scattering techniques discussed in Section 12.6 have used a

combination of visible light and molecules, so that the dimension of the particle is smaller than the wavelength of the light. When using light of smaller wavelengths such as X-rays, the overall dimension of a molecule is large as compared to the incident light. Electrons in the different parts of the molecule are now excited by the incident beam with different phases. The coherent waves of the scattered light therefore show an interference that is dependent on the geometrical shape of the molecule. As a result

- in the forward direction (at 0°), there is no phase difference between the waves of the scattered light, and one observes maximum positive interference, i.e. highest scattering intensity;
- at small angles, there is a small but significant phase difference between the scattered waves which results in diminished scattering intensity due to destructive interference.

Small-angle X-ray or **neutron scattering** (SAXS or SANS) are experimental techniques used to derive size and shape parameters of large molecules. Both X-ray and neutron scattering are based on the same physical phenomenon, i.e. scattering due to differences in scattering mass density between the solute and the solvent or indeed between different molecular constituents. An advantage for protein structure determination is the fact that samples in aqueous solution can be assessed.

Experimentally, a monodisperse solution of macromolecules is exposed to either X-rays (wavelength $\lambda = \text{ca. } 0.15 \text{ nm}$) or thermal neutrons ($\lambda = \text{ca. } 0.5 \text{ nm}$). The intensity of the scattered light is recorded as a function of momentum transfer q ($q = 4\pi \sin \theta \lambda^{-1}$, where 2θ is the angle between the incident and scattered radiation). Due to the random positions and orientations of particles, an isotropic intensity distribution is observed that is proportional to the scattering from a single particle averaged over all orientations. In neutron scattering, the **contrast** (squared difference in scattering length density between particle and solvent) can be varied using $\text{H}_2\text{O}/\text{D}_2\text{O}$ mixtures or selective deuteration to yield additional information. At small angles the scattering curve is a rapidly decaying function of q , and essentially determined by the **particle shape**. Fourier transformation of the scattering function yields the so-called **size distribution function** which is a histogram of interatomic distances. Comparison of the size distribution function with the particle form factor of regular geometrical bodies allows conclusions as to the shape of the scattering particle. Analysis of the scattering function further allows determination of the **radius of gyration** R_g (average distance of the atoms from the centre of gravity of the molecule), and the mass of the scattering particle from the scattering in the forward direction.

Shape restoration

Software programs have been developed that enable the calculation of three-dimensional structures from the one-dimensional scattering data obtained by SAXS. Due to the low resolution of SAXS data, the structural information is restricted to the shape of the scattering molecules. Furthermore, the scattering data do not imply a single, unique solution. The reconstruction of three-dimensional structures might thus result in a number of different models. One approach is to align and average a set of independently reconstructed models thus obtaining a model that retains the most persistent features.

13.8 SUGGESTIONS FOR FURTHER READING

General

Ciulli, A. and Abell, C. (2007). Fragment-based approaches to enzyme inhibition. *Current Opinion in Biotechnology*, **18**, 489–496.

Infrared spectroscopy

Beekes, M., Lasch, P. and Naumann, D. (2007). Analytical applications of Fourier transform-infrared (FT-IR) spectroscopy in microbiology and prion research. *Veterinary Microbiology*, **123**, 305–319.

Ganim, Z., Chung, H. S., Smith, A. W., Deflores, L. P., Jones, K. C. and Tokmakoff, A. (2008). Amide I two-dimensional infrared spectroscopy of proteins. *Accounts of Chemical Research*, **41**, 432–441.

Tonouchi, M. (2007). Cutting-edge terahertz technology. *Nature Photonics*, **1**, 97–105.

WEBSITES

<http://www.cem.msu.edu/~reusch/VirtualText/Spectrpy/InfraRed/infrared.htm>

<http://www.chem.uic.edu/web1/ocol/spec/IR.htm>

<http://orgchem.colorado.edu/hndbksupport/irtutor/tutorial.html>

<http://www.umd.umich.edu/casl/natsci/slc/slconline/IR/>

<http://www.biophysik.uni-freiburg.de/Spectroscopy/Time-Resolved/spectroscopy.html>

Raman spectroscopy

Benevides, J. M., Overman, S. A. and Thomas, G. J. Jr. (2004). Raman spectroscopy of proteins.

Current Protocols in Protein Science, Chapter 17, Unit 17.8. New York: Wiley Interscience.

Wen, Z. Q. (2007). Raman spectroscopy of protein pharmaceuticals. *Journal of Pharmaceutical Sciences*, **96**, 2861–2878.

WEBSITES

<http://www.jobinyvon.com/Raman%20Tutorial%20Intro>

<http://people.bath.ac.uk/pysdw/newpage11.htm>

Surface plasmon resonance

Anker, J. N., Hall, W. P., Lyandres, O., Shah, N. C., Zhao, J. and Van Duyne, R. P. (2008). Biosensing with plasmonic nanosensors. *Nature Materials*, **7**, 442–453.

Campbell, C. T. and Kim, G. (2007). SPR microscopy and its applications to high-throughput analyses of biomolecular binding events and their kinetics. *Biomaterials*, **28**, 2380–2392.

Majka, J. and Speck, C. (2007). Analysis of protein–DNA interactions using surface plasmon resonance. *Advances in Biochemical Engineering and Biotechnology*, **104**, 13–36.

Neumann, T., Junker, H. D., Schmidt, K. and Sekul, R. (2007). SPR-based fragment screening: advantages and applications. *Current Topics in Medicinal Chemistry*, **7**, 1630–1642.

Phillips, K. S. and Cheng, Q. (2007). Recent advances in surface plasmon resonance based techniques for bioanalysis. *Analytical and Bioanalytical Chemistry*, **387**, 1831–1840.

WEBSITES

<http://www.biacore.com/>

<http://www.uksaf.org/tech/spr.html>

<http://people.clarkson.edu/~ekatz/spr.htm>

Electron paramagnetic resonance spectroscopy

Matsumoto, K., Subramanian, S., Murugesan, R., Mitchell, J. B. and Krishna, M. C. (2007). Spatially resolved biologic information from in vivo EPRI, OMRI, and MRI. *Antioxidants and Redox Signaling*, **9**, 1125–1141.

Schiemann, O. and Prisner, T. F. (2007). Long-range distance determinations in biomacromolecules by EPR spectroscopy. *Quarterly Reviews in Biophysics*, **40**, 1–53.

WEBSITES

<http://hyperphysics.phy-astr.gsu.edu/hbase/molecule/esr.html>

<http://www.chemistry.nmsu.edu/studntres/chem435/Lab7/intro.html>

Nuclear magnetic resonance spectroscopy

- Blamire, A. M. (2008). The technology of MRI: the next 10 years? *British Journal of Radiology*, **81**, 601–617.
- Ishima, R. and Torchia, D. A. (2000). Protein dynamics from NMR. *Nature Structural Biology*, **7**, 740–743.
- McDermott, A. and Polenova, T. (2007). Solid state NMR: new tools for insight into enzyme function. *Current Opinion in Structural Biology*, **17**, 617–622.
- Skinner, A. L. and Laurence, J. S. (2008). High-field solution NMR spectroscopy as a tool for assessing protein interactions with small molecule ligands. *Journal of Pharmaceutical Science*, **97**, 4670–4695.
- Spieß, H. W. (2008). NMR spectroscopy: pushing the limits of sensitivity. *Angewandte Chemie International Edition (English)*, **47**, 639–642.

WEBSITES

- <http://www.cem.msu.edu/~reusch/VirtualText/Spectrpy/nmr/nmr1.htm#nmr1>
- http://arrhenius.rider.edu/nmr/NMR_tutor/pages/nmr_tutor_home.html
- <http://www.cis.rit.edu/htbooks/nmr/>
- <http://teaching.shu.ac.uk/hwb/chemistry/tutorials/molspec/nmr1.htm>
- <http://www.chem.queensu.ca/FACILITIES/NMR/nmr/webcourse/>

X-ray diffraction

- Hickman, A. B. and Davies, D. R. (2001). Principles of macromolecular X-ray crystallography. *Current Protocols in Protein Science*, Chapter 17, Unit 17.3. New York: Wiley Interscience.
- Miao, J., Ishikawa, T., Shen, Q. and Earnest, T. (2008). Extending X-ray crystallography to allow the imaging of noncrystalline materials, cells, and single protein complexes. *Annual Reviews in Physical Chemistry*, **59**, 387–410.
- Mueller, M., Jenni, S. and Ban, N. (2007). Strategies for crystallization and structure determination of very large macromolecular assemblies. *Current Opinion in Structural Biology*, **17**, 572–579.
- Wlodawer, A., Minor, W., Dauter, Z. and Jaskolski, M. (2008). Protein crystallography for non-crystallographers, or how to get the best (but not more) from published macromolecular structures. *FEBS Journal*, **275**, 1–21.

WEBSITES

- <http://www.colorado.edu/physics/2000/xray/index.html>
- <http://www.physics.upenn.edu/~heiney/talks/hires/hires.html>
- <http://www.matter.org.uk/diffraction/x-ray/default.htm>

Small-angle scattering

- Lipfert, J. and Doniach, S. (2007). Small-angle X-ray scattering from RNA, proteins, and protein complexes. *Annual Reviews of Biophysical and Biomolecular Structure*, **36**, 307–327.
- Neylon, C. (2008). Small angle neutron and X-ray scattering in structural biology: recent examples from the literature. *European Biophysics Journal*, **37**, 531–541.
- Putnam, C. D., Hammel, M., Hura, G. L. and Tainer, J. A. (2007). X-ray solution scattering (SAXS) combined with crystallography and computation: defining accurate macromolecular structures, conformations and assemblies in solution. *Quarterly Reviews in Biophysics*, **40**, 191–285.

WEBSITES

- <http://www.ncnr.nist.gov/programs/sans/tutorials/index.html>
- <http://www.isis.rl.ac.uk/largescale/loq/documents/sans.htm>
- <http://www.embl-hamburg.de/workshops/2001/EMBO/>